Encapsulation of fluorogenic probes and pharmacologically active molecules into nanoparticles for enhancing cellular uptake

Eliza Anna Glowka Martenka

Poznan University of Medical Sciences

Nancy University

ELIZA GŁÓWKA

Encapsulation of fluorogenic probes and pharmacologically active molecules into nanoparticles for enhancing cellular uptake

Doctoral dissertation

Doctorat *co-tutelle*

Mentors: Prof. Dr Janina Lulek
Prof. Dr Philippe Maincent

Members of the Committee:

Prof. Dr Janina Lulek
Prof. Dr Małgorzata Sznitowska
Prof. Dr Edmund Grześkowiak
Prof. Dr Philippe Maincent
Prof. Dr Elias Fattal
Dr Anne Sapin-Minet

Poznań 2009

Keywords: nanoparticles, nanospheres, nanoencapsulation, encapsulation, salmon calcitonin, glutathion, sustained release, oral delivery, intracellular targeting, bioavailability

Słowa kluczowe: nanocząstki, nanosfery, inkorporowanie, kalcytonina łososiowa, glutation, przedłużone uwalnianie leku, podanie doustne, przenikanie dokomórkowe, biodostępność

Mots clés: nanoparticules, nanosphères, nanoencapsulation, encapsulation, calcitonine de saumon, glutathion, libération prolongée, administration orale, pénétration intracellulaire, biodisponibilité

ACKNOWLEDGEMENTS

The present work was carried out between July 2005 and June 2009 in the framework of the doctoral studies (*doctorat co-tutelle*) between Poznan University of Medical Sciences (Poland) and Nancy University (France).

First of all, I would like to express my deepest gratitude to my supervisors. **Professor Janina Lulek** (Department of Pharmaceutical Technology, Poznan University of Medical Sciences) and **Professor Philippe Maincent** (Department of Pharmaceutical Technology, Nancy University) are gratefully acknowledged for offering me the opportunity to work in this project, for the constructive discussions, support and constant interest, the friendly atmosphere within both departments and for involving me in the program of *Euro PhD in Advanced Drug Delivery Systems* provided by the GALENOS Network.

Professor Pierre Leroy (Nancy University), who co-supervised the first part of this thesis (Encapsulation of fluorogenic probes into nanoparticles), is also gratefully acknowledged for the generous support concerning mainly analytical issues of this project, for reviewing the present thesis, and in principle for inspiring me to do the doctoral studies.

Professor Małgorzata Sznitowska (Medical University of Gdansk) and **Professor Elias Fattal** (University of Paris-XI) are thanked for kindly being co-referees for this thesis.

Very special acknowledgements to **Dr Anne Sapin-Minet** for her continual support with all scientific, administrative and technical issues during my stay in Nancy. Furthermore, I would like to address sincere thanks to all my colleagues and friends within both departments for their invaluable support, good cooperation, professional and private discussions, and for the friendly atmosphere and great time we spent as co-residents in the laboratory. I am especially grateful to: **Dr Ahmed Sheik Hassan**, **Julien Scala Bertola, Fatima El Ghazouani**, and **Javier Camargo** (special thanks for taking SEM micrographs) within the Department of Pharmaceutical Technology in Nancy, and to **Bartłomiej Milanowski, Magdalena Olejniczak-Rabinek, Hanna Wosicka**, **Małgorzata Geszke**, and **Dr Joanna Karolewska**, within the Department of Pharmaceutical Technology in Poznań.

Professor Jadwiga Jodynis-Liebert and **Dr Marek Murias** (Department of Toxicology, Poznan University of Medical Sciences) are thanked for offering me facilities to work in their laboratory.

Moreover, I am obliged to **Dr hab. Janusz Kasperczyk** and **Dr Katarzyna Jelonek** (Center of Polymer and Carbon Materials, Polish Academy of Science, Zabrze) for generously performing ^{1}H-NMR measurements and giving a word of advice. Additional thanks to **Dr hab. Arkadiusz Szymański** (Faculty of Chemistry, Adam Mickiewicz University, Poznań) for performing the DSC analysis.

Above all, I am in debt of **my husband Bartosz** and **my parents** for their encouragement, understanding and continuous support during all the years of my pharmaceutical education.

The **GALENOS NETWORK** is acknowledged for providing the financial support with the Galenos Fellowship in the Framework of the EU Project "Towards a European PhD in Advanced Drug Delivery", Marie Curie Contract MEST-CT-2004-504992.

The part of the *in vivo* study (oral administration in rats) was supported by a grant from the Polish Ministry of Science and Education (the project number: N405 040 32/2741).

Additionally, the DSC and ^{1}H-NMR studies were supported by the financial resources from Poznan University of Medical Sciences (the project numbers: 501-01-3307415-50387/2007 and 501-01-03314429-50387/2008).

Parts of this thesis have been presented at the following conferences/workshops:

1. **E. Główka**, A. Lamprecht, N. Ubrich, P. Leroy, J. Lulek, J. Coulon, P. Maincent, *Nanoparticles increase the uptake of glutathione selective fluorogenic probes in yeast cells* (poster presentation), 6th International Conference and Workshop on Cell Culture and In vitro Models for Drug Absorption and Delivery, Saarland University, Saarbrücken, Germany, March 1-10, 2006.
2. **E. Główka**, *Encapsulation of fluorogenic probes and salmon calcitonin in polymeric nanoparticles* (oral presentation), 4th Marie Curie Early Stage Training Galenos Thematic Workshop, University of Cagliari, Cagliari, Italy, September 7-9, 2006.
3. **E. Główka**, *Preparation, characterization, and in vivo evaluation of salmon calcitonin nanoparticles* (oral presentation), 3rd Lab Course at Charles University (Galenos Intensive Course), Charles University, Hradec Králové, Prague, Czech Republic, January 29 - February 8, 2007.
4. **E. Główka**, N. Ubrich, A. Sapin, P. Leroy, J. Lulek, P. Maincent, *Preparation and in vitro study on polymeric nanoparticles as drug delivery system for salmon calcitonin* (poster presentation), Young Pharmaceutical Scientists Meet in Amsterdam - Pre-Satellite Meeting of the 3rd Pharmaceutical Sciences World Congress (Poster Award) and 3rd Pharmaceutical Sciences World Congress: Optimizing Drug Therapy - an Imperative for World Health, Amsterdam, the Netherlands, April 20-25, 2007.
5. **E. Główka,** N. Ubrich, P. Maincent, P. Leroy, J. Lulek**,** *Otrzymywanie i charakterystyka nanocząstek jako nośników substancji o różnych właściwościach fizykochemicznych* (poster presentation), I Krajowa Konferencja Nanotechnologii, Politechnika Wrocławska, Wrocław, Poland, May 26-28, 2007.
6. **E. Główka**, N. Ubrich, P. Maincent, P. Leroy, J. Lulek, *The preparation and evaluation of polymeric nanoparticles containing a lipophilic or hydrophilic active agent* (poster presentation), 4th Polish-German Symposium, Martin Luther University Halle-Wittenberg, Halle, Germany, June 6, 2007.
7. **E. Główka**, A. Szymański, A. Sapin-Minet, P. Maincent, J. Lulek, *Charakterystyka fizykochemiczna polimerowych nanosfer do transportu leków* (poster presentation), II Krajowa Konferencja Nanotechnologii, Uniwersytet Jagielloński, Kraków, Poland, June 25-28, 2008.
8. **E. Główka**, A. Szymański, A. Sapin-Minet, P. Maincent, J. Lulek, *Kalcytonina łososiowa w polimerowych nanosferach* (oral presentation), Innowacyjne rozwiązania w technologii postaci leku w celu optymalizacji farmakoterapii. 80-lecie Katedry Technologii Postaci Leku i Biofarmacji, Uniwersytet Jagielloński, Kraków, Poland, October 24-25, 2008.

Parts of this thesis have been published in the following journals:

1. **E. Główka**, A. Lamprecht, N. Ubrich, P. Maincent, J. Lulek, J. Coulon, P. Leroy
   Enhanced cellular uptake of a glutathione selective fluorogenic probe encapsulated in nanoparticles
   Nanotechnology, 17, 2546-2552 (2006)

2. **E. Główka,** A. Sapin-Minet, P. Leroy, J. Lulek, P. Maincent
   Preparation and in vitro-in vivo evaluation of salmon calcitonin loaded polymeric nanoparticles
   Accepted by **Journal of Microencapsulation** (January, 2009)

TABLE OF CONTENTS

LIST OF ABBREVIATIONS

A	Absorbance
ACN	Acetonitrile
AIDS	Acquired immunodeficiency syndrome
AUC	Area under the curve
BCA	Bicinchoninic acid
BMD	Bone mineral density
BSA	Bovine serum albumin
BSO	Buthionine sulfoximine
CE	Capillary electrophoresis
CGRP	Calcitonin-gene related peptide
CLSM	Confocal laser scanning microscopy
CTR	Control solution
DDS	Drug delivery systems
DMSO	Dimethylsulfoxyde
DSC	Differential scanning calorimetry
E.C.	Enzyme Commission number
EDTA	Ethylenediaminetetraacetic acid
ELF	Epithelial lining fluid
ELISA	Enzyme-linked immunosorbent assay
FC	Flow cytometry
FDA	Food and Drug Administration
GFP	Green fluorescence protein
GSH	Reduced glutathione (γ-L-glutamyl-L-cysteinyl-glycine)
GSHPx	Glutathione peroxidases
GSSG	Glutathione disulfide
GST	Glutathione transferase
hCT	Human calcitonin
HIV	Human immunodeficiency virus
HPLC	High performance liquid chromatography
im	Intramuscular
IU	International units
iv	Intravenous
LDE	Laser Doppler electrophoresis
LOD	Limit of detection
LOQ	Limit of quantification
MBB	Monobromobimane
MCB	Monochlorobimane
MPS	Mononuclear phagocyte system
MS	Mass spectrometry
MTT	3-(4,5-dimethylthiazol-2-yl)-2,5-diphenyl tetrazolium bromide
MW	Molecular weight
NADPH	Nicotinamide adenine dinucleotide phosphate
NDA	Naphthalene-2,3-dicarboxaldehyde
ODS	Octadecylsilica
OPA	*Ortho*-phthaldialdehyde
PBS	Phosphate buffered saline

PCS	Photon correlation spectroscopy
PEG	Polyethylene glycol
pI	Isoelectric point
PLA	Poly(lactic) acid
PLGA H	Poly(lactic-co-glycolic) acid - uncapped (unesterified)
PLGA	Poly(lactic-co-glycolic) acid
PLGA S	Poly(lactic-co-glycolic) acid - capped (esterified)
PVA	Polyvinyl alcohol
r	Correlation coefficient
R.S.D.	Relative standard deviation
ROS	Reactive oxygen species
RS	Eudragit® RS
S.D.	Standard deviation
sc	Subcutaneous
sCT	Salmon calcitonin
SDS	Sodium dodecyl sulfate
SEM	Scanning electron microscopy
SNAC	N-[8-(2-hydroxybenzoyl)amino] caprylate
SOD	Superoxide dismutase
STD	Standard solution
TEM	Transmission electron microscopy
TFA	Trifluoroacetic acid
T_g	Glass transition temperature
tGSH	Total glutathione
TMB	Tetramethylbenzidine
UV	Ultraviolet
VIS	Visible

γ-GluCys	γ-Glutamylcysteine
γ-GT	γ-Glutamyltranspeptidase
5-CNAC	N-(5-chlorosalicyloyl)-8-aminocaprylic acid

1. INTRODUCTION

Nanotechnology is still an emerging and attractive technology, though it has been under the spotlight for the last few decades. Nanotechnology is not a field of science as such, but, the term covers a multidisciplinary complex of tools, techniques, and processes for the manipulation and utilization of materials or devices at the nanometer scale, where unique properties enable novel applications (Hayter, 2003). Moreover, nanotechnology has been expected to be a critical driver of technological development in the nearest future. It was inevitable that nanotechnology would be applied in biology, biotechnology and medicine, giving rise to the term nanobiotechnology and nanomedicine.

Nanomedicine, the medical application of nanotechnology, encompasses mainly drug delivery systems (DDS), tissue engineering (Kretlow*, et al.*, 2007), and imaging (Yu*, et al.*, 2006). Generally, nanotechnology deals with structures of the size 100 nm or smaller. However, biological and biopharmaceutical benefits are already observed for submicron-sized structures, hence, pharmaceutical nanotechnology involves drug-loaded structures with diameters ranging from 1 to 500 (Devalapally*, et al.*, 2007) or even 1 000 nm (Pinto Reis*, et al.*, 2006). The overall goal of nanomedicine is the same as it always has been in medicine: to diagnose as accurately and early as possible, to treat as effectively as possible without side effects, and to evaluate the efficacy of treatment noninvasively (Caruthers*, et al.*, 2007).

Depending on the physical form, DDS can be molecular or particulate. Molecular carriers include, for instance, soluble polymers to which drug molecules have been covalently attached, drug-antibody conjugates, conjugates with other natural macromolecules or lipophilic prodrugs, as well as drugs trapped within the central cavity of water-soluble cyclodextrins. Molecular carriers allow a wide distribution of the associated drug, however, one drug molecule can be carried by each molecular carrier. In contrast, particulate delivery systems can carry a large number of drug molecules in one entity. In this category, there are e.g. cells from the patient which have been loaded with a drug *ex vivo*, and various microparticulate (microspheres or microcapsules with a diameter from 1 to 250 μm) or nanoparticulate DDS, including nanoparticles and liposomes (referred to as 'colloidal drug carriers') (Couvreur*, et al.*, 2002, Barratt, 2003).

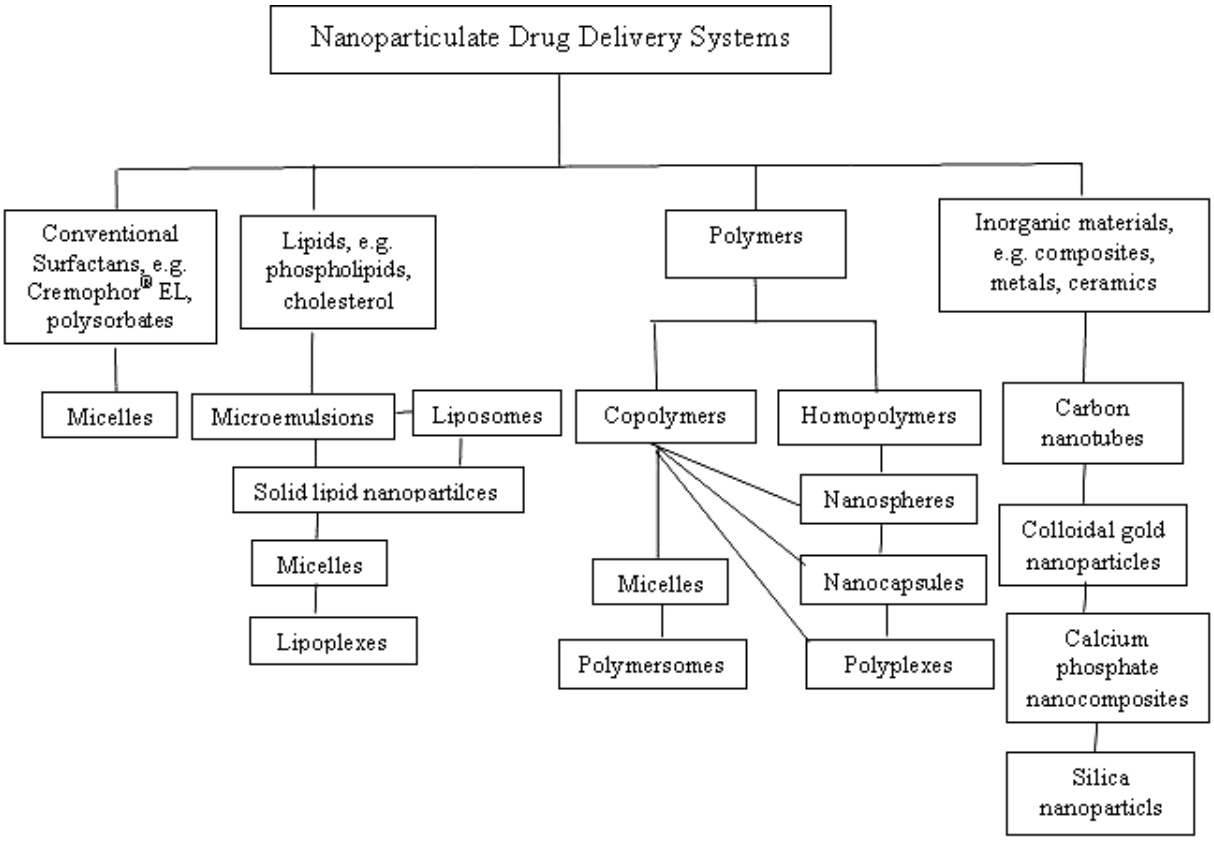

Figure 1. Classification of nanoparticulate drug delivery systems (adopted form Letchford & Burt, 2007).

A wide variety of nanoparticulate DDS composed of a range of materials including lipids, polymers and inorganic materials have been developed (Figure 1), resulting in delivery systems that vary in their physicochemical properties and thus their potential applications. The popularity of these systems is due in part to the several advantages they provide for drug delivering (Letchford & Burt, 2007).

According to the functional properties of particulate DDS, a division into 3 generations has been proposed (Couvreur*, et al.*, 2002). The first-generation systems are capable of releasing the active substance at the intended target, but because of their size (microparticles with a diameter > 1 μm), they have to be implanted as closely as possible to the site of action, e.g. systems for the controlled drug release within the brain. In contrast, the second- and third-generation systems are true carriers (< 1 μm in diameter), i.e. they are capable of carrying a drug at the intended target and releasing from after administration by a general route, including an intravenous one. The second-generation carriers do not contain any specific recognition elements in comparison with the third generation. The second-generation carriers includes 'passive' colloidal carriers (classical liposomes and nanoparticles)

as well as certain 'active' carriers such as temperature-sensitive liposomes and magnetic nanoparticles, which release a drug after a specific signal. Sterically stabilized carriers ('stealth' carriers) also belong to this group. They may remain in the blood compartment for a considerable time due to the modification of surface properties allowing to reduce the deposition of plasma proteins resulting in diminished recognition by phagocytes. Furthermore, stealth particles may cross capillary endothelium characterized by a greater permeability in the region of solid tumors, inflammation or infection. Whereas, the third-generation carriers are capable of specific recognition of the target, e.g. antibodies, certain second-generation particulate systems piloted by monoclonal antibodies or other ligands. Additionally, these carriers will be more effective if they are also sterically stabilized (Couvreur*, et al.*, 2002, Barratt, 2003).

Nanotechnology-based DDS used for drug formulations, with a special emphasis on polymeric nanoparticles, have the potential to improve drug delivery to the desired site of action and enable delivery of poorly soluble, poorly absorbed or unstable drugs. The current focus is on targeted drug delivery. Nanoparticles can improve drug delivery by the following approaches (Jain, 2008):

- Particle size of a drug, which has poor water solubility, is reduced to nanometer range (nanonisation in contrast to micronization) to increase the surface area, thereby increasing the rate of drug dissolution and absorption, resulting in better bioavailability. This way, drug nanoparticles form so-called nanocrystals or nanosuspensions of pure drugs, often containing only a small amount of surfactants (Keck & Muller, 2006),
- An aqueous solubility of a poorly soluble hydrophobic drug can be improved *via* solubilization within the hydrophobic core of nanoparticles,
- Nanoparticles can be injected directly into the systemic circulation without the risk of blocking blood vessels. Due to their very small diameter, nanoparticles can flow easily through the narrowest gauge needles. After an intravenous administration, opsonization and subsequent recognition and phagocytosis by macrophages is dependent on the particle size. It has been found that particles under 200 nm in diameter display a decreased rate of clearance, and thus an extended circulation time as compared to those with a larger diameter. The circulation time of nanoparticles could be further increased by the surface modification with polyethylene glycol (PEG) chains (PEGylation). The circulation time of nanoparticles is additionally prolonged

by their reduced renal excretion due to their sufficiently large particle size which prevents glomerular filtration (Letchford & Burt, 2007),

- Nanoparticles administered by an oral route have better stability both during storage and *in vivo* compared to liposomes (Barratt, 2003), and reveal some advantageous over the microparticles. It has been observed that the number of nanoparticles which cross the intestinal epithelium is greater than the number of microparticles, and that not only the M cells of the Peyer's patches, but also normal enterocytes are involved in the uptake of nanoparticles from the gastrointestinal tract (Vila, *et al*., 2002),
- Development of novel nanoparticle formulations with improved drug stability and absorption resulting in better bioavailability can potentially reduce the amount of dose required and increasing safety through reduced side effects,
- Nanoparticle formulations can provide sustained or controlled release profiles up to 24 h for oral delivery (e.g. due to mucoadhesive properties) or over a longer period of time (days, months) for injectable or implantable formulations, hence improve patient compliance with drug regimens,
- Nanoparticles can be combined with ligands (e.g. folic acid, lectins, specific antibody) for targeted drug delivery (e.g. to the brain, tumor, specific receptors or antigens on the cell surface). Such functionalized nanoparticles should be protected from opsonization and recognition by immune system and efficiently targeted to particular tissue types. Targeted drug carriers reduce drug toxicity and provide more efficient drug distribution (Vasir, *et al*., 2005),
- Nanoparticles may be capable of intracellular targeting of drugs whose site of action is located in the intracellular compartment e.g. glucocorticoids (cytoplasmic receptors) or anticancer drugs (nucleus) (Vasir, *et al.*, 2005),
- Nanoparticles can make possible the delivery of labile peptides and proteins by non invasive routes of administration, especially an oral one (Delie & Blanco-Prieto, 2005),
- Nanoparticles can be useful as non-viral vectors for gene delivery (Panyam & Labhasetwar, 2003).

Polymeric nanoparticles are defined as submicronic solid colloidal carriers made of polymers. This general term includes nanospheres and nanocapsules (Figure 2). In a polymeric nanosphere (matrix system), a drug can be entrapped into the matrix (dissolved or

dispersed), chemically bound or adsorbed to the particle surface. On the other hand, a nanocapsule is a vesicular system in which the drug is confined to a cavity surrounded by a polymer membrane. Typically, the core is an oily liquid and the surrounding polymer is a single layer of polymer, but the preparation of nanocapsules with an aqueous core is also feasible (Couvreur, *et al.*, 2002). Alternatively, if the core of the vesicle is an aqueous phase and the surrounding coating is a polymer bilayer, the particle is referred to as a polymersome. These vesicles are analogous to liposomes, but they differ from liposomes in that the external bilayer is composed of amphiphilic block copolymers (Letchford & Burt, 2007).

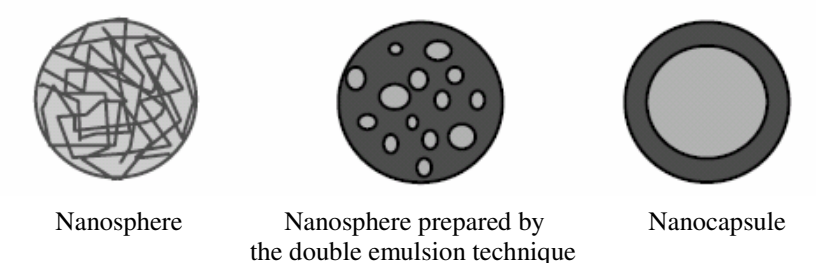

Figure 2. Different types of polymeric nanoparticles (adopted from Delie & Blanco-Prieto, 2005).

It should be mentioned that when arriving in the bloodstream after administration, clearance of nanoparticles is immediate because of the capture by the mononuclear phagocyte system (MPS) sequestering particles within organs such as the liver and spleen. However, elimination may be slowed down due to the submicron particle size. In order to suppress opsonization by plasma proteins, thus resisting phagocytosis by macrophages and decreasing clearance by the MPS, resulting in prolonged circulation times, several approaches have been proposed such as steric modification of the particle surface (e.g. with PEG or surfactants), increasing the particle hydrophilicity, decreasing the particle size, making the particle neutral (Devalapally*, et al.*, 2007).

Different methods for the preparation of nanoparticles have been formerly described by many authors (for extensive general review see Bodmeier & Maincent, 1996, Soppimath*, et al.*, 2001, Pinto Reis*, et al.*, 2006). Generally, preparation of nanoparticles is based on either the dispersion of preformed polymers (water-soluble or water-insoluble, synthetic, semi-synthetic or natural polymers) or polymerization of lipophilic or hydrophilic monomers. A drug can be incorporated during or after the preparation of the polymer dispersions. The choice of a particular preparation method and a polymer depends mainly on the physicochemical properties of the drug substance, the desired release characteristics, the

therapeutic goal and the route of administration. From a technological point of view, the successful selection of a preparation method is determined by the ability to achieve high drug loadings, high encapsulation efficiencies, high product yields, and the potential for easy scale-up (Bodmeier & Maincent, 1996). Overall, the polymerization methods are classified into emulsion polymerization (organic or aqueous continuous phase), interfacial polymerization and interfacial polycondensation. On the other hand, preparation of nanoparticles from synthetic preformed polymers can be mainly achieved using emulsification/solvent evaporation, emulsification/solvent diffusion, salting out, interfacial deposition (often referred to as nanoprecipitation) and solvent displacement techniques (Pinto Reis*, et al.*, 2006). Based on the previous listed methods and depending on the experimental conditions and various modifications of these techniques, it is possible to obtain either nanospheres or nanocapsules. It should be emphasized that it is often difficult to distinguish between different structures and morphologies of the particles, thereby, the term 'nanoparticles' is generally preferred (Bodmeier & Maincent, 1996).

In conclusion, nanoparticles have been experimentally used in a very extensive way in order to demonstrate their potential clinical applications. However, until now, only several nanotechnology-based products are already approved and present in the market, such as Doxil® (doxorubicin-loaded liposomes) and Abraxane® (130 nm-sized paclitaxel nanoparticles sterically stabilized by human albumin to prevent aggregation), both used as injectable suspensions for the treatment of cancer. Although clinical trials are very limited and progress in clinical applications of nanoparticulate DDS has been slow, the achieved experimental results have been promising and the potential of nanoparticles as DDS should be great.

2. THEORETICAL PART

2.1. Encapsulation of glutathione-selective fluorogenic probes

2.1.1. Biochemistry of glutathione

Reduced glutathione (GSH) is a tripeptide (γ-L-glutamyl-L-cysteinyl-glycine) (Figure 3) playing a crucial role in many biochemical reactions. GSH is the most abundant cellular non-protein low molecular weight thiol (MW = 307.32 g/mol), and is almost ubiquitous in all human, animal, plant and microbial cells. A disulfide dimer (GSSG – 'oxidized glutathione') usually accounts for less than 1% of the total intracellular glutathione content (tGSH; sum of the content of the reduced form and oxidized forms). However, an important fraction of GSH can be found in cells also as thioesters or mercaptides in combination with other low molecular weight thiols or proteins (GSH conjugates) (Franco*, et al.*, 2007).

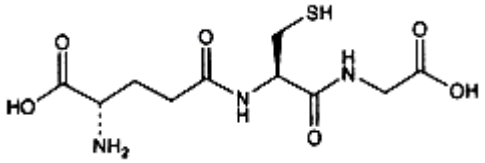

Figure 3. The structure of GSH.

The intracellular concentration of GSH is homeostatically controlled and reflects a dynamic balance between *de novo* GSH synthesis, its recycling from GSSG, consumption rate (by peroxidases, transferases and transpeptidases), and transport (Kidd, 1997). GSH is 85 to 90% freely distributed in the cytosol, where it is synthesized. However, it can be compartmentalized in organelles such as mitochondria, nuclear matrix, endoplasmic reticulum and peroxisomes (Wu*, et al.*, 2004, Franco*, et al.*, 2007). The mitochondrial pool of GSH represents 10-15% of cellular tGSH and is tightly held because mitochondria are normally under high oxidative stress (Kulinsky & Kolesnichenko, 2007).

De novo GSH synthesis from individual amino acids is an operation of two successive enzymes: γ-glutamylcysteine ligase (or γ-glutamylcysteine synthase, E.C. 6.3.2.2) and GSH synthase (E.C. 6.3.2.3). In the first step, an untypical peptidic γ-linkage, that protects GSH from hydrolysis by intracellular peptidases, is formed between glutamate and cysteine. The

availability of cysteine is usually the rate-limiting factor in GSH synthesis. Finally, glycine is added to γ-glutamylcysteine (γ-GluCys) by the activity of GSH synthase. The synthesis is controlled by a negative feedback from GSH on the γ-glutamylcysteine ligase activity (Sies, 1999, Dickinson & Forman, 2002, Wu*, et al.*, 2004, Franco*, et al.*, 2007). Some factors and processes, such as oxidative stress, cancer or GSH depletion, increase γ-glutamylcysteine ligase transcription and activity (Wu*, et al.*, 2004). On the other hand, GSH is synthesized *via* its recycling from GSSG by means of GSH reductase (E.C. 1.6.4.2).

The key enzyme implicated in GSH catabolism is a γ-glutamyl transpeptidase (or γ-glutamyl transferase, γ-GT, E.C. 2.3.2.2), the active center of which is localized on the outer side of the plasmatic membrane. Since GSH is continuously effluxed by cells e.g. with the use of the multidrug resistance proteins, γ-GT allows component amino acids to be available for intracellular GSH resynthesis. By the activity of γ-GT, the γ-glutamyl moiety from GSH and GSH-conjugated compounds is removed and transferred to other acceptors (amino acids, dipeptides) producing cysteinylglycine or cysteinylglycine-conjugates. These latter are then hydrolyzed by ectoprotein dipeptidases giving cysteine and γ-glutamyl amino acids which are taken up into the cytosol by the activity of specific membrane transporters (Franco*, et al.*, 2007).

GSH is a very reactive molecule participating in a wide variety of metabolic processes. Theses reactions can be divided into those involving the γ-glutamyl moiety of the molecule, such as reactions mediated by γ-GT, and those involving the thiol moiety that include oxidation-reduction (redox), nucleophilic or addition reactions.

2.1.2. Functions of glutathione

GSH was initially recognized as a potent reducing agent and a major cellular antioxidant, however, many other cellular functions have been ascribed to GSH.

As an antioxidant, GSH maintains a tight control of the cellular redox status. GSH effectively scavenges free radicals and other reactive oxygen species (ROS) and reactive nitrogen species, directly or indirectly through enzymatic reactions, thus preventing oxidation of biomolecules. The mechanism of direct GSH reactions with carbon centered radicals ($R^{\bullet}$) is the following (Winterbourn, 1993):

$$R^{\bullet} + GSH \rightarrow RH + GS^{\bullet}$$

$$GS^{\bullet} + GS^{-} \rightarrow GSSG^{\bullet -}$$

$GSSG^{\bullet -} + O_2 \rightarrow GSSG + O_2^{\bullet -}$

$2\ O_2^{\bullet -} + 2H^+ \rightarrow H_2O_2 + O_2$ (catalyzed by SOD)

In this so-called 'free radical sink', GSH operates together with superoxide dismutase (SOD, E.C. 1.15.1.1) to produce species which are less reactive and not being radicals. It has been also proved that GSH reacts directly with superoxide anion, hydroxyl radical, singlet oxygen, protein- or DNA-radicals. On the other hand, GSH reacts indirectly with hydroperoxides being a substrate for selenoproteins GSH peroxidases (GSHPx, E.C. 1.11.1.9) as follows:

$H_2O_2 + 2\ GSH \rightarrow 2\ H_2O + GSSG$ (catalyzed by GSHPx)

$ROOH + 2GSH \rightarrow ROH + GSSG + H_2O$ (catalyzed by GSHPx)

These reactions are recognized as the predominant cellular mechanism for reduction of hydrogen peroxide and lipid hydroperoxides (Dickinson & Forman, 2002). GSSG is then reduced to GSH by NADPH through the GSH reductase activity (E.C. 1.6.4.2).

The cellular content of GSH and the ratio GSH/GSSG are responsive to many different environmental factors. Under conditions of oxidative stress, GSH is consumed in the first cellular response by scavenging free radicals, while GSSG level increases. That is why, GSH and the GSH/GSSG ratio are considered as sensitive indicators of oxidative stress. Moreover, due to very low redox potential, high concentration in cells and the fact that its reduced state is maintained by GSH reductase, GSH is regarded as main cellular redox buffer.

Furthermore, GSH is involved in a reversible post-translational modification of proteins by oxidation consisting of the formation of a mixed disulfide bond between a cysteine residue on a protein and the GSH molecule. This process, so-called S-glutathionylation, similarly to phosphorylation, can act as a mechanism of regulation of the cellular functions of many important proteins by modulating their activity, either positively (activation) or negatively (inhibition), but it can also protect protein thiols from irreversible inactivation by oxidants during oxidative stress (Rouhier*, et al.*, 2008). It has already been identified approximately 150 different protein targets (e.g. enzymes, receptors, transport proteins, and transcription factors) regulated by S-glutathionylation. However, the precise mechanism of S-glutathionylation and its control still remain unknown (Mieyal*, et al.*, 2008). The reverse reactions consisting in disulfide bond reduction, controlled by thioredoxins and glutaredoxins, play an important role in redox signaling together with GSH/GSSG system (Michelet*, et al.*, 2006).

Moreover, GSH, being a nucleophile, can react with many electrophiles including endogenous compounds and xenobiotics *via* either a direct reaction or reaction catalyzed by a

GSH transferase (GST). In this way, depending on a substrate, GSH forms thioether or thioesther conjugates and mercaptides with metals (Franco, *et al.*, 2007). It is now well established that GSH and GST play a crucial role in phase II of detoxification process leading to the conversion of lipophilic, non-polar xenobiotics into more water-soluble and therefore less toxic metabolites, which can then be eliminated easily from the cell/body. What is more, conjugation of electrophiles to GSH, which initiates the formation of mercapturates, is quantitatively the major phase II detoxification reaction in many species, but it is also an essential aspect of normal physiological metabolism (Sheehan, *et al.*, 2001). The binding of GSH to endogenous compounds serves to regulate their activity, facilitate their membrane transport and elimination from the cell and organism, and result in the formation of important intermediates (Franco, *et al.*, 2007). In this manner, GSH participates in metabolism of some important molecules such as estrogens, prostaglandins and leukotrienes.

Adequate GSH concentrations are also necessary, e.g. for the regeneration of reduced ascorbate, proliferation of cells, conversion of methylglyoxal to D-lactate in the glyoxalase system, cytokine production, spermatogenesis and sperm maturation (Wu, *et al.*, 2004). Interestingly, both *in vitro* and *in vivo* data suggest that GSH inhibits infection by the influenza virus (Cai, *et al.*, 2003).

Moreover, in microorganisms, GSH can be involved in some specific processes such as yeast-to-mycelium transition in *Candida albicans* (Thomas, *et al.*, 1991) or regulation of intracellular level of potassium, whose transport and accumulation play a main role in maintenance of cell turgor and pH homeostasis, or adaptation to various oxidative stresses in bacteria (Smirnova & Oktyabrsky, 2005). As an example of the latter, Saby *et al*. (1999) have demonstrated that high oxygenation or starvation of the wild-type *Escherichia coli* strain shifts GSH homeostasis towards higher concentration of GSH and increases resistance to chlorine. It has been concluded that GSH could protect bacteria against other disinfectants, such as chloramines, H_2O_2 and ozone, by acting as an oxidant scavenger and activator of defense system, which could make the drinking water disinfection process less effective (Saby, *et al.*, 1999).

2.1.3. Significance of glutathione in medicine and pharmacy

Alterations in GSH/GSSG homeostasis and in GSH-dependent enzymes or processes have been widely reported to be correlated with several human diseases. Most of these

pathological conditions are associated with depletion of GSH content which can lead to the progression of cellular death and cytotoxicity. GSH depletion has been shown to either predispose cells to apoptosis or directly trigger cell death in response to different apoptotic stimuli such as ROS generation (Franco*, et al.*, 2007). However, protective effect of GSH in preventing cell death in the absence of any ROS formation is also observed (Deas*, et al.*, 1997). Hence, the precise mechanism of apoptosis modulation by GSH still remains elusive. Nevertheless, shifting the GSH/GSSG redox toward the oxidizing state activates several signaling pathways, thereby progressing the pathogenesis of many diseases including cancer, neurodegenerative diseases (Alzheimer's disease, Parkinson's disease), HIV, AIDS, inflammation, kwashiorkor, liver disease, cystic fibrosis, infection, heart attack, stroke, ischemia, and metabolic diseases (diabetes, obesity) (Wu*, et al.*, 2004, Franco*, et al.*, 2007). On the other hand, in carcinogenous cells, high intracellular GSH concentrations associated with increased expression of GST and GSH-transporters are responsible for resistance to anticancer drugs (Franco*, et al.*, 2007).

By its extraordinary antioxidant properties, GSH belongs to the group of molecules looking for clinical applicability. Since GSH deficiency is due to an aberration in efflux rather than synthesis, supplementation with GSH is desirable rather than the use of GSH precursors (Townsend*, et al.*, 2003). As is the case of peptide and protein drugs, the clinical use of GSH is limited only to parenteral administration for approved indications such as the treatment of alcohol and drug poisoning and protection against toxicity induced by cytotoxic chemotherapy, radiation trauma, or AIDS-associated cachexia. Nevertheless, rapid enzymatic degradation brings the GSH plasma concentration to negligible levels within a few minutes after intravenous (iv) administration of high GSH doses (Trapani*, et al.*, 2007).

Therefore, the development of dosage forms enabling GSH administration by alternative routes (such as oral or pulmonary) may provide increased clinical value to GSH. Due to GSH stability and uptake, inhalation methods appear quite promising. GSH in the epithelial lining fluid (ELF) of the lower respiratory tract is thought to be the first line of defense against oxidative stress involved in many respiratory tract diseases. Inhalation is the only known method that increases GSH levels in the ELF and exhibits the effectiveness for the treatment of several pulmonary diseases (Prousky, 2008).

To assess the feasibility of supplementing oral GSH, Witschi *et al.* (1992) have determined the systemic availability of GSH in 7 healthy volunteers. However, after a single GSH dose of 3 g, the concentrations of GSH, cysteine, and glutamate in plasma did not increase significantly, suggesting that the systemic availability of GSH is negligible in man.

Because of hydrolysis of GSH by intestinal enzymes, it is not possible to increase circulating GSH to a clinically beneficial extent by the oral administration of GSH (Witschi*, et al.*, 1992).

In order to be administered by the oral route, GSH needs to be protected against both chemical (risk of oxidation of GSH to GSSG) and enzymatic hydrolysis during gastrointestinal transit. There have been only a few studies with oral GSH. In the work of Gate *et al.* (2001), GSH was incorporated into liposomes and GSH-loaded liposomes restored intracellular GSH in cells previously treated with buthionine sulphoximine (BSO), which is a γ-glutamylcysteine synthase inhibitor (Gate*, et al.*, 2001). On the other hand, Trapani *et al.* (2007) have encapsulated GSH alone or in combination with hydroxypropyl-β-cyclodextrin in Eudragit RS 100 - based microparticles by an emulsification solvent evaporation method and evaluated this delivery system for an oral administration. In their report, it has been suggested that the system could be useful for the oral administration of GSH based on the *in vitro* enzymatic stability and frog intestinal permeability studies (Trapani*, et al.*, 2007). Nevertheless, this GSH delivery system was not tested in animals.

From a pharmaceutical technology standpoint, it is worthy of note that GSH is able to act itself as a permeation enhancer by inhibition of protein tyrosine phosphatase activity *via* a disulfide bond formation. In this way, the tight junctions of the intestinal epithelium become open and paracellular permeability increases for hydrophilic macromolecular drugs (Bernkop-Schnurch*, et al.*, 2003). Since GSH can be rapidly oxidized to GSSG on the surface of epithelial cells, better results have been obtained with the use of thiomer/GSH system. In this system, a thiolated polymer (thiomer) cooperates by reducing GSSG and remaining for a prolonged period of time at the site of absorption because of its mucoadhesive properties. The potential usefulness of this system is already supported by *in vitro* and *in vivo* studies e.g. for calcitonin, insulin or heparin (Clausen*, et al.*, 2002, Bernkop-Schnurch*, et al.*, 2003).

2.1.4. Analytical methods for glutathione detection and determination

High constant interest in the determination of the glutathione status (concentration of GSH, GSSG and other oxidized forms, and the ratio GSH/GSSG) in various cells, tissues and organs is related to the role of GSH in respect with its biochemical, physiological, toxicological and clinical aspects. As mentioned above, glutathione status constitutes a dynamic equilibrium between GSH synthesis, catabolism, transport, oxidation and reduction depending on cellular state and environmental conditions. Changes in glutathione status occur

under both normal physiological situations and stresses, or result from genetic defects (e.g. *E. coli* mutants in genes encoding enzymes of GSH metabolism) or the action of some chemicals (e.g. BSO) (Smirnova & Oktyabrsky, 2005).

Generally, GSH is found in cells in high concentrations up to 10 mM in most cells. However, GSH concentration in human plasma is relatively low (~ 0.01 mM), because of its rapid catabolism (Franco*, et al.*, 2007). Consistent with the function as an antioxidant and detoxifier, GSH concentrations are particularly high in the liver (~ 10 mM), which is frequently exposed to xenobiotics, but also high concentrations can be found in the kidney, lungs and intestine. The GSH/GSSG ratio, which is often used as an indicator of the cellular redox state, is above 10 under normal physiological conditions in mammalian cells (Wu*, et al.*, 2004). In microbial and plant cells, GSH is present with concentrations in the milimolar range as well. In *E. coli* cells, the ratio GSH/GSSG is very high and comes to 300-600 in cytoplasm. Interestingly, the extracellular concentration of GSH in the growth medium can be controlled by cells and modulated depending on bacterial growth conditions and phase, thus the extracellular GSH can probably play a role in physiology of bacteria (Smirnova & Oktyabrsky, 2005).

Since GSH is present in relatively high concentrations, sensitivity of quantitative analytical methods should not be critical for measurement of physiological GSH levels. However, high sensitivity is important when inhibitors of GSH synthesis are used or when determined in extracellular fluids. On the other hand, specificity (discrimination of GSH from other thiols present in cells) or selectivity (separation of GSH from possible interfering molecules in matrices) are required for an accurate GSH determination. In the case of GSSG, the method should always be very sensitive if measured in cells and extracellular compartments because of low concentrations of this compound (Camera & Picardo, 2002).

Many analytical tools are available for the analysis of GSH including non-separative spectrometric techniques, such as spectrophotometry, spectrofluorimetry, and a wide variety of separative methods (high performance liquid chromatography - HPLC, capillary electrophoresis - CE) allowing to measure GSH in different fluids such as cellular or tissue extracts, body fluids or microbial growth medium. Regardless of the method, in order to minimize oxidation and proteolysis of GSH during the sample handling, special precautions must be always taken (maintenance of pH below 7, refrigeration, protein precipitation by acidification) (Camera & Picardo, 2002).

Direct determination of GSH molecule with ultraviolet (UV) detection is possible, but highly devoid of sensitivity. Therefore, most of analytical approaches developed to assay

GSH involves chemical derivatization of GSH followed by quantitation of the obtained adduct using an appropriate detection system. Incidentally, chromatographic and electrophoretic methods coupled with electrochemical detector or mass spectrometry (MS) enables very sensitive and specific GSH measurement without derivatization process. It is important to mention that common spectrometric, chromatographic and electrophoretic techniques typically measure the average concentration of GSH in a cell population after preparation of cell homogenates (GSH or tGSH level averaged across all cellular compartments). That is why, *in situ* techniques, such as fluorescence microscopy or flow cytometry (FC), have been developed in response to the need to analyze GSH in individual cells or in a specific cellular compartments.

As known, a derivatization reagent (label, dye, stain) introduces an appropriate tag (chromophore, fluorophore) into a molecule in order to permit its analysis with better detectability or separation properties. A good derivatization reagent should quickly and specifically react with the molecule and does not contribute to the matrix interference reactions and loss of sample during the reaction or does not require removing its excess prior to analysis. The obtained derivative must be relatively stable. In HPLC systems, this reaction can be applied as a pre-column or post-coulmn derivatization. However, derivatization process is an additional, often time-consuming step in sample preparation and the process can lead to varying and incomplete recovery of GSH (Rahman*, et al.*, 2006). In the GSH molecule, the thiol moiety is susceptible to derivatization and preferred for its specificity compared to free carboxylic and amino functional groups present in this molecule (Camera & Picardo, 2002). Many derivatization reagents for GSH are available and their use has been already broadly described in the literature (Shimada & Mitamura, 1994). Nevertheless, a classical spectrophotometric assay with the use of 5',5'-dithiobis(2-nitrobenzoic acid) (so-called Ellman's reagent) and its modification (enzymatic recycling method) are until today widely used and have been accepted as routine for the determination of GSH in biological fluids like blood (Rahman*, et al.*, 2006).

Most methods devoted to the measurement of GSH rely upon separative techniques like HPLC and CE (Shimada & Mitamura, 1994, Camera & Picardo, 2002). Chromatographic methods provide high degree of specificity and low detection levels, however, they imply time consuming handling, and are expensive and not readily available in most clinical laboratories. The enzymatic spectrophotometric assays are laborious and complicated. Spectrofluorimetric method is widely used in the field of biological science for its sensitivity and low cost, but, as a matter of fact, a required derivatization process needs an additional

sample treatment. Moreover, all the techniques mentioned above are mostly characterized by a low sample throughput due to the sequential mode of analytical runs. However, a non-separative technique with a high sample throughput (fluorescence assay using the universal 96-well microplate format for the measurement of GSH in cells) have been also developed (Lewicki*, et al.*, 2006). Nevertheless, new trends in the development of methods devoted to GSH monitoring are focused on its fluorescence labeling in living cells to allow GSH localization and/or determination using e.g. FC and confocal microscopy (*in situ* techniques). Therefore, there is a need for the development of GSH-selective fluorogenic or fluorescent probes.

2.1.5. *In situ* methods for glutathione and glutathione redox state imaging

Fluorescence imaging has been widely used in the life sciences for investigation of many cellular processes as it offers nanometer-scale resolution, fast, sensitive, reliable, and reproducible detection of ions, biomolecules and organelles in cells (Santra*, et al.*, 2004, Resch-Genger*, et al.*, 2008). However, the potential of a detection or imagining method is to a great extent determined by the properties of the probe used. Such a probe is a tag molecule designed to detect a particular component within a specific region of a biological specimen (including whole intact live cells, tissues) with adequate sensitivity and selectivity. To be suitable for these techniques, the probe must (a) be excitable without simultaneous excitation of the biological sample; (b) be detectable with conventional instrumentation; (c) posses a high molar absorption coefficient at the excitation wavelength; and (d) posses a high fluorescence quantum yield. Additionally, an ideal probe must exhibit non-toxicity, water solubility, stability, ability to penetrate intact cells, high reaction rate at neutral pH, and its adduct with a target molecule must have sufficient photostability (Resch-Genger*, et al.*, 2008). A fluorescence probe is already a fluorophore, while a fluorogenic probe natively does not fluoresce, but forms a fluorescent adduct with a target molecule.

Owing to *in situ* methods, the target of a fluorescence probe can be localized in cells if examined under a fluorescence microscope. Whereas, application of fluorescence probes to cells followed by FC analysis allows subpopulations within a large sample to be identified and quantitated. Additionally, these *in situ* techniques even enable multicolor labeling experiments of cellular or subcellular components when simultaneously introduced two or more probes (Haugland, 2005). Some of reagents for GSH derivatization reacting with a thiol

group are also useful as probes for GSH fluorescence imaging by means of *in situ* techniques. Fluorescent probes reported in the literature for *in situ* GSH imaging can be categorized into 3 major types: organic fluorogenic or fluorescent dyes, fluorophores of biological origin like genetically encoded fluorescent proteins and fluorescent nanoparticle probes (Wang*, et al.*, 2006).

2.1.5.1. Organic fluorogenic or fluorescent probes for glutathione

A wide variety of thiol-reactive probes is available and used to label various cellular peptides, proteins and thiolated oligonucleotides for investigating their biological structure, function and interactions. The common thiol-reactive probes form with sulfhydryls chemically stable thioethers, e.g. maleimide dyes which are not appreciably fluorescent until after conjugation with thiols (Figure 4). On the other hand, there are thiol-reactive probes that have a structure of symmetric disulfide and undergo a thiol-disulfide interchange reaction to yield a new asymmetric disulfide. Reaction of most probes with thiols proceeds rapidly at room temperature in the physiological pH range (Haugland, 2005).

Figure 4. Reaction scheme of a maleimide with a thiol to form a thioether (adopted from Haugland, 2005).

The general division of thiol-reactive probes into probes excited with visible light or UV light is used since such probes have very different chemical structures and reactive groups. In the class of the organic dyes excited with visible light, there are probes having visible absorption maxima beyond 410 nm, such as the Alexa Fluor, BODIPY, fluorescein and rhodamine derivatives. Then, the thiol-reactive probes exited with UV light have peak absorption below 410 nm, e.g. coumarin, naphthalene derivatives, dansyl aziridine and bimanes. Typically, UV light-excitable dyes exhibit blue fluorescence and less photostability than that of visible light-excitable dyes (Haugland, 2005).

Additionally, the fluorescent probes for GSH are categorized into GST-dependent and GST-independent probes. In both cases, adducts are formed between the dye and the sulfydryl group of GSH, resulting in a dramatic increase in fluorescence intensity and/or altered

excitation/emission spectral properties of the dye. More specifically, GST-independent probes (non selective probes) react directly (non enzymatically) with the thiol group of GSH, e.g. monobromobimane (MBB), N-(1-pyrene)maleimide, BODIPY® maleimides (Haugland, 2005), and aromatic dialdehydic probes. The major weak point of these probes is a serious possibility of occurrence of side reactions with intracellular thiols other than GSH, such as low molecular weight compounds, e.g. cysteine, γ-GluCys and protein sulfydryls, often resulting in high levels of background fluorescence. However, GST-dependent probes for GSH (GSH selective or specific probes) contain a chloromethyl group and the formation of an adduct between the GSH molecule and a dye molecule is catalyzed by GST. Due to the fact that this binding is only possible in presence of GST, it has been conferred a high degree of specificity of these dyes to GSH with very low background labeling (Tauskela*, et al.*, 2000). The following are examples of GST-dependent probes: monochlorobimane (MCB), 5-chloromethylfluorescein diacetate and 7-amino-4-chloromethylcoumarin.

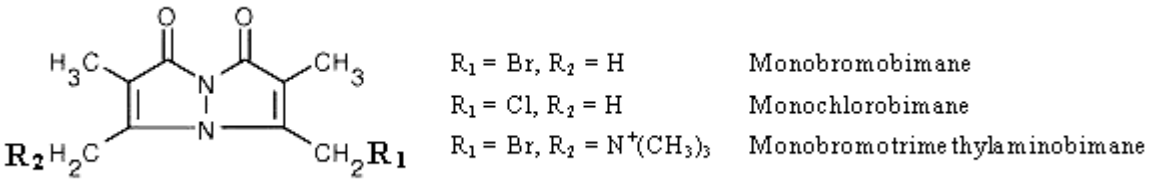

Figure 5. The structure of bimanes.

Of these, bimanes, derivatives of 1,5-diazabicyclo(3.3.0)octadiendione, are the important class of GSH probes (Figure 5). They are essentially non fluorescent, but react rapidly with thiols at pH 8.0 to produce thioethers characterized by a strong blue fluorescence. Apart from MCB and MBB, there is also a monobromotrimethylaminobimane (Figure 5) which serves for labeling of extracellular thiols and dead or permeabilized cells (Bellomo*, et al.*, 1997). MCB is cell-permeant, highly selective for GSH, and has long been widely used for visualization of intracellular distribution and fate of GSH and GSH conjugates in living cells (Bellomo*, et al.*, 1997), or for quantitating GSH levels and measuring GST activity (Barhoumi*, et al.*, 1995). However, major drawbacks to using GST-dependent probes result from: (a) existence of several GST isoenzymes with different abilities to catalyze adduct formation, i.e. different specificities for probes; (b) heterogeneous distribution of GST isoenzymes in different tissues and within different intracellular compartments; (c) low expression levels and GST activities in some cell types; (d) feedback inhibition by the adduct

on GST activity (Orwar, *et al.*, 1995, Tauskela, *et al.*, 2000). However, in the case of MCB, the isoenzymes of GST present in most human cell lines have a low affinity for MCB and GSH is incompletely labeled. Therefore, it has been reported that MBB is an alternative dye for human cells, because it reacts non enzymatically but less selectively with GSH than does MCB (Ublacker, *et al.*, 1991, Hedley & Chow, 1994).

In conclusion, in order to choose an optimal probe for use in given cells many factors must be taken into consideration, including cell type, dye properties, transport of the fluorescent adduct out of the cell, decomposition to other fluorescent products, experimental conditions such as dye concentration, loading time, temperature, and so on (Barhoumi, *et al.*, 1995, Tauskela, *et al.*, 2000). A useful strategy is to test several GSH sensitive dyes, both those requiring GST activity, and GST-independent probes, under controlled experimental conditions in which GSH is depleted (Tauskela, *et al.*, 2000).

The next group of GSH organic probes is the group of aromatic dialdehydes including *ortho*-phthaldialdehyde (OPA) and naphthalene-2,3-dicarboxaldehyde (NDA). They have been extensively used in HPLC or CE techniques as derivatizing reagents for the analysis of various amines, polyamines, amino acids, peptides, endo- and exogenous amino group containing compounds. With regard to HPLC method, OPA and NDA have been applied either in precolumn or postcolumn derivatization (for review, see Kutlan, *et al.*, 2002, Rammouz, *et al.*, 2007). To determine primary amines as their OPA derivatives, the reaction must be carried out in the presence of a SH group containing nucleophile (co-reagent), e.g. 2-mercaptoetahnol, N-acetylcysteine, 3-mercaptopropionic acid, or ethanethiol (Kawamura, *et al.*, 2000, Kutlan, *et al.*, 2002, Hanczko, *et al.*, 2007). NDA has been known to react with primary amines in the presence of cyanide ion to produce N-2-substituted 1-cynobenz-[*f*]-isoindole derivatives (Rammouz, *et al.*, 2007, Lamba, *et al.*, 2008).

In the case of a heterobifunctional analyte, such as GSH containing both an amino and a thiol group, OPA and NDA are used without co-reagent. Since two functional groups of GSH are involved in the reaction, these probes are highly specific for GSH. OPA and NDA are reagents that do not intrinsically fluoresce, but together with a sulfhydryl and a primary amino group of the GSH molecule, they produce highly fluorescent isoindole adducts (OPA-GSH, NDA-GSH) (Figure 6). The fluorescence spectrum of the OPA-GSH adduct (λ_{ex}= *ca.* 350 nm, λ_{em}= *ca.* 420 nm – green fluorescence) is shifted from those of protein adducts (λ_{ex}= *ca.* 350 nm, λ_{em}= *ca.* 405 nm – blue fluorescence) which permits distinction between GSH and protein fluorescence by FC (Treumer & Valet, 1986). Unlike OPA, NDA does not require UV excitation, and therefore is suitable for the flow cytometers and confocal microscopes in

most laboratories that use the 488 nm line of an argon laser. Moreover, NDA derivatives are typically more stable than the OPA-derivatives, and, as mentioned above, they are excited in the visible spectrum (λ_{ex}= *ca.* 400-470 nm, λ_{em}= *ca.* 490-530 nm) and exhibit higher fluorescence quantum yields (Manica*, et al.*, 2003).

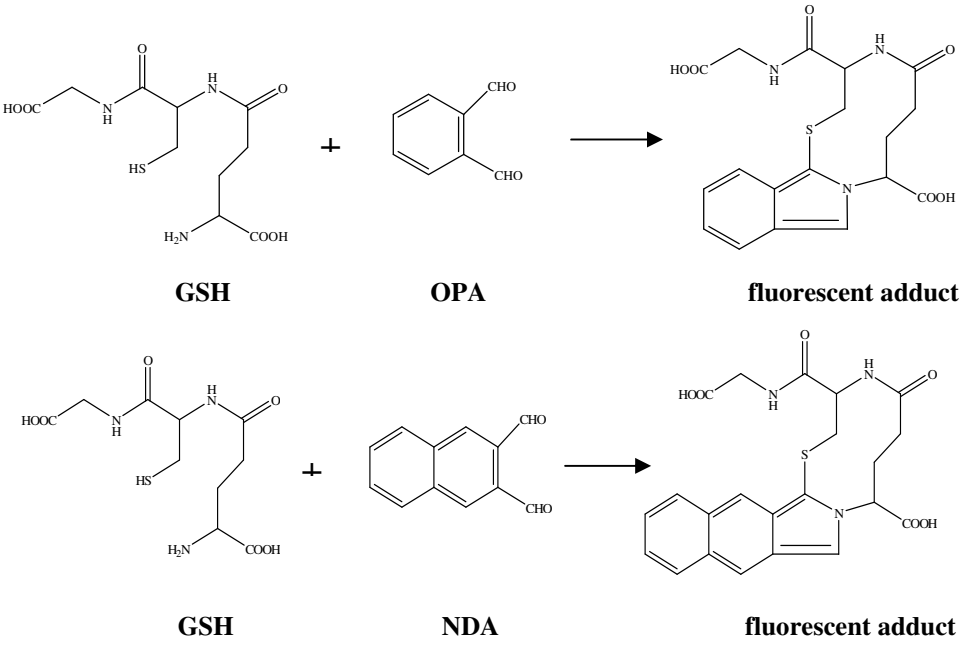

Figure 6. Scheme of derivatization reaction of OPA and NDA with GSH.

A large number of applications has been already described in the literature on the use of OPA or NDA for measuring variations of GSH concentrations under physiological conditions, during oxidative stress or after exposure to BSO in different samples (mammalian cells, cellular extracts, plasma, tissue homogenates) using HPLC (Leroy*, et al.*, 1993, Paroni*, et al.*, 1995, Lenton*, et al.*, 1999, Cereser*, et al.*, 2001, Dziurla*, et al.*, 2004, Diez*, et al.*, 2005), CE (Orwar*, et al.*, 1995, Parmentier*, et al.*, 1999, Qin*, et al.*, 2005), FC techniques (Treumer & Valet, 1986, Hedley & Chow, 1994), or a microplate assay to measure GSH derivatized with NDA (Lewicki*, et al.*, 2006). Interestingly, OPA has also been demonstrated to be bactericidal by interacting with primary amino groups of the microbial cell wall (Simons*, et al.*, 2000, Akamatsu*, et al.*, 2005).

Generally, organic dyes are the earliest class of fluorescent probes, and they are still widely used because of their small size, water solubility, ease of usage, the existence of standard protocols, and low cost (Wang*, et al.*, 2006). However, they are some limitations in their use such as susceptibility to photobleaching under a powerful excitation source (laser) or lack of stability in the cellular environment causing changes in photophysical and

photochemical behavior. The disadvantage of organic dyes is also having a narrow excitation and broad emission spectra. Thus, the ultrasensitive detection of biomolecules and real-time analysis of biological processes is almost not possible with organic dyes (Santra*, et al.*, 2004).

2.1.5.2. Redox-sensitive fluorescent proteins

The most important member of the fluorescent protein family is a green fluorescent protein (GFP). The wild type GFP, originally isolated from the jellyfish *Aequorea victoria,* emits green fluorescence under light excitation, requiring no exogenously added proteins, substrates or co-factors, in contrast to other bioluminescence systems. The absorbance and fluorescence of GFP stem from a 4-(*p*-hydroxybenzylidene)-5-imidazolinone fluorophore, which is formed by the post-translational intramolecular cyclization of the amino acid sequence at positions 65–67 (serine, tyrosine and glycine, respectively) followed by oxidation of the tyrosine side chain by oxygen (Figure 7). The fluorophore is located in the center of the GFP β-barrel, thus protected from the bulk solvent (Schultz, 2009).

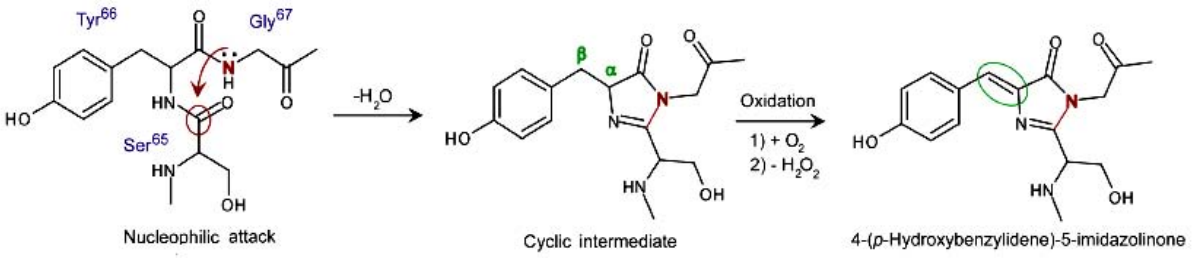

Figure 7. Mechanism of the GFP fluorophore formation (adopted from Schultz, 2009).

Introduction of certain mutations in the fluorophore of the wild type GFP yielded variants, such as blue, cyan or yellow fluorescent proteins, with improved properties that stimulated the widespread use of fluorescent proteins. The currently known GFP variants may be divided into seven classes based on the distinctive component of their fluorophores. Each class has a distinct set of excitation and emission wavelengths (Wang*, et al.*, 2006). GFPs have been used as tools in numerous applications. Initially, GFP was used to track protein localization and monitor gene expression by producing GFP fused to the protein of interest or by placing GFP under the control of a promoter of interest. Using genetic engineering, GFP and its variants can be fused as tags to any protein of interest often without altering the function of the protein in living cells. Chimeric GFP fusions have the advantage that they can be expressed *in situ* by gene transfection. The resulting chimera often retains parent protein

targeting and function when expressed in cells (Schultz, 2009). Moreover, GFP has made real-time imaging in living cells a common technique. Fluorescence proteins were also used as probes to monitor protein–protein interactions by a method called bimolecular fluorescence complementation (Kerppola, 2006). However, there is always a possibility that GFP may interfere with the expression and properties of the labeled protein or dimerize with neighboring fluorescent proteins inside the cells (Schultz, 2009).

Recently, genetically encoded probes based on fluorescent proteins have been applied for the measurement of the spatiotemporal intracellular redox changes within cellular compartments. These redox-sensitive GFP-based biosensors are engineered by inserting an additional dithiol-disulfide pair into the protein barrel. The two cysteine residues are sufficiently close to form a disulfide bridge depending on the redox-environment of the protein. Formation or release of this disulfide bridge then leads to slight conformational changes in the protein barrel and alters the protonation state of the fluorophore. This change in protonation leads to a change in the absorption properties, and hence in a change of fluorescence (Gutscher*, et al.*, 2008, Schwarzlander*, et al.*, 2008). In the case of yellow fluorescence protein, the introduction of a pair of cysteine residues confers reversible redox-dependent changes in fluorescence intensity, but no shift in either the excitation or emission spectrum. By contrast, the oxidized and reduced forms of GFPs are preferentially excited at two different wavelengths, facilitating quantitative ratiometric imaging of redox dynamics (Schwarzlander*, et al.*, 2008). In the study of Schwarzlander *et al.* (2008) two redox-sensitive GFPs were expressed in different subcellular compartments of *Arabidopsis* and tobacco leaves to determine their performance as redox sensors for confocal imaging *in planta*. Both GFPs consistently indicated redox potentials of about –320 mV in the cytosol and –360 mV in the mitochondria. The only oxidizing compartment was the lumen of the endoplasmic reticulum, in which GFP was almost completely oxidized (Schwarzlander*, et al.*, 2008). However, the usefulness of redox-sensitive GFPs could be limited by slow response to changes in redox potential and undefined specificity due the poor evidence of which endogenous cellular redox system interact with GFP. That is why, Gutscher *et al.* (2008) demonstrate that the fusion of glutaredoxin to GFP facilitates specific real-time equilibration between the sensor protein and the glutathione redox couple. The fusion protein allowed dynamic live imaging of the GSH redox potential in different cellular compartments with high sensitivity and temporal resolution. The biosensor detected nanomolar changes in GSSG against a backdrop of millimolar GSH on a scale of seconds to minutes (Gutscher*, et al.*, 2008). Previously, Ostergaard *et al.* (2004) determined the cytosolic glutathione redox status

to be –289 mV using a genetically encoded probe (yellow fluorescent protein) in yeast (Ostergaard, *et al.*, 2004).

Since genetically encoded GFPs are made by the cells itself, the problems of low membrane permeability of the probe and cytotoxicity have been overcome (Schultz, 2009). Moreover GFPs have only minimal photobleaching allowing the performance of long term measurements, however a drawback of GFP family is its low emission wavelength, which could overlap with the cellular autofluorescence (Sharma, *et al.*, 2006).

2.1.5.3. Fluorescence nanoparticle probes

Recently, a growing number of papers has reported the development and application of various types of nanoparticles, roughly divided into organic and inorganic ones, for the labeling, imaging and analysis of biomolecules (Riegler & Nann, 2004, Santra, *et al.*, 2004, Sharma, *et al.*, 2006, Wang, *et al.*, 2006).

For instance, Wang *et al.* (2005) described the applicability of a highly sensitive method with organic nanoparticles as fluorescence probe for the quantification of GSH. They prepared and characterized water-soluble fluorescent 1-pyrenemethylamine nanoparticles. These nanoparticles had approximately 25 nm in diameter and a good colloidal stability. In the presence of OPA, the primary amino groups of 1-pyrenemethylamine nanoparticles reacted with GSH at pH 9.0 and formed a highly fluorescent derivative with a longer emission wavelength compared to nanoparticles and limit of GSH detection of 0.071 μM. Though, the influence of some potentially interfering substances on the determination of GSH was studied, the method had not been applied for GSH measurement in biological samples (Wang, *et al.*, 2005).

Another approach in the study of the subcellular distribution of GSH is the immunocytochemical detection of GSH by transmission electron microscopy (TEM). This became possible with the use of an immunogold labeling method. In this method, the samples are first treated with the primary antibody against glutathione, then anti-glutathione rabbit polyclonal immunoglobulin G, and finally incubated with the secondary antibody, goat anti-rabbit immunoglobulin G conjugated to 10 nm-diameter colloidal gold particles. The primary antibody does not discriminate between GSH and GSSG, hence, the labeling within the cells reflects tGSH content. As a result, gold particles are indirectly bound to GSH and their density in cell compartments is investigated by TEM. With reference to GSH, the use of this technique was described by the group of Muller *et al.* for the investigation of the GSH

distribution in cells of *Cucurbita* (Muller*, et al.*, 2004, Zechmann*, et al.*, 2006) or *Arabidopsis* (Zechmann*, et al.*, 2008). In another report, the authors have compared the above immunogold labeling/TEM method with an HPLC assay studying the subcellular changes in tGSH content during virus infection in *Cucurbita*. It has been concluded that during infection local increases in tGSH contents can occur in intact cells and can be detected by immunogold labeling, but it will not be detected if a homogenate of a whole or parts of a leaf is investigated by HPLC (Zechmann*, et al.*, 2005). A more advanced technology is the combination of ultrasmall gold nanoparticles and a fluorescence dye into a single probe for imaging a specimen both by fluorescence and electron microscopy (e.g. FluoroNanogold® - combination of the Monomaleimido Nanogold® and fluorescein) (Takizawa & Robinson, 2000).

Gold nanoparticles were also used by Lu *et al.* (2007). They have developed a new postcolumn colorimetric detection method for HPLC assay of GSH and other low molecular weight biothiols (cysteine, homocysteine, cysteinylglycine, γ-GluCys) based on the analyte-induced aggregation of the colloidal Brij®-capped gold nanoparticles with average diameters of 12 nm. Compared with conventional thiol-reactive probes, the gold nanoparticles colloids are much more stable in aqueous solution over a wide pH range and exhibit relatively high selectivity toward small biothiols (Lu*, et al.*, 2007). Next, gold nanoparticles were used by Tseng *et al*. (2005) to locate GSH and determine its concentration within individual human erythrocyte cells. The cells were loaded with an aqueous solution of Nile Red-adsorbed 32-nm gold nanoparticles, and when the Nile Red product is displaced by GSH on the gold nanoparticles surface, the fluorescence of the solution increases and the gold nanoparticles aggregate. The microscopic images clearly indicated the location of GSH inside erythrocytes and were supported by images recorded using NDA as a probe. Moreover, the average GSH concentration in a single erythrocyte cell was determined to be *ca.* 1.3 mM by microscopic fluorescence measurements in intact cells and by CE measurements in conjunction with laser-induced fluorescence (as a reference method) in lysed erythrocytes. In both measurements, Nile Red-adsorbed gold nanoparticles and NDA were used for GSH labeling and similar results were obtained (Tseng*, et al.*, 2005). Furthermore, gold nanoparticle-based monitoring of the reduction of GSSG to GSH has been proposed by He *et al.* (2007). In this paper, combination of an organic fluorophore (perylene bisimide derivative) and gold nanoparticles was produced. However, as a photoluminescent quencher, gold nanoparticles highly efficiently quenched the fluorescence of the organic component in the composite. After the reduction of GSSG by GSH reductase, GSH could displace the organic component from the

composite, so that its fluorescence could be recovered. In this way, the fluorescence quenching properties of gold nanoparticles were utilized to monitor the reversion of GSSG to GSH in the presence of GSH reductase, which provides a new concept to measure the balance of glutathione in biological systems (He, *et al.,* 2007). In conclusion to gold nanoparticles, these labels can be almost as small as organic fluorophores, but due to their metallic nature they offer the additional possibility to be imaged with electron microscopy. Since the resolution for electron microscopy is much better than for optical microscopy, biological structures can be visualized with nanometre resolution. Unfortunately, electron microscopy is typically only possible with fixed and thus dead samples. However, many interesting labeling experiments have also been reported in which gold particles have been imaged with optical microscopy. Using gold particles instead of fluorophores circumvents the drawbacks of photobleaching and blinking (Parak*, et al.*, 2005).

Finally, recent literature demonstrates the great potential of quantum dots, new types of fluorescent materials for biological and medical labeling (Gao*, et al.*, 2005, Medintz*, et al.*, 2008). Quantum dots are fluorescent inorganic nanoparticles (semiconductor nanocrystals) with all three dimensions in the 1–10 nm size range, and with unique size-dependent optical and electrical properties due to quantum confinement effect. Since these nanoparticles are inorganic solids (the most often used semiconductor materials are: CdSe, CdS, CdTe, ZnS), they can be expected to be more robust than organic fluorophores (e.g. towards photobleaching) and in addition they can also be observed with high resolution by both fluorescence and electron microscopy. Typically, quantum dots intended for biomedical purposes are of the core-shell type, water soluble and often functionalized with specific ligands (e.g. biotin, folic acid, proteins like avidin or streptavidin, the lectin wheat germ agglutinin, or antibodies) allowing the molecular *in vivo* recognition of the target. There are different strategies for conjugation of quantum dots to biological molecules such as a covalent linkage between functional groups on the quantum dot surface and functional groups of the biological molecule (e.g. thiols), a covalent attachment by means of cross-linker molecules, and finally an attachment *via* the streptavidin–biotin system or adsorption to the hydrophilic shell by electrostatic interaction (Parak*, et al.*, 2005). The following advantages in fluorescence labeling are ascribed to quantum dots, especially when compared to organic dyes (Sharma*, et al.*, 2006):

- Particle size-tunable (so-called quantum size effect) and particle composition-tunable absorption and emission wavelengths (width of the emission band mainly determined by size distribution of quantum dots),

- Large absorption coefficients across a wide spectral range,
- Broad excitation spectra (facilitating the use of a single excitation wavelength that excite quantum dots of different colors) and narrow emission spectra of mostly symmetric shape (possible multiple color labeling due to reduced spectral overlap of multiple fluorophores), thus allowing free selection of the excitation wavelength and straightforward separation of excitation and emission,
- High fluorescence quantum yields and photostability, long lifetimes.

However, there are several limitations associated with the use of quantum dots such as optical blinking, which causes difficulties for quantitative assays, influence of quantum dots on the function of attached ligand molecules, lack of biocompatibility and possible cytotoxicity, thus they have to be surface modified before they are used in live cells or animal experiments. Therefore, quantum dots are only complementary to conventional organic dyes, but they are better suited for multicolor, long-term and high-sensitivity fluorescence imaging and for applications where good photostability is required (Wang, 2006). However, if the issues related to the potential toxicity can be resolved, these materials will have the potential to become valuable tools for medical imaging.

Recently, Clarke *et al.* (2006) have reported the cell-based biosensor based on electron transfer between a small molecule (dopamine) and semiconductor CdSe/ZnS quantum dots. In their study, living cells were labeled with quantum dots - dopamine conjugates in a redox-sensitive pattern: under reducing conditions, fluorescence was only seen in the cell periphery and lysosomes. As the cell was becoming more oxidizing, quantum dots labeling appeared in the perinuclear region. With the most-oxidizing cellular conditions, quantum dots labeling throughout the cell was seen. Cell cultures with different intracellular redox potentials were generated by enhancing GSH level (GSH monoethyl ester makes the cellular environment more reducing) or suppressing GSH synthesis (BSO makes it more oxidizing) (Clarke, *et al.*, 2006). On the other hand, GSH is often conjugated to quantum dots. As an example, such GSH functionalized fluorescent quantum dots were used for staining a freshwater invertebrate called *Hydra vulgaris*. It was demonstrated that these GSH-quantum dots were internalized by endotermal cell layer in *Hydra*, and GSH conjugated to quantum dots retained its biological activity (induction of mouth opening by GSH in *Hydra*) (Tortiglione*, et al.*, 2007).

2.2. Encapsulation of salmon calcitonin

2.2.1. Physiologic action and clinical use of calcitonin

Calcitonin, discovered more that 40 years ago (Copp*, et al.*, 1961), is a natural polypeptide hormone produced and secreted by the parafollicular cells (C-cells) of the thyroid gland in mammals, and in many animals by the ultimobranchial body. Calcitonin is one of the regulators of calcium homeostasis. It counteracts parathyroid hormone, prevents calcium excess and maintains normal calcium blood levels during episodes of calcium stress (e.g. postprandial hypercalcemia, pregnancy). The main factor controlling the calcitonin secretion is the extracellular concentration of ionized calcium, e.g. increased blood calcium levels stimulating calcitonin secretion, and the secretion is suppressed when the calcium level falls below normal. Calcitonin can exert various physiologic effects by binding with calcitonin receptors abundantly distributed on the surface of osteoclasts. There are approximately one million calcitonin receptors per osteoclast (Zaidi*, et al.*, 2002). All calcitonin receptors bind calcitonin peptides with high affinity, according to the general following comparative potency: salmon calcitonin (sCT) > porcine calcitonin > human calcitonin (hCT), and low affinity for the alternative ligands such as amylin, calcitonin-gene related peptide (CGRP) and adrenomedullin (Purdue*, et al.*, 2002).

Predominantly, calcitonin acts on bone metabolism, more specifically, by directly affecting the osteoclasts. Calcitonin inhibits bone resorption, which means protection against calcium release from skeleton, thus indirectly lowering blood calcium level. For this reason, calcitonin has been known and clinically used for many years as an antiresorptive drug for the treatment of osteoporosis, especially a postmenopausal type of osteoporosis. Due to the hypocalcemic activity, it is also used in other disease involving accelerated bone turnover such as Paget's disease and hypercalcemia. However, it should be mentioned that calcitonin is not any more the first drug of choice for the treatment of all these disorders (Karsdal*, et al.*, 2008).

Due to the activation of calcitonin receptors, a series of effects is observed in osteoclasts. Calcitonin reduces the recruitment and activity of these bone-resorbing cells (Plosker & McTavish, 1996). Within a few minutes after receiving calcitonin, secretory activity of osteoclasts ceases, its ruffled borders (active site of bone resorption being a specialized cellular membrane of an osteoclast from which hydrogen ions and proteolytic

enzymes are released) disappear, the cytoplasmic motility decreases and the osteoclast detaches itself from the bone surface (Zaidi*, et al.*, 2002, Ikegame*, et al.*, 2004).

Moreover, the calcitonin receptor was also identified on chondrocytes, and there is experimental evidence, both *in vitro* and *in vivo*, that calcitonin acts on cartilage and subchondral bone (Manicourt*, et al.*, 2005). Due to the positive effects of calcitonin on articular cartilage degradation and pain alleviation, osteoarthritis has arisen as a new potential therapeutic indication for calcitonin (Karsdal*, et al.*, 2007). Data from a clinical trial show that calcitonin is safe and effective in osteoarthritis by reducing cartilage degradation and thereby providing therapeutic benefit in terms of chondroprotection (Bagger*, et al.*, 2005).

Interestingly, calcitonin may interact somehow with osteoblasts despite no convincing evidence for calcitonin receptors on any osteoblast-like cells. However, this interaction is not well understood. Both *in vitro* and *in vivo* data suggest that calcitonin has an anabolic effect on bone (Wallach*, et al.*, 1993). It might promote bone formation through stimulation of osteoblasts (Azria*, et al.*, 1995). In addition, compared to bisphosphonates, calcitonin seems to act in a more physiologic way to counteract excessive bone resorption. The effect of calcitonin is stronger when the osteoclasts are more active, and is more apparent in the trabecular bone than in the cortical bone, which is in alignment with the higher turnover at this site (Karsdal*, et al.*, 2008).

It has been suggested that treatments of osteoporosis with a better effect on bone quality are those that are able to uncouple bone formation and resorption. However, the current antiresorptive drugs (bisphosphonates, raloxifene, denosumab) cause the secondary reduction in bone formation due to coupling between bone resorption and formation (Karsdal*, et al.*, 2008), because bone formation is only limited on resorbed surfaces. With regard to calcitonin, it has been shown that it decreases osteoclast activity, but not osteoclasts number (Ikegame*, et al.*, 2004). Hence, reduction in bone formation in patients treated with calcitonin is either absent or much lower that the reduction in bone resorption. It could be also explained by the fact that calcitonin does not cause a sustained reduction in bone resorption and resorption returns to baseline before additional calcitonin administration. This is in contrast to bisphosphonates that, because of different pharmacokinetic properties, inhibit resorption for longer time periods, and thereby do not allow resorption to return to basal levels, and simultaneously lead to a reduction in bone formation (Karsdal*, et al.*, 2008).

Since the only acceptable endpoint for treatments of osteoporosis is a reduction in the number of fractures in patients, but not an increase in bone mineral density (BMD), the PROOF (Prevent Recurrence of Osteoporotic Fractures) trial has definitely showed that sCT

reduces vertebral fractures (Chesnut III*, et al.*, 2000). In this clinical study in postmenopausal women with osteoporosis, the risk of new vertebral fractures was significantly reduced compared with placebo by 33% when 200 IU of sCT per day was administered intranasally and for up to 5 years. In addition, there was a 36% risk reduction in new vertebral fractures in patients who had one to five previous vertebral fractures. Nevertheless, the reductions in vertebral fractures in the 100-IU and the 400-IU groups were not significantly different from placebo. It was also observed that calcitonin caused a very small increase in BMD (Chesnut III*, et al.*, 2000). As a matter of fact, bisphosphonates and raloxifene have better-proven effectiveness in reducing the risk of fracture (Ettinger*, et al.*, 1999, Harris*, et al.*, 1999). For instance, risedronate, a potent bisphosphonate, decreased the new vertebral fractures by 41% over 3 years, compared with placebo, in postmenopausal women with established osteoporosis at a once daily dose of 5 mg. A fracture reduction of 65% was observed after the first year. The cumulative incidence of non-vertebral fractures over 3 years was reduced by 39%. BMD increased significantly compared with placebo and the therapy during this study seemed to be well tolerated (Harris*, et al.*, 1999).

Furthermore, *in vitro* studies have demonstrated that continuous or repeated administration of calcitonin cause the disappearance of calcitonin ability to inhibit bone resorption and osteoclast activity with time, which was confirmed *in vivo* by a loss of calcitonin ability to decrease blood calcium levels. Mainly in the presence of sustained calcitonin blood levels, calcitonin receptors are downregulated, the effect of calcitonin on osteoclasts diminishes rapidly due to the withdrawal of the receptors, and osteoclast activity escapes the suppressive effects of calcitonin ('escape phenomenon') (Zaidi*, et al.*, 2002, Ikegame*, et al.*, 2004). This is probably related to clinical resistance to calcitonin treatment. Another potential explanation of the resistance is the development of calcitonin antibodies in response to non-human calcitonin administration, but it still remains unclear (Chesnut III*, et al.*, 2008).

The bone is the most important target organ of calcitonin, however, this hormone also acts with a lesser extent on the normal function of the kidney. Pharmacological calcitonin concentrations increase renal calcium and phosphate excretion and 1,25-dihydroxycholecalciferol production (Zaidi*, et al.*, 2002). Furthermore, calcitonin can affect the secretions of the gastrointestinal glands by regulating local calcium concentration (Azria*, et al.*, 1995).

Additionally, calcitonin receptors are found in the central nervous system, especially in zones involved in the control of pain perception. A direct central action is probably

responsible for the analgesic effect of calcitonin, but the exact mechanism is unknown. It is assumed that the analgesic effects of calcitonin are at least to some extent mediated centrally, with serotonergic pathways involved. However, neither a direct receptor-mediated action nor an indirect endorphin-mediated effect can be ruled out. From the clinical point of view, the analgesic effect of calcitonin is beneficial throughout the whole period of treatment, i.e. sCT is effective in pain relief in long-term use and no 'escape phenomenon' occurs. The analgesic action of calcitonin has been formerly confirmed in bone pain associated with acute vertebral fractures, metastatic bone disease, Paget's disease and osteoporosis (Lyritis & Trovas, 2002, Silverman & Azria, 2002). The value of early treatment with calcitonin in order to alleviate pain in the population of osteoporotic patients with an acute vertebral fracture was confirmed in the clinical study, and the pain relieving effects of nasal spray (200 IU/day) and injectable sCT (50 IU/day) were equivalent (Combe*, et al.*, 1997).

2.2.2. Structural properties and stability of calcitonin

Regardless of the origin, calcitonin is a single-chain polypeptide consisting of 32 amino acid residues and having a molecular weight of approximately 3.4 kDa. The following features of the primary structure are typical for all the calcitonin peptides (Figure 8): (a) a disulfide bridge between the cysteine residues in positions 1 and 7 forming a loop of seven amino acid residues at the N-terminal (this region is critical for the agonist activity of calcitonin peptides); (b) an amphiphilic α-helix between amino acids 8 and 22 (maintenance of this α-helical secondary structure is important for high affinity binding to calcitonin receptors); (c) a proline amide group at the C-terminal at position 32 (crucial for peptide activity and absolutely conserved in all species) (Purdue*, et al.*, 2002). In sCT molecule, the presence of the disulphide bridge is not required for full agonist activity, but helix formation in the region 8–16 and the presence of leucine at position 12 appears to be important, at least in part, for the higher affinity of sCT to calcitonin receptors. However, the C-terminal residues 22–32 are the most critical for the higher affinity binding and potency of sCT compared to other calcitonin peptides (Purdue*, et al.*, 2002).

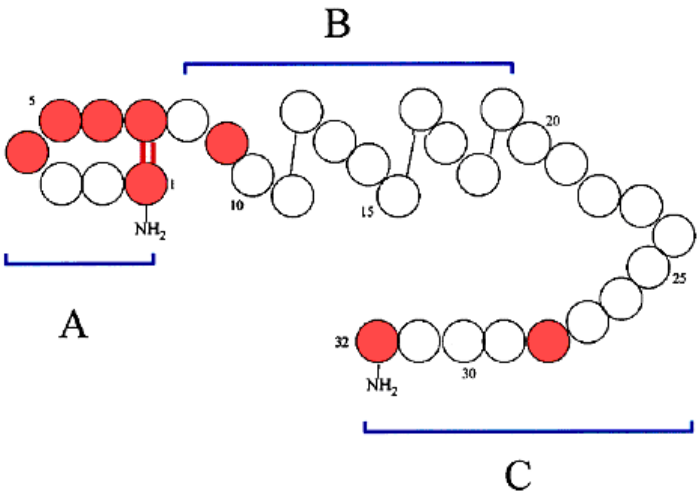

Figure 8. Schematic diagram of the sCT structure: A - a loop bridged by a disulphide bond between cysteines 1 and 7; B - central amino acids forming α-helix; C – the C-terminal residues and the C-terminal proline amide at position 32. Colored residues represent amino acids that are very highly conserved among calcitonin peptides from different species (adopted from Purdue, *et al.*, 2002).

There is a high homology within mammalian calcitonins as well as within fish calcitonins, but significant sequence variation between these two classes, e.g. there are 2 different amino acids in the polypeptide chain between human and rat, but 16 between human and salmon (Table 1). Eight residues are conserved in all species, six of them clustering at the N-terminus (Zaidi, *et al.*, 2002). This suggests that differences in pharmacological potency between different calcitonins have to be related to structural differences in the central and C-terminal regions. Additionally, calcitonin peptides are homologous with the related peptides such as CGRP, amylin, and adrenomedullin (Purdue, *et al.*, 2002).

Many therapeutic peptides and proteins, including calcitonin, may be sensitive to a variety of environmental factors (e.g. aqueous/organic or air/water interfaces, temperature, light, oxidation, pH, ionic strength, cations, vigorous shaking, freeze-thawing, freeze-drying, spray-drying) leading to their degradation which can be classified either as chemical or physical instabilities (Cholewinski, *et al.*, 1996, Fu, *et al.*, 2000). Chemical stability involves the integrity of the amino acid sequence (primary structure) and the reactivity of the side chains. The chemical stability can be impaired during various degradation reactions, often typical for a given amino acid residue, as seen in Table 2, leading to the degradation products that might be therapeutically inactive, or cause unpredictable side effects (toxicity, antigenicity). On the other hand, physical instability involves reversible or irreversible conformation changes, adsorption to surfaces, aggregation (self association) and precipitation, often with further chemical degradation (Bilati, *et al.*, 2005).

Table 1. Comparison of the primary structures (amino acid sequences) of human, rat and salmon calcitonin (bold type - amino acids different from those of human calcitonin, * indicates disulfide bridge).

Position	**Human calcitonin**	**Rat calcitonin**	**Salmon calcitonin**
1*	Cys	Cys	Cys
2	Gly	Gly	**Ser**
3	Asn	Asn	**Asn**
4	Leu	Leu	Leu
5	Ser	Ser	Ser
6	Thr	Thr	Thr
7*	Cys	Cys	Cys
8	Met	Met	**Val**
9	Leu	Leu	Leu
10	Gly	Gly	Gly
11	Thr	Thr	**Lys**
12	Tyr	Tyr	**Leu**
13	Thr	Thr	**Ser**
14	Gln	Gln	Gln
15	Asp	Asp	**Glu**
16	Phe	**Leu**	**Leu**
17	Asn	Asn	**His**
18	Lys	Lys	Lys
19	Phe	Phe	**Leu**
20	His	His	**Gln**
21	Thr	Thr	Thr
22	Phe	Phe	**Tyr**
23	Pro	Pro	Pro
24	Gln	Gln	**Arg**
25	Thr	Thr	Thr
26	Ala	**Ser**	Asn
27	Ile	Ile	**Thr**
28	Gly	Gly	Gly
29	Val	Val	**Ser**
30	Gly	Gly	Gly
31	Ala	Ala	**Thr**
32	ProNH2	ProNH2	ProNH2

The interaction of peptide molecules with each other can lead to the formation of linear, biologically inactive aggregates (fibrils). In aqueous solutions many peptides and proteins tend to show marked physical (adsorption and aggregation phenomena) and chemical instabilities (hydrolytic degradation) upon processing, manufacturing of drug formulations, during storage and release *in vivo*. One of the benefits of formulation under non aqueous conditions is the minimization of hydrolytic degradation and stabilization of conformational structures (Stevenson & Tan, 2000).

As mentioned in the previous section, hCT does not generate antibodies during the long term therapy, as is likely to be the case for sCT. However, due to the lower potency, hCT

needs higher doses to be administered. On the other hand, the therapeutic use of hCT is hampered by its physical instability in aqueous solutions, especially near neutral pH. This could be explained in part by the different isoelectric point (pI) values of hCT (pI = 8.7) and sCT (pI = 10.4) which seems to be responsible to a certain extent for the faster fibrillation of hCT compared to sCT around neutral pH (Baudys, *et al.*, 1996). This is because of the partial loss of the net electrical charge carried by the molecule, when a peptide is found in an aqueous medium at pH approaching its pI resulting in precipitation out of the solution.

Table 2. Common degradative reactions in peptides and proteins (adopted from Fu, *et al.*, 2000).

Reaction	**Protein moiety involved**
Deamidation	Asparagine and glutamine residues
Peptide bond hydrolysis	Primarily at aspartic residues
β-Elimination	Cystine residues
Disulfide bond reshuffling	Cystine residues
Oxidation	Cysteine and methionine residues
Crosslinking	Lysine residues
Thiol-disulfide exchange	Cystine and cysteine residues
Aggregation	Whole molecule
Intramolecular conformational scrambling	Whole molecule

Several studies of calcitonin secondary structure have been performed (Arvinte, *et al.*, 1993, Arvinte & Drake, 1993, Moriarty, *et al.*, 1998, Amodeo, *et al.*, 1999, Stevenson & Tan, 2000). Generally, calcitonin shows little ordered secondary structure in aqueous solutions including a random coil or α-helix conformation, but it becomes more helical in non aqueous or mixed organic solvents (Moriarty, *et al.*, 1998). The central amino acids of the chain (approximately the sequence 8–22) are expected to form the helix, in which one side is hydrophobic and the other side is hydrophilic. Amodeo *et al*. (1999) listed in their paper many authors who studied conformational flexibility of hCT and sCT in different aqueous, non aqueous environments or mixtures and described the exact amino acid positions in the central fragment of the polypeptide chain involved in helical conformation (Amodeo, *et al.*, 1999). The presence of organic solvents, like methanol and trifluoroethanol, favors the α-helix secondary structure, while the presence of dimethylsulfoxyde (DMSO) or sodium dodecyl sulfate (SDS) induces the β-sheet conformation. Nevertheless, the protein shows conformational reversibility after substitution of the organic solvent with water (Arvinte & Drake, 1993). Interestingly, in the study of Stevenson and Tan (2000), a non gelled solution formulation containing a high dose of sCT (50 mg/ml) in pure DMSO demonstrated good

chemical stability over 12 months and was chosen to determine sCT *in vitro* release rate from DUROS® implants (Stevenson & Tan, 2000).

With regard to hCT, it is considered to have a weaker secondary structure compared to sCT, as a shorter helix is observed for hCT. As mentioned above, the ability to form the helical conformation, the exact sequence and number of amino acid residues involving in this process depend on time, concentration, temperature, solvent, pH and presence of additives (Amodeo*, et al.*, 1999, Gaudiano*, et al.*, 2005). hCT has a marked tendency to aggregate and precipitate in aqueous solutions, resulting in viscous and turbid dispersions (gel) consisting of long fibrils. In this process, monomeric hCT molecules modify their secondary structure from the random coil, occurring in water, to a mixture of α-helical and β-sheet structure occurring in initial aggregation states conformed at first as granules and then evolving to protofibrils (Arvinte*, et al.*, 1993).

Extensive research has been performed on the degradation pathway of hCT and sCT in aqueous solutions (Lee*, et al.*, 1992, Windisch*, et al.*, 1997, Lu*, et al.*, 1999, Stevenson & Tan, 2000, Capelle*, et al.*, 2009). In one of the first studies, the most chemical stability of sCT tested at 70°C was observed at pH 3.3 since no additional peak was detected by means of HPLC (Lee*, et al.*, 1992). Apart from the reduced sCT (no disulfide bridge), the authors did not identify other degradation products. Instead, the structures of several major degradation products of sCT have been elucidated in the work of Windisch *et al.* (1997). In their study, sCT was most stable at pH 3 and 4, but when the pH is raised to 5 and 6, the rate of degradation and the number of degradation products increase dramatically. The degradation pathways of sCT include hydrolytic deamidation of the Gln^{14} and Gln^{20} residues to glutamic acid residues and dimerization. However, sCT also displayed a hydrolysis between residues Cys^{1} and Ser^{2} and underwent an unusual degradation pathway to form a trisulfide bridge between Cys^{1} and Cys^{7}. The chemical pathways for this degradation could be rationalized from known chemical mechanisms. Moreover, some degradation products showed similar activity to sCT, as determined by the rat bioassay (Windisch*, et al.*, 1997). Very recently, Capelle *et al*. (2009) have published the results of the sCT stability studies in which one hundred aqueous solutions of sCT were prepared on the basis of 20 buffer types characterized by pH values between 2.5 and 10.5. After 7 days, only 12 out of the 100 formulations were stable. The best sCT formulation was in 10 mM sodium acetate buffer with pH values between 3.5 and 5.5 which was in accordance with the sCT formulation commercially used (Capelle*, et al.*, 2009).

One of the major challenges in the field of formulation of peptide and protein drugs is to ensure adequate stability of incorporated proteins/peptides during the entire life of a formulation from manufacturing to *in vivo* release. Many research articles and extended reviews have been devoted to the stability problems of therapeutic peptides and proteins and how to overcome or minimize the impact of the potentially damaging conditions (Cholewinski*, et al.*, 1996, Lai & Topp, 1999, Wang, 1999, Weert*, et al.*, 2000, Bilati*, et al.*, 2005, Capelle*, et al.*, 2007). More specifically, in order to improve stability of calcitonin both *in vitro* and *in vivo*, several strategies were suggested including PEGylation (Na*, et al.*, 2004), cyclodextrins (Sigurjonsdottir*, et al.*, 1999), various excipients as stabilizers e.g. SDS (Baudys*, et al.*, 1996, Dijkhuizen-Radersma*, et al.*, 2002) or co-administration of protease inhibitors protecting the peptide from an enzymatic degradation in the gastrointestinal tract (Shah & Khan, 2004 A). However, the first and simplest step toward calcitonin stabilization in aqueous solution is to maintain acidic pH with the use of acetic acid (Baudys*, et al.*, 1996, Cholewinski*, et al.*, 1996, Dijkhuizen-Radersma*, et al.*, 2002).

2.2.3. Pharmaceutical preparations, side effects and pharmacokinetics

Synthetic or recombinant calcitonins from different species have been used for therapeutic purposes. Calcitonins do not have equal potency in exerting their inhibitory effects on the osteoclasts. Fish calcitonins, notably salmon and eel, are about 40-fold more potent (weight by weight) compared with mammalian (human or porcine) calcitonins in lowering plasma calcium or reducing markers of bone resorption. Four forms are clinically used, namely, human, salmon, porcine calcitonin, and a synthetic analogue of eel calcitonin (elcatonin), which has equal potency to sCT (Zaidi*, et al.*, 2002). However, sCT is, by far, the most widely used in clinical practice due to its higher intrinsic potency, stability and improved analgesic properties when compared to hCT (Chesnut III*, et al.*, 2008).

The first sCT product (Calcimar®) was approved in 1975 by the Food and Drug Administration (FDA). A hCT product (Cibacalcin®) was first approved by the FDA in 1986 (Capelle*, et al.*, 2009). Pharmaceutical calcitonin preparations are available in the market as an injectable formulation for iv, subcutaneous (sc) or intramuscular (im) use, and as a nasal spray. An oral sCT preparation is currently under clinical development (phase III clinical trial, see section 2.2.4.2.). According to European Pharmacopoeia, the activity of hCT is 200 IU/mg, whereas that of sCT is 6 000 IU/mg. At present, sCT nasal spray is recommended at a therapeutic dose of 200 IU per day for treatment of established post-menopausal osteoporosis.

For injectable formulations, dosing recommendations for sc administration range from 50 IU every second day to 100 IU per day, depending on the indication and the severity of disease. For emergency treatment of hypercalcemia, sCT has been recommended at a dose of 5-10 IU per kg body weight either as sc or im injection or as infusion in physiologic saline (Chesnut III*, et al.*, 2008). In managing osteoporotic patients, the clinical monitoring of therapeutic response to the calcitonin medication, as for other antiresorptive drugs, should be confirmed by a preservation of BMD, a significant decrease in markers of bone resorption and mainly the absence of further fractures.

A unique advantage of sCT, unshared by any other antiresorptive agent, is its analgesic effect on bone pain previously demonstrated in clinical studies (Gennari, 2002, Munoz-Torres*, et al.*, 2004). Calcitonin is especially recommended for patients who fail to respond to or cannot tolerate bisphosphonate medications or are unable to take bisphosphonates because of impaired renal function (Silverman, 2003). Nasal administration of sCT constitutes a therapeutic option that is particularly attractive for women who do not wish to take or do not tolerate estrogens, or for whom estrogens are contraindicated (Silverman, 1997).

Injections of sCT (Miacalcin® Injection, Novartis Pharma) are available as sterile acetic acid buffered solutions ready to use containing phenol (preservative) and sodium chloride. Whereas hCT (Cibacalcin®, Novartis Pharma), owing to its lesser stability, has to be dissolved by mixing the freeze dried powder consisting of 0.5 mg hCT and mannitol with a solution of 30 mg mannitol in water for injection prior to use. With regard to storage conditions, sCT vials for injection must be refrigerated at 2-8°C, whereas hCT can be stored at ambient temperature as the dry powder. The nasal spray formulation (Miacalcin® Nasal Spray, Novartis Pharma) is an aqueous solution of sCT containing benzalkonium chloride as a preservative and sodium chloride as tonicity agent, pH is set with hydrochloric acid. It has to be stored in refrigerator at 2-8°C until first usage (unopened bottle), afterwards it can be stored at ambient temperature for up to 35 days. The bottles must be protected from freezing (manufacturer's data).

Calcitonin injections have been widely used for over 30 years in many countries and the drug has now a well investigated and established safety profile (Karsdal*, et al.*, 2008). Calcitonin is usually very well tolerated. The most common adverse effects after injection of sCT are nausea with or without vomiting (10% of patients) disappearing with time, local inflammatory reactions at the site of injection (10% of patients) and flushing of face or hands (2-5% of patients). Because calcitonin is protein in nature, the possibility of a systemic

allergic reaction exists. The adverse effects associated with the use of injectable sCT occur less frequently in patients treated with nasal spray. However, sCT nasal spray administration can evoke some discomfort and trigger mild to moderate local irritation including rhinitis, dryness, redness, nasal sores, itching (manufacturer's data). In terms of safety profile, calcitonin is more advantageous than the bisphosphonates. Gastrointestinal toxicity is a classic and frequent side effect associated with the oral bisphosphonates therapy. In addition, serious complications have been recently ascribed to bisphosphonates therapy such as osteonecrosis of the jaw, atrial fibrillation, musculoskeletal pain and severe suppression of bone turnover (Arum, 2008).

Early pharmacokinetic studies in humans evaluated the disposition of calcitonin following iv, im and sc administration. The absolute bioavailability of sCT after sc or im administration in humans was found to be 71 and 66%, respectively (Beveridge*, et al.*, 1976). sCT is quickly absorbed both from the site of injection or by the nasal mucosa. It appears to distribute quickly and extensively into extravascular tissue sites and then is quickly eliminated from the body. Plasma protein binding is 30-40%. sCT is degraded mainly in the kidneys, the metabolites are inactive, and only about 2% of the administered dose of sCT is excreted in urine as unchanged hormone. After parenteral administration of sCT at a dose of 100 IU, the highest plasma concentrations ranges from 200 to 400 pg/ml. The higher sCT plasma concentration is, the more frequent possibility of nausea and vomiting can occur (manufacturer's data). Peak plasma concentration appear approximately 31-39 min after the nasal administration compared to 16-25 min after parenteral administration (Plosker & McTavish, 1996). The systemic absorption of sCT in humans after nasal administration is low, with the bioavailability being in the range 1-15% (Lee*, et al.*, 2003). The nasal spray offers a convenient route for self administration, but is far from being optimal. At present, clinical usage of calcitonin is limited, due almost entirely to its poor bioavailability as in the case of other peptide or protein drugs. The lack of a potent therapeutic effect when the peptide is administered intranasally is not surprising, even though sCT is the most potent direct inhibitor of osteoclast function both *in vitro* and *in vivo*. Thus far, intranasal administration of sCT produces nominal effects at best, especially when compared with the newer potent bisphosphonates (Zaidi*, et al.*, 2002)

2.2.4. Novel calcitonin delivery systems and routes of administration

The development of recombinant DNA and analytical separation technologies paved the way for the mass scale production of highly purified biopharmaceuticals, namely therapeutic peptides and proteins, without the drawbacks of animal-derived products such as immunogenicity. Despite this fact, there are many hurdles that have to be overcome to the delivery of peptide and protein drugs. As mentioned earlier, physical or chemical instability, one of the most challenging tasks in the development of peptide/protein pharmaceuticals, is the major reason why they are administered traditionally through injection rather than taken orally like most low molecular weight chemical drugs and why they need careful attention in their storage to achieve an acceptable shelf life and maintain a full activity (Wang, 1999). Therefore, it is crucial to develop novel delivery systems for peptides and proteins, in order to reduce the gap between the vast number of discovered and biotechnologically prepared peptides/proteins and the low number of efficient delivery systems (Dorkoosh*, et al.*, 2002).

In the case of calcitonin, its clinical usage is currently limited because of the necessity of regular injections and poor bioavailability when administered non-parenterally. However, several new strategies are presently being studied to enhance calcitonin access to the osteoclast such as various technological approaches as well as a chemistry approach by synthesis of small molecules that would either enhance the secretion of endogenous calcitonin or allosterically activate the calcitonin receptor (Zaidi*, et al.*, 2002). It is expected that the next few years should therefore see the revival of calcitonin as an important therapeutic agent mainly for the treatment of osteoporosis, but not exclusively. Finally, there is a possibility for the development of an oral or injectable sustained release delivery system for calcitonin. Moreover, several other alternative routes of calcitonin delivery have been also studied.

2.2.4.1. Parenteral sustained release calcitonin delivery systems

It is obvious that repeated parenteral drug administration, using typically a syringe and needle, is inconvenient for patients, can have negative effects on compliance and often requires additional costs when done under the supervision of a healthcare professional. An alternative to the investigation of non parenteral routes is the development of parenteral formulations, capable of delivering the polypeptide drug for prolonged periods of time (days, weeks, months) in order to avoid daily injections. Such systems can achieve fairly constant

blood levels of protein therapeutics leading to improved drug efficiency, higher drug safety and fewer adverse side effects (Stratton, *et al.*, 1997).

Several systems for the sustained or controlled delivery of therapeutic peptides/proteins have been investigated and some of them are already available in the market. These are formulations based on the poly(lactic-co-glycolic) acid (PLGA)-composed microparticles containing e.g. leuprolide (Lupron Depot®), growth hormone (Nutropin Depot®) or triptorelin (Trelstar® Depot) (Mundargi, *et al.*, 2008). In the case of calcitonin, a sustained release system could both improve the patient compliance and facilitate the maintenance of therapeutic plasma levels. Especially as the latter is particularly difficult to achieve with non parenteral delivery systems. Most of technological approaches, formerly described in literature with the aim of developing injectable sustained release systems for calcitonin, have involved encapsulation of the polypeptide drug within biodegradable polymer-based particles. The obvious advantage of biodegradable polymers for drug delivery over non degradable systems is that they do not have to be removed from the body at the end of the therapy.

PLGA copolymers, being approved by most of drug agencies worldwide, are the most widely studied for the sustained release of proteins, peptides, vaccines and genes (Mundargi, *et al.*, 2008). These polymers were first used in the production of biodegradable sutures and later found to have properties desirable for controlled release devices. As a result of their use for several decades, much is known about their biocompatibility, biodegradation and physicochemical characteristics. PLGA copolymers are well suited for application in delivery systems since they can be fabricated into a variety of morphologies including films, rods, microspheres, and nanospheres (Gombotz & Pettit, 1995). PLGA copolymers are prepared by polycondensation reactions with lactic and glycolic acids, and they belong to the group of aliphatic polyesters. On exposure to water, PLGA undergoes random chain scission by hydrolysis of the ester bond linkage to form non toxic monomeric acids (lactic acid, glycolic acid) that are eliminated from the body through the Krebs cycle, primarily as carbon dioxide and water. Devices made from PLGA copolymers undergo bulk erosion. In fact, the degradation of these materials allows a simultaneous release of incorporated therein high molecular weight drugs that, due to their physicochemical properties (large size), would otherwise not be able to diffuse through the non biodegradable polymer matrix. It is supposed that enzymes are also involved in the biodegradation process of PLGA. The rate of degradation, and thus drug release kinetics, is controlled by manipulating the chemical

composition and ratio of monomers used in the polycondensation reaction (Gombotz & Pettit, 1995).

Polymeric nanoparticles based on biodegradable and biocompatible polymers are suitable candidates for delivering drugs *via* parenteral routes (no risk of embolization, easy flowability through the narrowest gauge needles). Surprisingly, there is only a few articles available in the literature on polymeric nanoparticles intended for the prolonged parenteral calcitonin delivery. Tasset *et al*. (1995) studied the potential of nanoparticles of polyisobutylcyanoacrylate (synthetic biodegradable polymer) as sustained release for hCT. The particles had an average size of 150 nm, and after sc injection in rats, two hCT-loaded nanoparticulate formulations showed a more important and more prolonged hypocalcemic effect than free hCT. The calcitonin level was sustained for more than 24 h after injection (Tasset*, et al.*, 1995). Additionally, Kawashima *et al*. (1998) did a comparative study of two different preparation methods of PLGA nanospheres containing eel calcitonin, but the authors did not test the systems in animals (Kawashima*, et al.*, 1998).

However, microparticles have been more intensively studied as sustained calcitonin delivery systems. Injectable biodegradable systems based on PLGA microspheres were studied by Lee *et al*. (1991) and Mehta *et al*. (1994). In their studies, the effect of the systems on the *in vivo* release behavior of sCT was evaluated and its efficiency was compared to free sCT. In both cases, a sustained hypocalcemic effect was obtained (Lee*, et al.*, 1991, Mehta*, et al.*, 1994). However, in the study of Mehta *et al*. (1994), a hypocalcemic effect was induced for an average of six days, when sCT was incorporated during microsphere preparation, while microspheres with adsorbed sCT (adsorption of sCT after the formation of the microspheres) had an effect for only four days. Moreover, their results indicated that serum calcium levels are not well correlated to calcitonin serum levels because of the negative and positive feedback action provided by serum calcium on endogenous calcitonin and parathyroid hormone, respectively. Nevertheless, it should be mentioned that in most published *in vivo* studies only the hypocalcemic activity is measured without determination of sCT concentration in blood.

Then, other researchers studied the suitability of biodegradable gelatin microspheres for nasal and im delivery of sCT in rats (Morimoto*, et al.*, 2001). In this study, negatively or positively charged gelatin microspheres were prepared. With regard to im administration, the area above the hypocalcemic–time curve values for both types of microspheres were significantly increased compared to free sCT. Furthermore, the hypocalcemic effect of the negatively charged gelatin microspheres tended to appear more slowly and last longer

compared to that of positively charged gelatin microspheres, and was not affected by the particle size.

Only a few authors have shown results from animal studies based on serum sCT levels. Dani and DeLuca (2001) have reported that elevated serum sCT levels could be sustained for about 10 days after sc administration of sCT-loaded PLGA microspheres to rats at a high dose of 1 mg/kg (Dani & DeLuca, 2001).

However, Diaz *et al*. (1999) have reported to obtain a one-month sustained release microspheres of ^{125}I-bovine calcitonin, which delivered calcitonin at a constant release rate of 25 µg/day, prepared with three biodegradable polymers (PLGA of MW = 12 000 or 30 000, PEG-PLGA of MW = 34 000) using the double emulsion method. The *in vitro* release results (PBS pH 7.4) indicated a very slow release rate for an optimal one-month sustained release formulation. ^{125}I-bovine calcitonin microspheres were administered subcutaneously in Wistar rats and the radioactivity at the injection site was measured over one month. The *in vivo* profiles were affected by the weight average molecular weight of the copolymers. Microspheres prepared with PLGA of molecular weight equal to 12 000 released 100% of the dose in 1 month, and *in vivo* release profiles presented two phases, during the first 2 weeks approximately 70% of the ^{125}I-bovine calcitonin injected was released, followed by a second slower release phase (Diaz*, et al.*, 1999).

An interesting study was performed by Prabhu *et al*. (2005) who designed an *in situ* biodegradable injectable implant as controlled release delivery system for sCT. In such an implant, a drug can be dissolved or suspended in a biodegradable polymer (e.g. PLGA) dissolved in a nontoxic, physiologically acceptable solvent(s), that upon injection forms a gel-like mass releasing drug over a period of time. This system has several advantages over the polymeric microspheres including less number of processing steps, less complex method of manufacture, easier to use, higher dose of drug delivered. Additionally, compared to microparticle preparations, *in situ* implants can be injected with smaller diameter injection needles and exhibit less tissue irritation and low initial burst release due to a low surface area to volume ratio (Prabhu*, et al.*, 2005). In the study of Prabhu *et al*. (2005), the *in situ* implants were prepared by dissolving/suspending sCT in a poly(lactic acid) (PLA) polymer solutions/suspensions containing combinations of a hydrophobic (benzyl benzoate) and a hydrophilic (benzyl alcohol) solvent, and the objective of the study was to assess the release of the drug as a function of these co-solvents. As a result, the higher the hydrophobic solvent content, higher the rate of drug release was observed. However, the long-term storage of sCT in organic solution may not be feasible in humans. Nevertheless, degradation of sCT in such

formulations over a 4-month period was much slower at 4°C. There was no *in vivo* study reported in this paper (Prabhu*, et al.*, 2005).

Finally, it is worth writing that some efforts have been made to prolong the systemic circulation half-life of sCT *via* PEGylation process as these polymers surrounding the polypeptide are considered to increase the stability toward proteolysis and to reduce renal excretion. The conjugation of sCT by covalent linkage with PEG was attempted by Lee *et al*. (1999). In clearance studies in rats, PEGylated sCT (mono-PEG-sCT and di-PEG-sCT) had significantly longer circulating half-lives than the intact sCT. Moreover, PEGylated sCT showed a substantially improved stability in rat liver homogenates as compared to the intact sCT, indicating that PEG molecules protected sCT from various degrading enzymes and exhibited similar biological activity to the unmodified sCT (Lee*, et al.*, 1999). Additionally, the approach of sCT PEGylation to make the polypeptide more resistant to enzymatic degradation was also undertaken to improve delivery and stability of sCT *via* pulmonary (Youn*, et al.*, 2008), intestinal (Youn*, et al.*, 2006) and nasal (Lee*, et al.*, 2003) route.

2.2.4.2. Oral calcitonin delivery systems

Compared to other routes of administration, the oral drug delivery has many advantages: (a) it is convenient for patients and encourages good patient compliance; (b) it is the most accepted route for the treatment of chronic diseases; (c) it has usually lower preparation costs (Dorkoosh*, et al.*, 2002). Major factors remaining hurdles for oral peptide/protein formulations are: large molecular size (high molecular weight), charge and hydrophilicity, instability in the gastrointestinal fluids, and poor intestinal membrane permeability. Of these, the particular barriers to developing a desirable oral formulation for peptides and proteins are extensive degradation by proteolytic enzymes in the intestine and instability at gastrointestinal pH, that typically result in oral bioavailability less than 1-2% (Lee & Sinko, 2000). However, there are polypeptide drugs, such as cyclosporin A and desmopressin that are already available in the market as oral dosage forms, indicating that oral delivery of peptides is feasible. Interestingly, the bioavailability of cyclosporine A and desmopressin from the oral dosage forms is 30% (Sandimmune® Soft Gelatin Capsules) and 0.08% (Minirin® Tablets), respectively, which must be clearly sufficient for the therapeutic efficiency (manufacturer's product information). In the case of calcitonin, it is supposed that its oral administration would enhance clinical usefulness, lead to higher patient compliance to long-term treatment and render calcitonin competitiveness towards oral bisphosphonates.

Several technological approaches are currently being considered for improving oral bioavailability of calcitonin. Some of them are mentioned or discussed below.

In the field of formulation, the coadministration of permeation (absorption) enhancers and protease inhibitors in peptide/protein drug formulations have been investigated for many years (Dorkoosh*, et al.*, 2002). Such approaches focus on either changing the permeability of the gut tissue or digestibility of a peptide/protein by deactivation of intestinal enzymes, both resulting in increase of drug absorption in the gastrointestinal tract. However, some of these agents can alter the integrity of the mucosal surface and can cause adverse effects either locally or systemically when absorbed from the intestine. However, possible solutions are the covalent attachment of protease inhibitors to unabsorbable polymeric matrix as well as the use of unabsorbable penetration enhancers of a high molecular weight selectively opening the tight junctions, in both cases to avoid their systemic absorption (Dorkoosh, et al., 2002, Shen, 2003). This strategy has been already used for calcitonin. Guggi *et al*. (2003) formulated minitablets (5 mg) by direct compression of sCT (50 µg), thiolated chitosan (chitosan – 4-thiobutylamidine conjugate; 3 450 µg), chitosan – protease inhibitor conjugate (chitosan – pepstatin A; 1 000 µg) and GSH (500 µg). In this way, a multifunctional polymeric carrier matrix combined the mucoadhesive features of the thiomer, the permeation enhancing properties of the thiomer – GSH system (seen section 2.1.3.), the enzyme inhibitory activity of a chitosan – pepstatin A conjugate, and simultaneously the prevention the inhibitor from being absorbed. Interestingly, this complex formulation was designed as a stomach targeted system since sCT is relatively stable at gastric pH and enzymatic activities in the stomach are limited. When administered orally in rats, the formulation allowed to reach a significant pharmacological efficacy by decreasing the plasma calcium level of 10% for at least 12 h, suggesting that stomach targeted oral delivery might be a promising approach for noninvasive systemic peptide administration (Guggi*, et al.*, 2003). The delivery of sCT *via* the stomach seems to be feasible, despite the permeability of sCT through the epithelium in the stomach is approximately 3-fold lower compared to the ileum (the region of maximum sCT permeability) (Shah & Khan, 2004 B).

Another example of the formulation approach is the use of Eligen® Technology created by Emisphere Technologies, Inc. (http://www.emisphere.com) which reflects the potential that for the first time sCT may also be available as a convenient oral medication. Novartis Pharma AG and its partner Nordic Bioscience are currently taking Eligen® Technology into Phase III clinical studies with an oral sCT product to treat osteoarthritis and osteoporosis. Eligen® technology employs low molecular weight compounds (termed drug

delivery agents or carriers), generally being caprylic acid derivatives, that interact non-covalently and reversibly with a peptide/protein increasing its lipophilicity, changing its conformation, and, consequently, its ability to cross the gastrointestinal epithelium. Simultaneously, the drug may be protected from proteolytic degradation. This class of absorption enhancers enables drug absorption by passive transcellular diffusion, without affecting the integrity of cell membranes or tight junctions and is practically devoid of toxic activity toward the intestinal epithelial cells (according to Emisphere). Once the drug crosses the membrane, the delivery agent dissociates from the drug and the drug adopts its natural conformation structure and retain its bioactivity (Goldberg & Gomez-Orellana, 2003, Malkov*, et al.*, 2005). The efficacy and safety of this technology for oral sCT, using N-(5-chlorosalicyloyl)-8-aminocaprylic acid (5-CNAC) as a carrier, has been demonstrated in Phase I clinical study in healthy male volunteers (Buclin*, et al.*, 2002) and in Phase IIa clinical study in healthy postmenopausal women (Tanko*, et al.*, 2004). The same technology was tested for insulin with the use of N-[8-(2-hydroxybenzoyl)amino] caprylate (SNAC) as a carrier at the cellular level (Malkov*, et al.*, 2005) and in healthy non-diabetic volunteers (Kidron*, et al.*, 2004). More specifically, in the phase I clinical trial (Buclin*, et al.*, 2002) sCT was absorbed with an absolute bioavailability of 1.4% at a single dose of 1.2 mg/tablet and the achieved serum concentrations could evoke pronounced biological responses in bone tissue. In the phase II clinical trial described by Tanko *et al*. (2004), the efficacy and safety of the same formulation have been investigated in the target population (healthy postmenopausal women) over a longer period of time (3 months). The results of the trial showed that this oral formulation is safe, well tolerated and has potential to become an effective treatment for postmenopausal bone loss. In addition to its pronounced effect on bone resorption, this novel formulation may also reduce cartilage degradation and thereby provide therapeutic benefit in joint diseases such as osteoarthritis and rheumatoid arthritis (Bagger*, et al.*, 2005).

Another strategy for oral peptide/protein delivery is a chemical modification by lipidization which appears to be a reasonable approach because there are examples of natural peptides with high lipophilicity, such as cyclosporin A, that can be absorbed from the gastrointestinal tract. In addition, lipidization can increase the stability of a peptide against digestion in the gastrointestinal tract. One of the limitations of this method is that lipid modification can reduce the bioactivity of a peptide/protein when an irreversible complex is produced (Shen, 2003). Wang *et al.* (2003) synthesized a sCT - fatty acid moiety conjugate using a reversible aqueous lipidization technology. This method of conjugation can be carried out in an aqueous solution and allow sCT to regenerate the original structure after oral

absorption. *In vivo* study conducted in mice and rats demonstrated better bioavailability and pharmacological efficacy of the lipidized sCT compared to unmodified polypeptide (Wang*, et al.*, 2003).

Most studied approach for oral peptide/protein delivery is encapsulation/incorporation into particulate carriers. Nanoparticles and microparticles can protect against degradation, enhance oral absorption of the drug and increase the residence time at a desirable absorption site in the gastrointestinal tract, during which the drug can be released and absorbed. The latter effect can be more pronounced when a mucoadhesive polymer is used (Allemann*, et al.*, 1998, Dorkoosh*, et al.*, 2002). It must be highlighted that only a few studies have been published on microencapsulation of calcitonin with the aim of oral administration. However, microparticles were mainly applied as an injectable depot formulation which releases the incorporated calcitonin after administartion over a prolonged period (see section 2.2.4.1.). Lamprecht *et al*. (2004) designed sCT-loaded microspheres for oral administration allowing the release of the peptide drug in the colon, where activities of proteolytic enzymes are relatively low. For colonic delivery of sCT, Eudragit P-4135F, a pH-sensitive polymer, was applied for the microspheres preparation by a double emulsion technique. The obtained microparticles were found to keep the *in vitro* release of sCT at pH 6.8 below 20% within 4 h, while at pH 7.4 a fast sCT release was observed. At a dose of 20 µg/kg (120 IU/kg), no significant hypocalcemic effects were found in rats, however, increasing the dose to 100 µg/kg (600 IU/kg) resulted in a distinct hypocalcemic effect (4-fold increase of the area under the curve - AUC compared to sCT solution) and revealed the sustained release properties of the microparticles (Lamprecht*, et al.*, 2004).

A perusal of the literature indicates that there is a greater number of research papers focusing on oral sCT delivery by means of nanoparticles than microparticles. The basic characteristics and major *in vitro* and *in vivo* outcomes for oral sCT using various nanostructures are summarized in Table 3. As seen in this Table, chitosan is quite often used for the preparation of nanoparticles or coating of nanoparticles. These delivery systems were able to enhance and prolong the intestinal absorption of sCT in rats resulting in a hypocalcemic effect. This positive action of chitosan on peptide delivery could be mainly ascribed to its permeation enhancing effect by opening the intercellular tight junction, proteolytic enzyme inhibitory capabilities, and mucoadhesive properties, which makes chitosan and its derivatives important excipients for peroral peptide/protein delivery systems (Bernkop-Schnurch, 2000).

Finally, it is worthy of note that some less typical, but interesting attempts have been made in order to develop an oral delivery system for calcitonin. These are oral multiple water/oil/water emulsion formulation (Dogru, *et al.*, 2000), dextran hydrogels for colon specific delivery (Basan, *et al.*, 2007) and pectin - liposome nanocomplexes (Thirawong, *et al.*, 2008).

Table 3. Nanoparticulate oral delivery systems developed for calcitonin

Reference	Delivery system	Polymer/ Lipid type	Size (nm)	Enca-psulation efficiency (%)	Experiments	
					In vitro release	*In vivo* study
(Lowe & Temple, 1994)	hCT-loaded nanocapsules	Polyiso-butylcyano acrylates	88	66	No data	Nanocapsules were administered duodenally in rats at a hCT dose of 0.2 mg/kg (40 IU). C_{max} was ~3 ng/ml after 15 min. After 2 h, the concentration was still 1 ng/ml. No more hCT measurements in rat plasma were done
(Kawashima, *et al.*, 2000)	Chitosan-coated nanospheres loaded with elcatonin	PLGA (75:25)	~ 250	~ 63	~ 30% of the drug was released immediately during the initial stage, then drug release lasted more than 2 weeks, at which time 40% of the elcatonin still remained in the nanospheres	Chitosan-coated nanospheres reduced significantly the blood calcium level in rats (dose: 500 IU/kg), and the reduced calcium level was sustained for a period of 48 h (~85% of basal). Under non fasting conditions, the mucoadhesion of chitosan coated nanospheres was unaltered and the reduction in blood calcium levels was maintained satisfactorily
(Takeuchi, *et al.*, 2003)	Carbopol- and chitosan-coated liposomes containing elcatonin	Dipalmitoyl phospha-tidylcholine and stearyl-amine	No data	greater than 90%	No data	Administration of both types of liposomes containing elcatonin showed an enhanced and prolonged reduction in blood calcium concentration for at least 12 h (administration in rats, dose 500 IU/kg). However, liposomes coated with chitosan reduced greater the calcium level (~80% of the initial value after 2 h)
(Yoo & Park, 2004)	Nanoparticles loaded with sCT-oleate complexes	PLGA (50:50)	200-300	53-95 depending on loading	Data not shown but mentioned that an initial burst of 40-50% at 1 day, then slow release over 1 week	For a sCT dose of 60 µg/kg (~300 IU) administered in rats, C_{max} was ~ 600 pg/ml after 2 h, and after 12 h the concentration was still high (~100 pg/ml)
(Garcia-Fuentes, *et al.*, 2005)	PEG-coated lipid nanoparticles and chitosan-coated lipid nanoparticles containing sCT	Tripalmitin (core of nano-particles)	226 for PEG-coated particles; 537 for chitosan-coated particles	>90 for PEG-coated particles; 31 for chitosan-coated particles	No data	PEG-coated nanoparticles did not produce any significant effect on plasma calcium levels in rats. In contrast, chitosan-coated nanoparticles revealed a rapid and drastic reduction in calcium levels which was maintained at ~ 75% of basal for at least 24 h
(Prego, *et al.*, 2006)	Nanocapsules containing sCT	Chitosan (medium MW)	266-333	44-52	Data not shown but mentioned that an initial burst of 20%	At a sCT dose of 500 IU/kg calcemia level in rats was significantly reduced to almost 70% of basal and the effect was maintained for 24 h

Extensive investigation on oral sCT delivery falls into the more general formulation problems facing oral delivery of peptides and proteins which have been approached from many different angles for many years. Several approaches have achieved an important increase in gastrointestinal absorption. However, none of these technologies has yet been fully developed into an oral dosage form for this class of drugs. The answer is that there are many criteria that must be fulfilled to bring an oral peptide/protein drug to the market (Shen, 2003).

For example, very low oral bioavailability might be acceptable for peptide/protein drugs that are both cheap and safe, such as the oral dosage form for desmopressin, but low bioavailability implies a large variation in absorption and a high manufacturing cost, which are both unacceptable for the development of most peptide and protein drugs. Furthermore, for drugs such as insulin that have a relatively narrow therapeutic window, the effects on gastrointestinal absorption of age, genomic factors, pathophysiological conditions and other individual variations must be carefully investigated. Finally, due to the chronic administration, the effects of long-term oral administration of carriers on both the gastrointestinal tract and systemic physiology must also be carefully evaluated (Shen, 2003). However, in the case of calcitonin, the hope has arisen as the Phase III clinical trial are currently under development (Eligen® technology).

2.2.4.3. Other alternative routes of calcitonin administration

Apart from the commercially available calcitonin preparations, and intensively researched oral formulations as well as sustained release formulations for parenteral applications, other routs of administration are also taken into consideration.

Pulmonary drug delivery for both local and systemic treatments has some advantages because the lungs have a large surface area for absorption of the drug, thin absorption barrier and low enzymatic metabolic activity making this route quite promising. There is the potential for possible systemic absorption of peptides and proteins through the alveolar region of the lungs (Yamamoto*, et al.*, 2005). The group of Kawashima has studied surface-modified PLGA nanospheres with chitosan for pulmonary delivery of elcatonin. The same system has been previously shown to be effective for oral delivery of elcatonin (Kawashima*, et al.*, 2000, see Table 3). The nanosphere suspension was successfully aerosolized with a nebulizer. After pulmonary administration, chitosan-modified PLGA nanospheres loaded with elcatonin were more slowly eliminated from the lungs, reduced blood calcium levels to 80% of the initial

calcium concentration, and prolonged the pharmacological action to 24 h with comparison to unmodified PLGA nanospheres (Yamamoto*, et al.*, 2005).

Instead, Youn *et al*. (2008) have demonstrated the usefulness of PEGylated sCT to improve the pulmonary delivery. Three PEG-sCT derivatives were synthesized by attaching PEG of different molecular weight (1, 2, or 5 kDa) to the Lys^{18}-amine of the sCT polypeptide chain. The results obtained showed that the pulmonary stability in rat lung homogenates and all pharmacokinetic parameters of these derivatives were greatly improved with increasing PEG molecular weight compared to unmodified sCT. Despite having the best properties, Lys^{18}–PEG_{5kDa}-sCT was found to have significantly lower hypocalcemic efficacy than other two sCT derivatives, probably due to its reduced intrinsic bioactivity, however all the sCT derivatives had greater hypocalcemic activity than unmodified sCT. Lys^{18}–PEG_{2kDa}-sCT showed the most promising pulmonary potential because of its well-preserved bioactivity (Youn*, et al.*, 2008).

Interesting approach was undertaken by Chaturvedula *et al*. (2005) who applied iontophoretic patch (a wearable electronic device with built-in electrodes in the patch - WEDD® - Wearable Electronic Disposable Drug Delivery, Birch Point Medical, Inc.) to deliver sCT transdermally. Iontophoresis utilizes a small amount of current to push charged drug molecules through and across the skin and into the systemic circulation. Advantages of this route include improved patient compliance, avoidance of first pass hepatic metabolism, controlled delivery and the possibility to modulate the rate of delivery. Such iontophoretic patches delivered sCT in hairless rats at an average infusion rate of 178 ng/(min kg) and an average steady state concentration of sCT in rat serum of 7.6 ng/ml was achieved. The calcium lowering effect of the iontophoretic patch was comparable with that after sc injection (Chaturvedula*, et al.*, 2005).

Despite potential advantages of administering drugs *via* the intranasal route, including the rapid absorption and avoidance of first-pass gastrointestinal and hepatic metabolism, there are also a number of limiting factors. The bioavailability of nasally administered peptide/protein drugs is low, which is mainly due to proteolytic degradation in the nasal mucosa, low permeability of the nasal epithelium, and physical removal from the site of deposition in the nasal cavity. Although nasal spray of sCT is commercially available for a long time, many attempts have been still made to improve nasal bioavailability of sCT such as PEGylation (Lee*, et al.*, 2003) or the use of mucolytic agents, such as N-acetyl-L-cysteine (Matsuyama*, et al.*, 2006).

3. OBJECTIVES OF THE THESIS

Polymeric nanoparticles can have many potential benefits in the field of drug delivery, as described in the Introduction. If designed appropriately, these submicronic carriers can be injected directly into the systemic circulation or they can deliver a drug in a prolonged or controlled way after parenteral administration over a long period of time. Development of the peptide or protein drug - loaded nanoparticles could be particularly advantageous with regard to their oral administration, since they can protect against enzymatic degradation, improve intestinal absorption of the drug, or the particles can be even entirely taken up from the gastrointestinal tract due to their very small size. Design of such formulations would potentially result in better drug bioavailability, improved patient compliance, reduced the amount of dose required and increased safety of the therapy. Moreover, this approach could be also applied in the field of *in situ* bioimaging of the important cellular biomarkers, since incorporation of selective dyes into nanoparticulate carriers can potentially influence their intracellular delivery and uptake.

Taking into account all these premises, this PhD project was divided into two parts. The first part involved nanoencapsulation of fluorogenic probes with the intention of improving GSH detection after applying in yeast cells. However, the second part dealt with nanoencapsulation of a pharmacologically active molecule, sCT, with the aim of enhancing the bioavailability of this labile polypeptide hormone after sc or oral administration in rats.

With regard to the first part of the thesis, the main scope was to evaluate the possible improvement of cellular uptake of GSH-selective fluorogenic probes by means of nanoparticles. More specifically, two fluorogenic probes, namely OPA and NDA, were selected as these aromatic dialdehydic probes are known to be useful as derivatization reagents for imaging and determination of GSH, which is an important biomarker of oxidative stress. *Candida albicans* yeast cells were chosen as a cell model. Since the probes do not penetrate easily into cells, and additionally the presence of cell wall in yeast cells hampers the penetration, the prime scope of the present work was to asses the possible influence of nanoparticles on the probe uptake by yeast cells. The objective was realized in the following steps:

- Development of polymeric nanoparticles loaded with OPA and NDA and investigating the influence of preparation process parameters on the properties of nanoparticles,

- Physicochemical and *in vitro* release characterization of the probe-loaded nanoparticles,
- Investigating the impact of nanoparticles on cellular uptake of the probe,
- Identifying the potential cytotoxicity effect of the free probe, the probe encapsulated in nanoparticles and blank nanoparticles on yeast cells.

The innovation of the study consists of the encapsulation of GSH probes in polymeric nanocarriers and their application in yeast cells. Since yeast cells are additionally surrounded by a cell wall, the extension of the present method to bacterial and mammalian cells seems easier by selecting yeast as the cell model.

With reference to the nanoencapsulation of sCT, the main objective was to develop sCT-loaded nanoparticles and evaluate as a possible sustained calcitonin release system (sc administration), or as a potential oral delivery system. In both cases, it would improve the patient compliance and comfort of administration leading to greater clinical usefulness of this natural and unique antiresorptive drug. Thereby, biodegradable and non-biodegradable nanoparticles containing sCT intended for a parenteral or an oral administration in rats were developed. The objective was realized in the following steps:

- Preparation of polymeric nanoparticles loaded with sCT and investigating the influence of polymer type on the properties of nanoparticles,
- Physicochemical and *in vitro* drug release characterization of the sCT-loaded nanoparticles,
- Subcutaneous administration of sCT-loaded nanoparticles and sCT determination in rat serum,
- Oral administration of sCT-loaded nanoparticles and sCT and calcium determination in rat serum.

Primarily, the development of the injectable and oral formulations were based on biodegradable and non biodegradable polymers, respectively. However, the non biodegradable nanoparticles were also injected subcutaneously in rats, to investigate the possible influence of polymer blending (producing positively charged nanoparticles for sc injection) on the *in vivo* behavior of nanoparticles and in order to get reference data that would allow the calculation of relative bioavailability after oral administration. This investigation on sCT delivery systems falls into the more general and challenging problems with injectable sustained or oral delivery of peptide and protein drugs.

4. EXPERIMENTAL PART

4.1. Encapsulation of glutathione-selective fluorogenic probes

4.1.1. Materials

- Naphthalene-2,3-dicarboxaldehyde (NDA; MW = 184.2 g/mol; Fluka): stock solution of NDA was prepared in absolute ethanol at a concentration of 1 mg/ml (= 5.43 mM) and stored at -80°C. Further dilutions were realized in 0.2 M borate buffer pH 9.2 for calibration curves or in sterile PBS solution for loading cultured cells and cytotoxicity assay,
- *Ortho*-phthaldialdehyde (OPA; MW = 134.14 g/mol; Fluka): stock solution of OPA was prepared in absolute ethanol at a concentration of 1 mg/ml (= 7.45 mM) and stored at -80°C. Further dilutions were realized in 0.2 M borate buffer pH 9.2 for calibration curves,
- Eudragit® E (MW = 150 kDa; Evonik Industries),
- Polyvinyl alcohol (PVA; MW = 30 kDa, 88% hydrolysed; Sigma Aldrich),
- Reduced glutathione (GSH; MW = 307.32 g/mol; Sigma Aldrich): solution of GSH was prepared *ex tempore* at a concentration of 1 mg/ml (= 3.25 mM) in 0.1 M HCl containing 2 mM ethylenediaminetetraacetic acid (EDTA, MW = 292.24 g/mol, Sigma Aldrich),
- Phosphate buffered saline solution of pH 7.0 (PBS) contained 120 mM NaCl (MW = 58.44 g/mol, Sigma Aldrich), 2.7 mM KCl (MW = 74.55 g/mol, Sigma Aldrich), 10 mM K_2HPO_4 (MW = 174.18 g/mol, Sigma Aldrich), adjusted to pH 7.0 with 1 M HCl before sterilization (autoclaving for 20 min, 120°C, pressure 2.5 bars),
- 0.2 M borate buffer of pH 9.2 prepared by dissolution of 2.47 g of boric acid (MW = 61.83 g/mol, Sigma Aldrich) in deionized water and adjusted to pH 9.2 with 40% NaOH solution,
- Bicinchoninic acid solution (BCA, Sigma Aldrich, ready for use),
- 4% (w/v) copper (II) sulfate pentahydrate solution in deionized water ($CuSO_4 \cdot 5H_2O$, MW = 249.69 g/mol, Sigma Aldrich), stored in the dark,
- 0.9% (w/v) NaCl solution in deionized water (MW = 58.44 g/mol, Sigma Aldrich),

- 0.5 g/l bovine serum albumin (BSA, MW = 66 kDa, Sigma Aldrich) solution in 0.9% NaCl,
- 125 mM buthionine sulfoximine (BSO; MW = 222.31 g/mol; Sigma Aldrich) solution prepared in deionized water, sterilized by filtration (filter 0.22 µm) and stored at 4°C,
- 3-(4,5-dimethylthiazol-2-yl)-2,5-diphenyl tetrazolium bromide (MTT; MW = 414.32 g/mol; Sigma Aldrich). MTT solution was prepared *ex tempore* at a concentration of 1 mg/ml in sterile fluid Sabouraud medium,
- prepared by dissolution of 2 g of anhydrous glucose (Sigma Aldrich) and 1 g of peptone (Sigma Aldrich) in 100 ml of deionized water (sterilization by autoclaving for 20 min, 120°C, pressure 2.5 bars),
- Fluid Sabouraud medium containing additionally 2g/100 ml of the yeast extract (Sigma Aldrich) and sterilized as above (modified fluid Sabouraud medium),
- *Candida albicans* VW 32 strain.

In all experiments deionized water was used. All chemical reagents were of analytical grade, except for HPLC-grade solvents.

4.1.2. Methods

4.1.2.1. Preparation of the probe-loaded nanoparticles

Nanoparticles loaded with the probe were prepared using a simple emulsion solvent evaporation method (Figure 9). First of all, 5 mg of OPA or NDA and 100 mg of Eudragit® E were dissolved in 3 ml of methylene chloride. The organic phase was then introduced into 10 ml of an aqueous solution containing PVA as the surfactant (PVA concentration: 3%). The mixture was then sonicated for 5 min in a cooled water bath at 10 W (ultrasonic homogenizer - Vibra Cell 75022, Bioblock Scientific). The organic solvent was then quickly eliminated by evaporation under vacuum (Rotavapor).

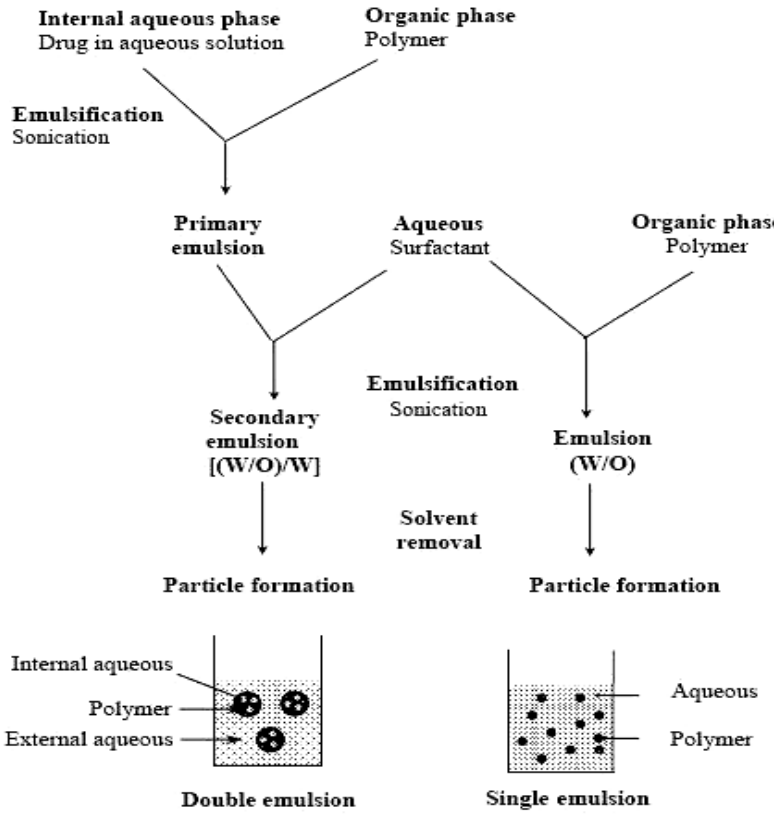

Figure 9. The scheme of the polymeric nanoparticle preparation by simple emulsion (encapsulation of a probe) or double emulsion solvent evaporation method (encapsulation of sCT) (adopted from Delie & Blanco-Prieto, 2005).

The resulting suspension of nanoparticles was fractionated into small portions (approximately 1 ml) and nanoparticles were recovered from the suspension by centrifugation in 1.5 ml Eppendorf tubes at 42 000 *g* for 20 min. The clear supernatant was withdrawn and refrigerated at -20°C. The pellets containing nanoparticles from all the tubes were put together

and redispersed in deionized water (approximately 3 - 4 ml), and the resulting suspension was lyophilized. Blank nanoparticles were obtained following the procedure described above without any addition of the probe. Lyophilized nanoparticles were protected from moisture (desiccator) and stored in the dark at 4°C for further analysis.

4.1.2.2. Characterization of the probe-loaded nanoparticles

The size, polydispersity index and zeta potential of nanoparticles were characterized using Zetasizer® 3000 HS (Malvern Instruments), in an aqueous suspension obtained directly after the evaporation of the organic solvent and following appropriate dilution in deionized water. The analyzer uses photon correlation spectroscopy (PCS) technique to determine the particle size and laser Doppler electrophoresis (LDE) for zeta potential measurement. Each sample was measured in triplicate.

The amount of the probe loaded in the nanoparticles was determined by direct recovery of the probe from the nanoparticles. In brief, 5 mg of nanoparticles was dissolved in 2.5 ml of 0.1 M HCl and then 2.5 ml of acetonitrile (ACN) was added. Samples of 100 µl were then derivatized and injected into the HPLC system (see section 4.1.2.5). Encapsulation efficiencies of NDA and OPA in nanoparticles were calculated as the ratio of the mass of the probe entrapped in nanoparticles to the theoretical mass of the probe initially added to the formulation. Additionally, the encapsulation efficiency was determined indirectly, i.e. the amount of non-encapsulated NDA was measured in the supernatant obtained after nanoparticles centrifugation during the preparation process. Yield of the preparation method was calculated as a percentage of weighed lyophilized nanoparticles to the sum of the mass of the probe and the polymer taken to the formulation process.

4.1.2.3. *In vitro* release of the probe from nanoparticles

10 mg of lyophilized NDA-loaded nanoparticles were suspended in 10 ml of sterile PBS solution pH 7.0 or 0.1 M HCl solution. The suspension was stirred at 250 rpm. All the experiments were carried out at 20 ± 2°C for 1 h. At predetermined time intervals (5, 15, 30 and 60 min), 1 ml samples were withdrawn and replaced by 1 ml of the fresh release medium. The samples were then quickly centrifuged at 42 000 *g* for 10 min and the obtained supernatants were frozen at -20°C until analysis. The amount of the probe in the supernatants

was determined after the derivatization process by the HPLC assay. The *in vitro* release experiment was conducted in duplicate for each batch formulations.

4.1.2.4. HPLC system and operating conditions

The HPLC system consisted of a low-pressure gradient solvent delivery pump (model PU 980, Jasco), a manual loop injector or an autosampler equipped with a cooling sample device, a column oven (model AS-300, Thermo), a spectrofluorimetric (model FP-920, Jasco) or a spectrophotometric detector (model L-4000, Merck). The tray compartment containing sample vials was cooled at 4°C. A guard column (4 mm ID × 8 mm) and an analytical column (4.6 mm ID × 125 mm) were packed with Spherisorb ODS-2, 5 µm (Macherey-Nagel) and maintained at a temperature of 40°C. NDA-GSH adduct was isocratically eluted with the mobile phase consisted of methanol and 0.05 M phosphate buffer pH 6.5 (20:80, v/v) at a flow rate of 0.8 ml/min. Spectrofluorimetric detection of the NDA-GSH adduct in cell extracts was operated at λ_{exc} = 472 nm and λ_{em} = 528 nm. However, for the determination of NDA in all other non-biological samples, the spectrophotometric detection was used with the absorption wavelength of 472 nm. Additionally, in the case of biological samples, the autosampler was used and the injection volume was 20 µl whereas, all the other samples were injected manually and the volume of injection was 10 µl.

For the determination of encapsulation efficiency of OPA, the same HPLC system was applied, with the difference that the mobile phase composition was methanol - 0.05 M phosphate buffer pH 6.5 (5:95, v/v) and the automatic injection was used. The spectrofluorimetric detection of the OPA-GSH adduct was operated at λ_{exc} = 340 nm and λ_{em} = 440 nm.

4.1.2.5. Pre-column derivatization of NDA

At first, the stock solution of NDA (1 mg/ml) was diluted with 0.2 M borate buffer pH 9.2 to obtain a primary standard solution of the concentration of either 1 or 100 µg/ml depending on the concentration range of standards to be prepared. A series of standard solutions was prepared according to the Table 4 with the final volume of 1 ml. Then, 1 ml of the NDA standard solution in 0.2 M borate buffer pH 9.2 was accurately mixed (vortexing for a few seconds) in a 1.5 ml Eppendorf tube with 100 µl of a freshly prepared GSH solution (1 mg/ml, in 0.01 M HCl containing 2mM EDTA) (Figure 6).

Table 4.Standard solutions of NDA for the determination of A) encapsulation efficiency of NDA in nanoparticles (spectrophotometric detection) or B) the NDA-GSH adduct concentration in yeast extracts (spectrofluorimetric detection).

A)

Standard	1_A	2_A	3_A	4_A	5_A
Volume (µl) of primary NDA standard of 100 µg/ml	20	50	100	200	300
Volume (µl) of 0,2 M borate buffer pH 9.2	980	950	900	800	700
NDA concentration (µg/ml)	**2**	**5**	**10**	**20**	**30**

B)

Standard	1_B	2_B	3_B	4_B	5_B
Volume (µl) of primary NDA standard of 1 µg/ml	20	50	100	200	500
Volume (µl) of 0,2 M borate buffer pH 9.2	980	950	900	800	500
NDA concentration (ng/ml)	**20**	**50**	**100**	**200**	**500**

The resulting mixture was kept at 20 ± 2°C for 15 min in the dark, then put into the autosampler at 4°C for a maximum time period of 1 h before injection or immediately injected by hand into the HPLC system in the case of the manual injector. OPA standard solutions were treated in a similar way (Table 5). For the NDA determination in non-biological samples (*in vitro* release study and encapsulation efficiency determination), 100 µl of the sample was first diluted by adding 900 µl of 0.2 M borate buffer pH 9.2, and then the derivatization reaction with GSH was carried out in a similar way (addition of GSH solution).

Table 5. Standard solutions of OPA for the determination of encapsulation efficiency of OPA in nanoparticles (spectrofluorimetric detection).

Standard	1_C	2_C	3_C	4_C	5_C
Volume (µl) of primary OPA standard of 1 µg/ml	50	100	250	500	1000
Volume (µl) of 0,2 M borate buffer pH 9.2	950	900	750	500	0
OPA concentration (ng/ml)	**50**	**100**	**250**	**500**	**1000**

4.1.2.6. Study on NDA stability at various pH

The stock solution of NDA (1mg/ml) was first diluted in borate buffer pH 9.2 to obtain the concentration of 100 µg/ml. The next dilution was performed at various pH as seen in Table 6 at NDA concentration of 20 µg/ml using 1.5 ml Eppendorf tubes. Afterwards, the sample was derivatized with GSH and injected into the HPLC system (see section 4.1.2.5.). The study was done in triplicate for each pH.

Table 6. The preparation of NDA dilutions at a concentration of 20 µg/ml at various pH

pH	**acidic**	**neutral**	**alkaline**
Volume (µl) of primary NDA standard of 100 µg/ml in 0.2 M borate buffer pH 9.2	200 µl	200 µl	200 µl
Volume of the medium (µl)	400 µl 0.1 M HCl 400 µl acetonitrile	800 µl PBS pH 7.0	800 µl borate buffer pH 9.2

4.1.2.7. Cell culture, probe loading and extraction conditions

Yeast cells (*Candida albicans* VW 32 strain) were obtained from a preculture and were grown in 20 ml of the yeast extract–peptone–glucose medium for 6 h at 25°C under stirring at 300 rpm to obtain an absorbance between 0.6 and 0.8. The absorbance was measured at 620 nm *versus* the cell free culture medium. In such conditions, cells are in their exponential growth phase. After incubation, 20 ml of cell suspension was centrifuged at 3 000 rpm for 5 min at 4°C. Then, cell pellets were washed twice by suspending in 10 ml of sterile PBS solution and centrifuging as above. The final pellets were suspended in 5 ml of sterile PBS solution. NDA was added to the obtained cellular suspension either as free NDA in sterile PBS solution (prepared as follows: 100 µl of the NDA stock solution diluted in 400 µl of the sterile PBS solution) or as a suspension of NDA-loaded nanoparticles (depending on the encapsulation efficiency, approximately 4-5 mg of nanoparticles suspended in 500 µl of sterile PBS solution), both at a final concentration of 100 µM. The resulting cell suspensions loaded with NDA were stirred in the dark on a rotary shaker at 20 ± 2°C for 20 min. After this

incubation, the cell suspensions were centrifuged at 3 000 rpm for 5 min at 4°C, and then washed twice by suspending in 10 ml of sterile PBS solution and centrifuging as before.

In some experiments, BSO was introduced, an inhibitor of GSH biosynthesis, in order to verify the ability of NDA-loaded nanoparticles to monitor variations of GSH concentration in cells. For this purpose, cells were exposed for 3 h at *ca.* 5 mM BSO in the culture medium (0.8 ml of 125 mM BSO solution was added to 20 ml of the culture suspension) before incubation of cells with NDA. Then, the cell suspensions were centrifuged and washed as described before and the protocol for loading with the probe was continued as above.

The final cell pellets received after the washing of NDA-loaded cells were first frozen at -80°C (at least for 1 day), then quickly thawed to trigger the lysis of cells, suspended in 1.1 ml of 0.2 M borate buffer of pH 9.2 and vortexing vigorously for 1 min. The obtained suspensions were then centrifuged at 14 000 rpm for 5 min at 4°C. After centrifugation, the resulting clear supernatants were immediately injected into the HPLC system, while the remaining pellets were frozen at -80°C until analysis for the total protein concentration. The concentration of the NDA-GSH adduct from the cells was calculated using a calibration curve of NDA derivatized with GSH. The NDA-GSH adduct concentration was expressed per the quantity of proteins remained in the corresponding pellets after the centrifugation of cell lysates. The protein concentration was determined in the pellets by the colorimetric method.

4.1.2.8. Protein determination by the bicinchoninic acid method

The total protein concentration was estimated in the pellets of *Candida albicans* lysates by the well known colorimetric microtiter plate bicinchoninic acid (BCA) method, using bovine serum albumin (BSA) as the standard for a calibration curve. This method combines the reduction of Cu^{+2} to Cu^{+1} by proteins in an alkaline medium (the biuret reaction) with the colorimetric detection of the cuprous cation Cu^{+1} using BCA. The purple-colored reaction product of this assay is formed by the chelation of two molecules of BCA with one cuprous ion. This water-soluble complex exhibits a strong absorbance at *ca.* 560 nm which increases linearly with protein concentrations. The macromolecular structure of protein, the number of peptide bonds and the presence of four particular amino acids (cysteine, cystine, tryptophan and tyrosine) are reported to be responsible for color formation with BCA. The total protein concentration generally is determined and reported with reference to standards of a common protein such as BSA. The microplate procedure enables high sample throughput and requires a smaller volume of protein sample compared to a test tube procedure with the

use of standard cuvettes and a spectrophotometer. A calibration curve, each time prepared in duplicate, was performed according to Table 7.

The pellets were first thawed and then diluted 50- or 100-fold in 0.9% NaCl. Next, 25 µl or 50 µl of each dilution was put into a microplate well in triplicate for each volume. For the first dilution, the volume was completed to 50 µl by addition of 0.9% NaCl. Finally, 200 µl of the reaction mixture (BCA + $CuSO_4 \bullet 5H_2O$) was added to each well. Then, the plate was mixed thoroughly on a plate shaker for 30 s, covered with the aluminum paper, and incubated at 37°C for 30 min. Thereafter, the plate was left at room temperature for the next 30 min. In the final step, the absorbance was measured at 560 nm on a plate reader (Metertech Σ960, Metertech Inc.).

Table 7. The preparation of a calibration curve for the total protein determination.

BSA concentration in the well (mg/l)	**0**	**20**	**40**	**60**	**80**	**100**
0.5 g/l BSA solution (µl)	0	10	20	30	40	50
0.9% NaCl (µl)	50	40	30	20	10	0
Voulme (µl) of the mixture of BCA solution and 4% $CuSO_4 \bullet 5H_2O$ (50:1)	200	200	200	200	200	200

4.1.2.9. Cytotoxicity studies

Cytotoxicity was assessed by the 3-(4,5-dimethylthiazol-2-yl)-2,5-diphenyl tetrazolium bromide (MTT) assay which is a well known colorimetric method using the metabolic competence of the cell to convert MTT to formazan as an indicator of cell viability.

Yeast cells were grown in 20 ml of the fluid Sabouraud medium for 15–18 h at 25°C under stirring. Under such conditions cells are in their stationary phase of growth and their number is stable. At first, cells were counted after appropriate dilution in sterile fluid Sabouraud medium using an optical microscope and a Malassez cell (a chamber facilitating cell counting under a microscope), in order to establish a linear relationship between absorbance resulting from formazan formation and cell number. After the counting of cells in the culture, a calibration curve was prepared in triplicate using a 96-well microplate as in Table 8. After preparation of standard suspensions of cells (A-E) with a final volume of 250 µl, the whole microplate was centrifuged (5 min, 4 000 rpm, room temperature), and the culture medium could be removed and replaced with 50 µl of the fresh medium containing MTT (1 mg/ml). Then, the cells were incubated with MTT for 1 h at 25°C under stirring in the dark. After this treatment, the medium with the excess MTT was again removed by centrifugation (5 min, 3 000 rpm, room temperature) and 100 µl of DMSO was added to the pellets to solubilize the resulting formazan product. Next, the microplate was stirred for *ca.* 30 min in the dark to homogenize accurately the content in each well, and then the absorbance was read at 560 nm using a microplate reader (Metertech Σ960, Metertech Inc.). The background absorbance of the blank in the absence of cells was subtracted.

To determine the cytotoxicity of blank nanoparticles, free or encapsulated NDA (Table 9), the constant volume of cell suspension in the culture medium (150 µl - which corresponds to a given number of cells calculating from the calibration curve) was exposed to blank nanoparticles, NDA solution or NDA-loaded nanoparticles (the final NDA concentration was 100 µM) in the dark for 20 min at 20 ± 2°C. Simultaneously, the control cells were treated in the same way but without adding any product (control). The experiment was done in triplicate for each culture treated with different products.

After this exposure, the procedure was continued as before under the same conditions i.e. centrifugation of the whole microplate and removal of the incubation medium with the tested product, addition of the fresh medium containing MTT, incubation with MTT, centrifugation of the whole plate and removal of the medium with the excess MTT, addition of DMSO, homogenization under stirring and finally the measurement of an absorbance at

560 nm with a microplate reader. The absorbance was read against the sterile fluid Sabouraud medium for the untreated control cells (Blank 1 – to calculate the number of vital cells from the calibration curve) and for the cells treated with the blank nanoparticles (samples type 1).

Table 8. The preparation of a standard curve for the cytotoxicity test.

Standard (with a known number of yeast cells)	Blank 1 (no cells)	A	B	C	D	E
Non-diluted cell culture (µl)	0	50	100	150	200	250
Sterile culture medium (µl)	250	200	150	100	50	0
Procedure	Centrifugation and removal of supernatant					
MTT dissolved in the sterile culture medium (µl)	50	50	50	50	50	50
Procedure	Incubation, then centrifugation and removal of supernatant					
DMSO (µl)	100	100	100	100	100	100
Procedure	Agitation and reading the absorbance					

However, in the case of cells exposed to free (samples type 2) or encapsulated NDA (samples type 3), the absorbance was read against the cells untreated with MTT, but exposed to NDA free or NDA encapsulated in nanoparticles at the corresponding concentration, respectively (Blank 2 and 3). The background absorbance of blanks was subtracted. Calculated viability of treated cells was expressed as a percentage of the number of untreated control cells which was considered to be 100 % using the calibration curve. With regard to the treatment with nanoparticles, approximately 8 mg (depending on the encapsulation efficiency) of blank or loaded nanoparticles was suspended in 1 ml of sterile PBS solution and added to the culture as described in Table 9 (final concentration: 0.8 mg of nanoparticles/ml).

Table 9. Scheme of blank and sample preparation way for cytotoxicity studies of free NDA, blank or NDA-loaded nanoparticles.

	Blank 1 (no cells)	Control (100 % viability)	Sample type 1	Blank 2	Sample type 2	Blank 3	Sample type 3
Non-diluted cell culture (µl)	0	150	150	150	150	150	150
Suspension of blank nanoparticles (µl)	0	0	25	0	0	0	0
NDA solution of 250 µM in PBS pH 7.4 (µl)	0	0	0	100	100	0	0
Suspension of NDA-loaded nanoparticles (µl)	0	0	0	0	0	25	25
Sterile culture medium (µl)	250	100	75	0	0	75	75
Procedure	Incubation for 20 min at 20 ± 2°C, then centrifugation and removal of supernatant						
MTT dissolved in the sterile culture medium (µl)	50	50	50	50 no MTT	50	50 no MTT	50
Procedure	Incubation, then centrifugation and removal of supernatant						
DMSO (µl)	100	100	100	100	100	100	100
Procedure	Agitation and reading the absorbance						

4.2. Encapsulation of salmon calcitonin

4.2.1. Materials

- Salmon calcitonin (sCT, MW = 3 432 Da, Calbiochem). The stock solution of sCT was prepared in 5% acetic acid solution (as recommended by the manufacturer) at a concentration of 1 mg/ml (w/v) and stored at - 20°C up to one month,
- Rat calcitonin (rCT, MW = 3 399 Da, Sigma Aldrich). The stock solution of rCT was prepared in deionized water at a concentration of 10 µg/ml (w/v) and stored at - 20°C,
- Poly(D,L-lactic-co-glycolic) acid 50:50 uncapped (unesterified) - Resomer® RG 504 H (PLGA H, Boehringer Ingelheim), inherent viscosity of 0.45 - 0.60 dl/g (0.1% in chloroform), stored at 2-8°C,
- Poly(D,L-lactic-co-glycolic) acid 50:50 capped (esterified) - Resomer® RG 504 S (PLGA S, Boehringer Ingelheim), inherent viscosity of 0.45 - 0.60 dl/g (0.1% in chloroform), stored at 2-8°C,
- Eudragit® RS PO (RS, MW = 150 000 Da, Evonik Industries),
- Polyvinyl alcohol (PVA, MW = 30 000 Da, 88% hydrolyzed, Sigma Aldrich). PVA was used as an aqueous solution at a concentration of 0.1% (w/v) and stored at 2-8°C,
- HPLC-grade acetonitrile (ACN),
- Trifluoroacetic acid (TFA, Sigma Aldrich),
- PBS pH 7.4,
- 2.3 M acetate buffer pH 4.3,
- 1.3 M acetate buffer pH 5.2,
- sCT enzyme-linked immunosorbent assay kit (Active® Ultra-Sensitive Salmon Calcitonin ELISA, Diagnostic Systems Laboratories, Inc.), stored at 2-8°C,
- Calcium kit Arsenazo III (Spinreact), stored at 2-8°C,
- Wistar rats.

Deionized water was used for all the experiments. All chemical reagents were of analytical grade, except for HPLC-grade solvents.

4.2.2. Methods

4.2.2.1. Preparation of salmon calcitonin-loaded nanoparticles

Nanoparticles were prepared by the double emulsion solvent evaporation technique (Figure 9), which has been well developed in the Department of Pharmaceutical Technology at Nancy University and previously described for nanoencapsulation of heparin (Hoffart, *et al.*, 2002) or insulin (Damge, *et al.*, 2007). Briefly, 0.5 ml of sCT solution (1 mg/ml) was first emulsified, by sonication for 30 s at 10 W (Vibra Cell 75022, Bioblock Scientific) in methylene chloride (3 ml) containing 250 mg of one polymer (PLGA H, PLGA S or RS) or a mixture of two polymers (1:1) (PLGA H/RS, PLGA S/RS). The obtained water/oil emulsion was then poured into 40 ml of 0.1% PVA solution (external aqueous phase) used as surfactant. The mixture was thereafter sonicated for 1 min at 10 W. The organic solvent was then quickly eliminated by evaporation under vacuum (Rotavapor) leading to immediate polymer precipitation in the form of nanoparticles. The resulting nanoparticles were recovered by centrifugation (42 000 × *g*, 20 min). After elimination of the clear supernatant, particles were suspended in deionized water and lyophilized. All the lyophilized nanoparticles were stored protected from light and moisture (desiccator) at 2-8°C for further analysis. Blank nanoparticles were obtained following the procedure described above with addition of a 5% acetic acid solution instead of sCT solution.

4.2.2.2. Characterization of salmon calcitonin-loaded nanoparticles

The mean diameter and polydispersity index of the nanoparticles were determined before lyophilization by PCS following appropriate dilution with deionized water. The zeta potential was measured by LDE upon dilution in a 1 mM NaCl solution. The PCS and LDE analysis were performed using a Zetasizer® 3000 HS (Malvern Instruments). Each sample was measured in triplicate. The surface topography and morphology of lyophilized nanoparticles were observed using scanning electron microscopy (SEM).

In order to determine the encapsulation efficiency (expressed in %) of sCT in nanoparticles, two alternative methods were used:

- Indirect method - the amount of non encapsulated sCT was measured in the supernatant obtained after centrifugation of the nanoparticle suspension just after

solvent evaporation during the particle preparation procedure. The encapsulation efficiency was calculated as the difference between the total amount of the drug used for the preparation and the amount of non encapsulated drug determined by HPLC.

- Direct (extraction) method - the amount of encapsulated sCT was determined after dissolving the nanoparticles in an organic solvent and extracting the peptide with an aqueous medium. The procedure was based on the established method of Blanco and Alonso (1997), but some modifications were introduced. Briefly, 10 mg of sCT-loaded nanoparticles were dissolved in 1 ml of ethyl acetate and the peptide was extracted into 3 ml of 0.1 M acetate buffer pH 5.2 containing 0.02% Tween 80 (w/v), by vortexing for 15 min. Thereafter, the aqueous phase containing the peptide was separated from the organic phase by centrifugation (3 900 rpm, 30 min). The extraction step was then repeated twice by adding the fresh buffer to the same organic phase followed by vortexing and centrifugation. The encapsulation efficiency of calcitonin in nanoparticles was calculated as the percentage of the encapsulated peptide (sum of the sCT amount derived from 3 extracts) with respect to the total amount of the peptide used for encapsulation.

4.2.2.3. Study on salmon calcitonin stability

The stability of calcitonin solution was studied at a concentration of 4 μg/ml at 37°C. The following media were used: 5% acetic acid solution, 2.3 M acetate buffer pH 4.3, PBS pH 7.4, 0.1 M HCl and 0.9% NaCl. Stability test was performed by adding sCT solution at a concentration of 100 μg/ml (0.8 ml) to the medium (19.2 ml) in flasks sealed and placed under magnetic stirring (200 rpm) into a constant-temperature water bath (37°C). Samples were periodically removed and the amount of the peptide was assayed by HPLC. The experiments were performed in triplicate.

4.2.2.4. Study on salmon calcitonin adsorption to blank nanoparticles

0.8 ml of sCT solution at a concentration of 100 μg/ml was added to 19.2 ml of 5% acetic acid solution or 0.1% PVA solution and incubated at 37°C under magnetic stirring (200 rpm) with 50 mg of blank nanoparticles. The samples were removed at predetermined time point, and then centrifuged (42 000 x *g*, 20 min). The amount of peptide in the supernatant was determined by HPLC. The experiments were performed in triplicate.

4.2.2.5. *In vitro* salmon calcitonin release from nanoparticles

50 mg of sCT-loaded nanoparticles were suspended in 20 ml of the release medium (5% acetic acid solution) containing 0.01% sodium azide (prevention of bacterial growth). The particle suspension was placed under gentle magnetic stirring (200 rpm) at 37°C. Then, 0.8 ml of suspension was withdrawn at each sampling time and replaced with an equal volume of the fresh release medium. Due to filter adsorption of sCT (established during the preliminary trials), each sample was centrifuged at 42 000 x *g* over 20 min. The supernatant was assayed by the HPLC method. The experiments were performed in triplicate.

4.2.2.6. HPLC assay for salmon calcitonin analysis

The method was developed on the basis of the literature data (Lee*, et al.*, 1992, Shah*, et al.*, 2003). The peptide was analyzed by reverse-phase HPLC using an LC-20AD pump, an on-line DGU-20A3 degasser, an SIL-20AC autoinjector, a CTO-20A column oven and a SPD-20A UV/VIS detector (all from Shimadzu Scientific Instruments, Inc.). The C_{18} column (Vydac 218TP54, 4.6 mm ID x 250 mm, 5 µm particle size, pore diameter of 300 Å) with a guard column (Vydac 218GD54) was equilibrated with 100% eluent A (25% ACN, 74.9% water, 0.1% TFA, v/v/v). The elution was performed using a linear gradient starting from 100% eluent A to 100% eluent B (55% ACN, 44.9% water, 0.1% TFA, v/v/v) over 20 min followed by the return to 100% eluent A and an isocratic step. The entire run program is presented in Table 10. A flow rate and column temperature were 0.8 ml/min and 35°C, respectively. Samples were injected into the column (injection volume - 50 µl) and detected at 210 nm. The tray compartment containing sample vials was cooled at 4°C. A calibration curve was constructed for each series of determinations. Concentrations of sCT in samples were quantified from integrated peak areas and calculated by interpolation from the calibration curve.

Each time, 5 standard solutions of sCT were performed for the calibration curve (1 injection per each standard) in an appropriate medium depending on the sample type:

- Standards prepared in a 5% acetic acid solution for the determination of sCT released from nanoparticles (*in vitro* drug release study, concentration range: 0.1 – 5 µg/ml)
- Standards prepared in a 0.1% PVA solution for the indirect determination of sCT encapsulation efficiency (concentration range: 1 – 20 µg/ml)

- Standards prepared in an acetate buffer pH 5.2 containing 0.02% of Tween 80 for the direct determination of sCT encapsulation efficiency (concentration range: 0.1 – 10 µg/ml).

Table 10. Composition of the mobile phase for sCT determination by HPLC (gradient elution).

Time (min)	Eluent A[a] (%)	Eluent B[b] (%)
0	100	0
20	0	100
25	100	0
35	100	0

[a] Eluent A – ACN : water : TFA (25 : 74.9 : 0.1), [b] Eluent B – ACN : water : TFA (55 : 44.9 : 0.1)

Table 11. Scheme of the preparation of sCT standard solutions in various media (5% CH_3COOH, 0.1% PVA or acetate buffer pH 5.2/0.02% Tween).

Standard	1_D	2_D	3_D	4_D	5_D	6_D	7_D	8_D
Volume (µl) of sCT primary standard (1 µg/ml)	100	250	500	-	-	-	-	-
Volume (µl) of sCT primary standard (10 µg/ml)	-	-	-	100	250	500	-	-
Volume (µl) of sCT primary standard (100 µg/ml)		-	-	-	-	-	100	200
Medium (µl)	900	750	500	900	750	500	900	800
sCT concentration in standard solution (µg/ml)	**0.1**	**0.25**	**0.5**	**1.0**	**2.5**	**5.0**	**10.0**	**20.0**

A series of standard solutions (5 different points depending on the concentration range) were performed in 1.5 ml Eppendorf tubes according to the Table 11, using sCT primary standards of appropriate concentration (1, 10 or 100 µg/ml) prepared from the sCT stock solution (1 mg/ml) in the appropriate medium.

4.2.2.7. DSC study

Differential scanning calorimetry (DSC) measurements were carried out using a DSC XP-10 apparatus (heat flux DSC, Thass). Samples were prepared by weighing ~ 3 - 6 mg of pure polymers, blank nanoparticles or sCT-loaded nanoparticles into an aluminum pan and then hermetically sealed. An empty pin-holed aluminum pan was used as a reference. Both the reference pan and the sample pan were allowed to equilibrate isothermally for 5 min at 0°C under nitrogen atmosphere. The pans were then heated at a rate of 10°C/min from 0 to 100°C, after 5 min quench cooled to -20°C at 20°C/min (to eliminate any sample history), and then heated again from -20°C to 100°C at 10°C/min. The glass transition temperature (T_g) was reported as the mid-point of the corresponding transition in the second heating.

4.2.2.8. *In vivo* studies

Subcutaneous administration in rats (Department of Pharmaceutical Technology, Nancy)

Experiments were carried out in accordance with the European Community Council Directive of November 24, 1986 (86/609/EEC) and the French system (personal authorization, certificate number of Prof. P. Maincent: 54-68 delivered on April 13, 2006 by Prefecture de Meurthe et Moselle).

Male Wistar rats weighing 250–450 g were maintained in conditions of 12 h-day light cycles and had free access to food and water. All rats were fasted overnight before and during all the experimentations, but allowed free access to water. Three or four groups (each group consisted of 5 rats) were subjected to the treatment. The animals were anaesthetized by an intraperitoneal injection of sodium pentobarbital (60 mg/kg) with additional doses given intraperitoneally when necessary during 10-12 h of the experiments, and finally once anaesthetized after 24 h after administration for the last sampling. The scheme of the procedure is presented in Figure 10. Solution of sCT (reference) in 0.9% NaCl was administered subcutaneously just below the neck region at a dose of 50 µg/kg (~ 300 IU/kg). The freshly prepared nanoparticles were suspended in 0.9% NaCl and injected as above at an equivalent calcitonin dose of 100 µg/kg (~ 600 IU/kg).

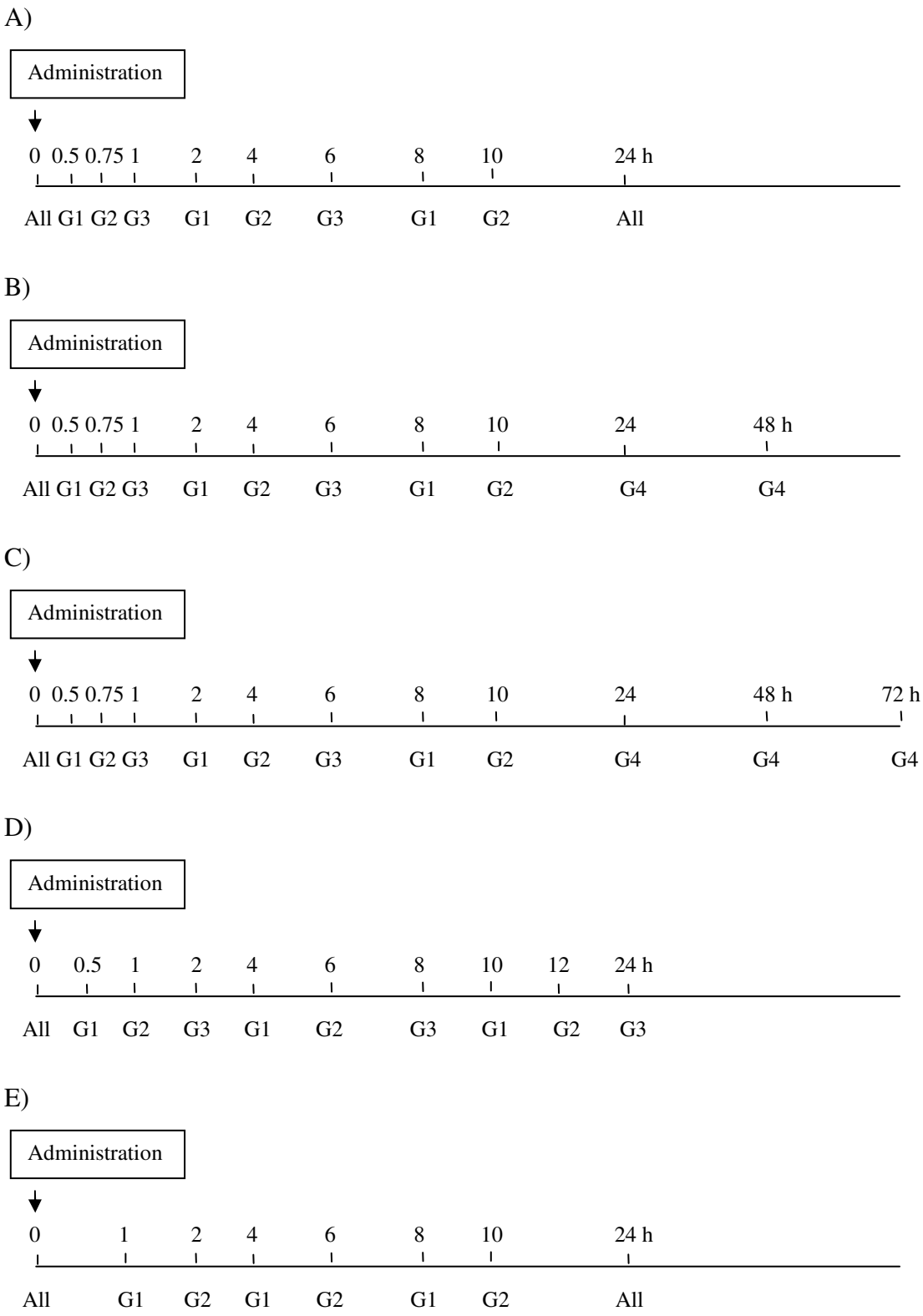

Figure 10. Blood sampling schedule for each group (G) of rats after single subcutaneous administration of: A) sCT solution; B) sCT-loaded RS nanoparticles; C) sCT-loaded PLGA H nanoparticles or sCT-loaded PLHA H/RS nanoparticles; or after single oral administration of: D) sCT solution and three types of sCT-loaded nanoparticles (RS, PLGA H/RS, PLGA H); and E) blank nanoparticles.

The doses were calculated on the basis of encapsulation efficiency for each formulation. The volume of sc injection was 250-500 µl depending on the body weight. Four series of the experiment were conducted for the single administration of the following: sCT solution, sCT-loaded PLGA H nanoparticles, sCT-loaded RS nanoparticles, sCT-loaded PLGA H/RS nanoparticles. Blood samples were collected through cardiac puncture from one group of rats at predetermined interval time after injection, and the groups were taken alternately. Thus, each animal had only 2-3 blood samplings within one day. After the experiment the rats were sacrificed. All the blood samples were allowed to clot over 30 min at 4°C, then centrifuged (3 000 × *g*, 15 min, 4°C) to separate the serum. Thereafter, the serum was frozen and stored at -20°C until the time of analysis. Serum samples were analyzed for sCT using an ELISA kit.

The area under the sCT concentration *versus* time curve (AUC) was calculated by the linear trapezoidal method from time 0 to the last time point. Relative bioavailability of sCT loaded in nanoparticles measured against sCT solution (both administered subcutaneously) was calculated as follows:

$$\textbf{\textit{Relative bioavailability [\%]}} = \frac{AUC_{nanoparticles} xDose_{solution}}{AUC_{solution} xDose_{nanoparticles}} x100$$

Oral administration in rats (Department of Pharmaceutical Technology, Poznań)

The experiments were approved by the Local Ethical Committee of the Poznan University of Medical Sciences (permission number 83/2006 delivered on May 15, 2006). The animals (male Wistar rats) were supplied by the Department of Toxicology, Poznan University of Medical Sciences, where the experiments were carried out. The principal of this *in vivo* study was similar to that described above, however, there were some essential differences:

- Weight of rats between 380-420 g,
- There were 3 groups consisted of 7 rats for single administration of sCT solution, sCT-loaded PLGA H nanoparticles, sCT-loaded RS nanoparticles, or sCT-loaded PLGA H/RS nanoparticles,
- There were 2 groups consisted of 4 rats for single administration of 3 blank nanoparticle formulations (RS, PLGA H/RS, or PLGA H),

- Additionally, the day before the experiment, a single blood taking was performed from all the rats in order to obtain samples for determination of normal serum calcium levels in rats (basal),
- Rats were anaesthetized for the duration of blood sampling with diethyl ether just before the cardiac puncture,
- All the formulations (sCT solution or suspension of nanoparticles loaded with sCT or blank nanoparticles) were given intragastrically (1 ml) and sCT dose was ~ 1 000 IU/kg (~ 167 µg/kg),
- All the formulations were lyophilized before administration (~50 mg of lyophilized nanoparticles/rat),
- Blood samples were taken as presented in Figure 10 D) and E),
- After blood centrifugation, the obtained serum from each rat was divided into 2 aliquots for the determination of either sCT or calcium concentration.

4.2.2.9. Determination of salmon calcitonin in rat serum by ELISA

The Active® Salmon Calcitonin Enzyme-Linked Immunosorbent (ELISA) kit is an enzymatically amplified 'two-step' sandwich-type immunoassay involving the biotin-streptavidin bridging detection system. The kit is originally intended for the quantitative measurement of sCT in human serum. The principle of the method is shown in Figure 11.

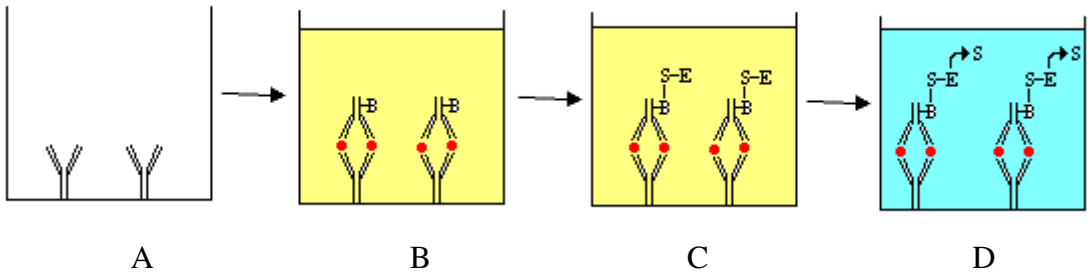

Figure 11. Schematic representation of the principle of ELISA for sCT determination in serum: A) primary antibody coated well; B) antigen (calcitonin) binds to primary antibody and a secondary biotinylated antibody binds to immobilized antigen; C) streptavidin-enzyme conjugate links to biotin-antibody conjugate; D) substrate is added and converted by enzyme into colored product (red circles - calcitonin, B - biotin, S - streptavidin, E - enzyme, S - substrate).

Ready to use 96-well plate with an anti-sCT primary antibody immobilized to the inside wall of wells is supplied in the kit (Figure 11 A). In the assay, standard (STD), control (CTR) or unknown serum sample is incubated with a biotinylated anti-sCT antibody in

microtitration wells which are already coated with another anti-sCT antibody (primary antibody) immobilized to the inside wall of each well (Figure 11 B). After incubation and washing, the wells are then incubated with streptavidin labeled horseradish peroxidase enzyme (Figure 11 C).

Table 12. ELISA procedure for preparation of a calibration curve and sCT determination in rat serum (subcutaneous administration).

	Blank	STD 1	STD 2	STD 3	STD 4	STD 5	CTR 1	CTR 2	Sample
Volume (µl) of primary sCT standard (100 pg/ml)	0	20	50	0	0	0	40	0	0
Volume (µl) of primary sCT standard (1000 pg/ml)	0	0	0	20	50	100	0	40	0
Volume (µl) of pooled rat serum	200	180	150	180	150	100	160	160	0
Volume (µl) of the unknown sample	0	0	0	0	0	0	0	0	200
sCT concentration in a well (pg/ml)	**0**	**10**	**25**	**100**	**250**	**500**	**20**	**200**	**unknown**
Antibody-biotin solution (µl)	50								
Procedure	Incubation for 3 h on an orbital microplate shaker (700 rpm, room temperature ~23°C)								
Procedure	Aspiration and washing of each well 5 times with the wash solution using an automatic microplate washer								
Streptavidin-enzyme conjugate solution (µl)	100								
Procedure	Incubation for 30 min on an orbital microplate shaker (700 rpm, room temperature ~23°C)								
Procedure	Aspiration and washing of each well 5 times with the wash solution using an automatic microplate washer								
TMB Solution (µl)	100								
Procedure	Incubation for 30 min on an orbital microplate shaker (700 rpm, room temperature ~23°C)								
Stopping Solution (µl)	100								
Procedure	Reading the absorbance (against pooled blank rat serum) of the solution in the wells using a microplate reader (dual wavelength measurement at 450 nm with background wavelength correction set at 600 nm)								

After this second incubation and washing step, the wells are next incubated with the substrate tetramethylbenzidine (TMB, supplied as a TMB solution in citrate buffer with hydrogen peroxide) (Figure 11 D). An acidic stopping solution (0.2 M sulfuric acid) is then added and the degree of enzymatic turnover of the substrate is determined by dual wavelength absorbance measurement at 450 and 620 nm (background) – if available. The absorbance of the coloured product is proportional to the concentration of sCT present in analyzed solutions. A set of sCT standards is used to plot a calibration curve of absorbance *versus* sCT concentration.

More specifically, the assay was performed as presented in Table 12. Standards and controls were supplied in the kit (vials with lyophilized human serum containing sCT for reconstitution in water). Nevertheless, the kit had to be validated for the determination of sCT in rat serum. Therefore, sCT standard solutions and controls were prepared each time (final volume of 200 µl/well) by a series of dilutions of the stock sCT solution in pooled normal rat serum (Table 12). Standards and controls were assayed in duplicate or triplicate. The unknown serum samples were assayed once or in duplicate if available without or with dilution if necessary. All the reagents were prepared according to the instructions. In more details, the concentrate of streptavidin conjugated to horseradish peroxidase in a protein-based buffer had to be diluted 10-15 min prior to use in the assay buffer. The concentrate of biotinylated anti-sCT detection antibody in a protein-based buffer was also diluted prior to use in the assay buffer. Wash solution containing buffered-saline with a nonionic detergent was prepared by diluting wash concentrate 25-fold with deionized water prior to use.

4.2.2.10. Spectrophotometric determination of calcium (II) in rat serum

Calcium (II) with the Arsenazo III reagent (120 mM of 1,8-dixydroxy-3,6-disulpho-2,7-naphthalene-bis(azo)-dibenzenearsonic acid and 100 mM imidazol buffer pH 6.5) yields a blue colored complex (λ_{max} = 650 nm) at neutral pH. The intensity of the color formed is proportional to the calcium concentration in the sample. The procedure is presented in Table 13. After agitating (vortex) of the reagent with the standard or sample, the mixture was left for 2 min at least before reading the absorbance (the color is stable for at least 1 h). Only one standard solution was used (calcium aqueous standard at a concentration of 10 mg/dl, supplied in the kit). In order to monitor the performance of the assay procedures, control sera were used: Spintrol H Normal (normal human serum, calcium concentration: 8.60 mg/dl) and

Spintrol H Pathologic (pathologic human serum with an increased calcium content: 13.4 mg/dl).

Table 13. Scheme of procedure for calcium determination in rat serum

	Blank	Standard	Sample
Arsenazo III reagent (ml)	1.0	1.0	1.0
Standard (µl)	-	10	-
Sample (µl)	-	-	10

4.2.2.11. Statistical analysis

Statistical data analysis was performed using the Student's *t*-test (normal distribution) or the Mann-Whitney U test (non-normal distribution) with $p \leq 0.05$ as the minimal level of significance. Calculations were done using the software Statistica version 6.0 (StatSoft).

5. RESULTS

5.1. Encapsulation of glutathione-selective fluorogenic probes

5.1.1. Validation of the HPLC method

The main scopes for the development of the HPLC technique were:

- to enable the determination of encapsulation efficiencies of NDA and OPA in the nanoparticles by the direct (complete dissolution of the probe-loaded particles allowing the measurement of the released probe) or indirect method (measurement of the non encapsulated probe in the external aqueous phase),
- to enable the determination of *in vitro* probe release from nanoparticles,
- to verify the real uptake of the probe by yeast cells and to estimate its reactivity level with GSH inside the cells (measurement of the NDA-GSH adduct in yeast extracts).

Thus, it was necessary to settle a common method which can identify and quantify both the free probe and the resulting probe-GSH adduct in biological samples. For this purpose, a classical isocratic reversed-phase HPLC technique was used and quantification was operated using standard solutions of the probe derivatized with an excess of GSH. Derivatization process and operating conditions for OPA were analogical to those for NDA with the exception of the mobile phase composition and the excitation-emission wavelengths (see section 4.1.2.4). The non-biological samples (determination of encapsulation efficiencies of NDA and OPA, *in vitro* probe release) needed the derivatization process before injection into the HPLC system, whereas the biological samples did not (yeast extracts). The fact that the derivatization of NDA was applied with the use of GSH, not in reverse, needs to be emphasized. The probe-GSH adducts could be detected both spectrophotometrically and spectrofluorimetrically. In the case of biological samples, which had lower levels of the analyte compared to non-biological samples, more sensitive spectrofluorimetric detection was used.

This method has been previously developed and validated (Martenka, 2004, Diez*, et al.*, 2005), but it has been slightly modified for the needs of this project. Some of previous results concerning the development and validation of the HPLC method are briefly listed herein.

Within the optimization of the derivatization process, formation of the NDA-GSH adduct in 0.2 M borate buffer pH 9.2 at room temperature as a function of reaction time and its stability at 4°C were studied. As a result, the optimal and retained in further analysis derivatization reaction time was 15 min. In terms of the adduct stability, no significant signal decrease was observed over an 1 h storage period at 4°C (Martenka, 2004, Diez*, et al.*, 2005). However, with regard to incubation of cells with NDA, formation of the NDA-GSH adduct in PBS medium pH 7.0 after 15-min derivatization was confirmed, but the adduct was not stable and the sample should be injected practically within 5 min after the adduct formation (Martenka, 2004).

The additional study was performed in order to compare the NDA-GSH adduct formation at various pH. Since the complete dissolution of Eudragit® E – composed nanoparticles can occur only in acidic pH, the ability of adduct formation from a very acidic sample was tested as well as for pH 7.0 (PBS) compared to standard pH 9.2. As seen in Table 14, after 15-min derivatization of NDA with GSH at a concentration of 20 µg/ml, the mean peak area was 92.4% and 110.3%, respectively, compared to the reference mean peak area for pH 9.2. Nevertheless, the samples were diluted 10-fold for the derivatization reaction with the borate buffer pH 9.2, the obtained results could indicate sufficient recovery of NDA from the acidic medium after the dissolution of nanoparticles.

Table 14. Stability results of NDA-GSH adduct formation at various pH.

Sample	Acidic pH		Neutral pH		Alkaline pH	
	Peak area	Mean	Peak area	Mean	Peak area	Mean
1	247,16	234,60	286,38	276,2	246,63	247,36
	222,04		266,02		248,08	
2	226,64	225,63	254,1	251,54	250,38	241,05
	224,62		248,98		231,72	
3	214,43	200,19	262,54	260,08	237,81	226,15
	185,95		257,61		214,48	
Mean	220,14		262,61		238,18	
S.D.	17,85		12,52		10,89	
R.S.D.(%)	8,11		4,77		4,57	

Validation of this HPLC technique was recently described in the report of Diez *et al.* (2005) and realized concerning the following points: selectivity, linearity of calibration curves, limit of detection (LOD), limit of quantification (LOQ) and repeatability of peak areas

for 3 levels of concentration. Selectivity was tested *versus* the blank reagent containing NDA but no GSH (no peak observed) and with regard to different amino acids (cysteine, histidine, histamine, arginine) and a dipeptide (γ-GluCys). All these amino acids and the dipeptide (precursor of GSH in cells which exists at very low levels in most cells) can potentially react with NDA in cells. The experimental approach consisted in derivatization of NDA with these compounds, instead of GSH, and at the same concentration than GSH. Based on the obtained results, the selectivity of the method was confirmed. The calibration curves were linear for the large range of the probe concentration with either the spectrophotometric (2-30 µg/ml) or spectrofluorimetric detection (2-500 ng/ml). LOD and LOQ were 0.7 ng/ml with a signal-to-noise ratio (S/N) of 3, and 1.7 ng/ml with S/N = 10, respectively (Diez*, et al.*, 2005).

A typical HPLC chromatogram corresponding to a NDA standard solution derivatized with GSH is shown in Figure 12 A.

5.1.2. Characterization of the probe loaded-nanoparticles

The preparation of the probe-loaded nanoparticles was based on an oil/water emulsification solvent evaporation method using 3% PVA solution as a surfactant and 5 min-period of ultrasonication for emulsion formation. The obtained nanoparticles were characterized in terms of size, polydispersity index, zeta potential, encapsulation efficiency and yield of production. These properties are summarized in Table 15.

The mean particle size of both blank nanoparticles (i.e. without OPA or NDA), and the probe-loaded particles was in the range 210 – 220 nm. Similarly, the zeta potential of OPA- and NDA-loaded nanoparticles was very close to that measured with blank nanoparticles (approximately +42 mV). Each formulation had a low polydisperisty index, meaning a narrow particle size distribution as seen in Table 15.

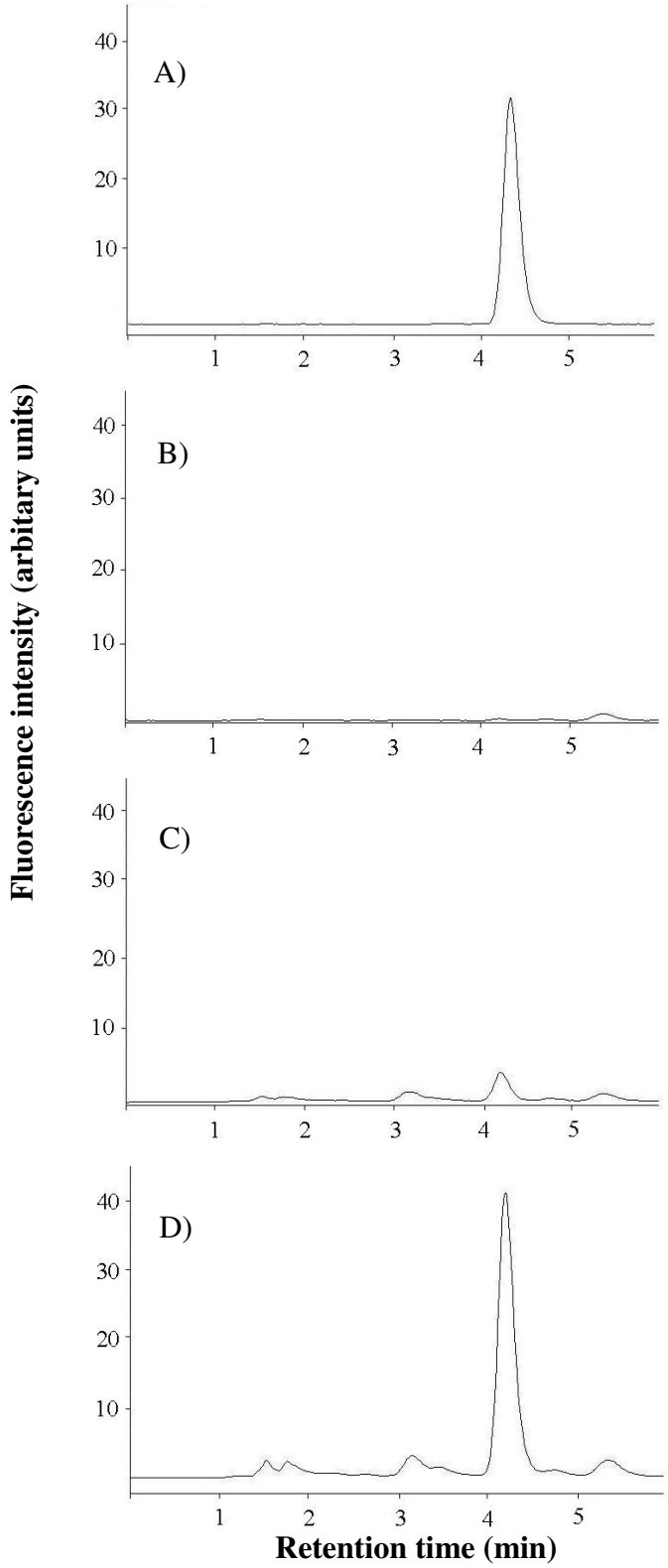

Figure 12. Typical HPLC chromatograms corresponding to: A) a NDA standard solution at a concentration of 0.54 µM derivatized with an excess of GSH; B) cells incubated without NDA; C) cells incubated for 20 min with 100 µM of NDA; D) cells incubated for 20 min with nanoparticles at a concentration of 100 µM of NDA. Cells were extracted with borate buffer pH 9.2 after a freezing cycle.

Table 15. General characteristics of the blank nanoparticles, OPA- and NDA-loaded nanoparticles. All results are shown as means ± S.D.

	Blank nanoparticles	OPA-loaded nanoparticles	NDA-loaded nanoparticles
Size (nm)	221.5 ± 5.5 (n = 3)	210.7 ± 6.6 (n = 3)	220.5 ± 14.0 (n = 4)
Polydispersity index	0.10 ± 0.03 (n = 3)	0.09 ± 0.04 (n = 3)	0.14 ± 0.02 (n = 4)
Zeta potential (mV)	42.1 ± 3.0 (n = 3)	44.9 ± 0.8 (n = 3)	41.5 ± 4.2 (n = 3)
Encapsulation efficiency (%) (direct method)	-	2.1 ± 0.2 (n = 3)	48.6 ± 8.2 (n = 3)
Encapsulation efficiency (%) (indirect method)	-	-	74.4 ± 4.2 (n = 3)
Production yield (%)	27.4 ± 8.5 (n = 3)	25.0 ± 0.4 (n = 3)	37.6 ± 12.1 (n = 4)

Encapsulation efficiency of OPA and NDA in lyophilized nanoparticles was determined directly by the complete dissolution of nanoparticles in acidic medium, and then HPLC analysis after derivatization reaction of the released probe. As indicated in Table 15, a higher encapsulation efficiency was observed for NDA than for OPA: 48.6 ± 8.2% and 2.1 ± 0.2%, respectively. However, the encapsulation efficiency of NDA determined by the indirect method (approximately 74%) was questionable and did not correlate with the results obtained by the direct method. The production yield of nanoparticles was rather low, but satisfying together with the encapsulation efficiency with respect to the dose needed for a biological application in yeast cells.

Figure 13 illustrates the *in vitro* release profiles of NDA from nanoparticles at pH 1.0 and 7.0, by representing the percentage of NDA release with respect to the amount of NDA encapsulated. In the acidic medium, a complete release of the probe was almost immediately observed. At pH 7.0 the release profile was characterized by a large initial amount of the probe released (about 70%), followed by a progressive and incomplete release up to 1 h. The incomplete release of the probe from nanoparticles resulted probably from the short time of the release study (60 min), but a complete release could be expected within 2 h. It should be

mentioned that a longer period of NDA release study was not appropriate to the fact that the cells loading with NDA encapsulated in nanoparticles was conducted within only 20 min.

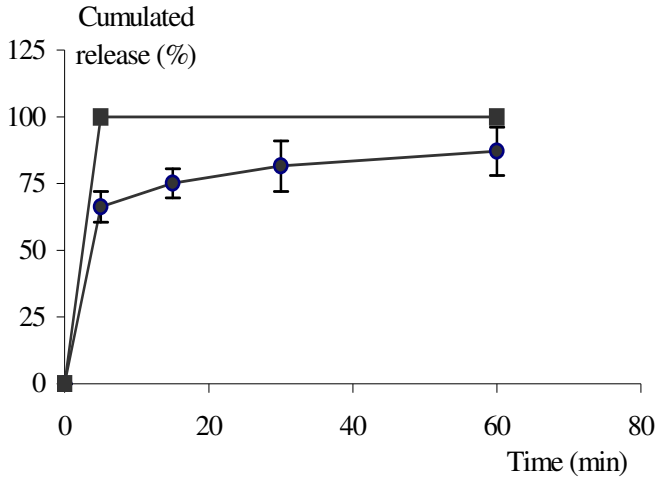

Figure 13. Percentage of NDA released from the corresponding loaded nanoparticles in PBS solution pH 7.0 (full circle) or in 0.1 M HCl solution (full square) at 20 ± 2°C. Data are presented as means ± S.D. (n = 3).

5.1.3. Loading of cells with NDA

The main scope of the present work was to evaluate the possible improvement of NDA uptake by cells using nanoparticles. The experiments were performed using previously optimized NDA concentration and loading time: 100 µM and 20 min, respectively (Diez*, et al.*, 2005) in order to compare between uptake of free NDA and NDA from nanoparticles. Typical chromatograms corresponding to extracts from yeast cells loaded with the free probe or the probe-loaded nanoparticles are shown in Figure 12 C-D. The concentration of the NDA-GSH adduct in each extract was calculated in pmol per mg of total protein. A calibration curve for the determination of the total protein concentration in cell extracts is presented in Figure 14.

A NDA-GSH adduct concentration of 22.74 ± 10.12 pmol/mg protein (n = 5) was found in cell extracts after incubation with NDA-loaded nanoparticles, which appears 9.2-fold more in comparison with incubation with the free NDA (2.46 ± 0.99 pmol/mg protein; n = 5) (Figure 15).

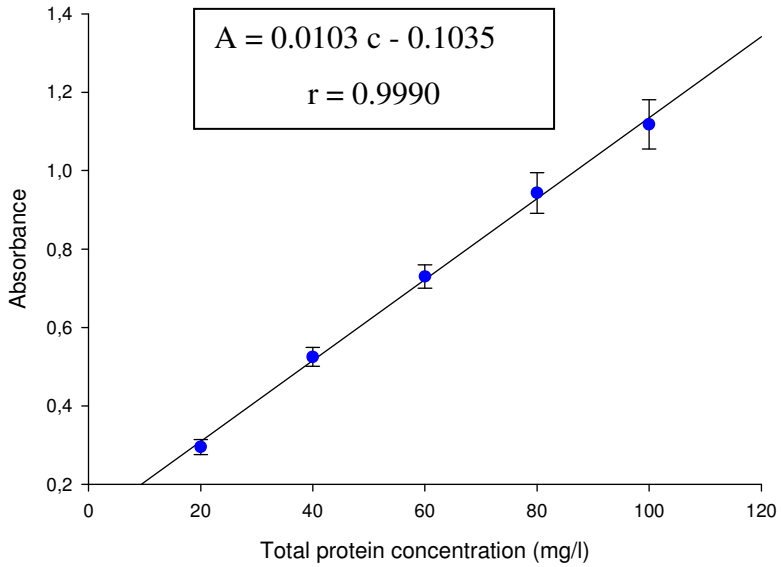

Figure 14. Calibration curve for the determination of total protein concentration according to BCA method (mean value from 5 independent curves ± S.D.).

In order to verify the ability of NDA-loaded nanoparticles to monitor variations of GSH concentration in the yeast strain, the cellular GSH level was varied with BSO. Cells were treated or not with 5 mM BSO added to the culture medium for 3 h before the incubation with NDA-loaded nanoparticles. The cellular NDA-GSH adduct concentration decreases of 39.0 ± 3.4% (n = 3) in presence of BSO, which demonstrates the usefulness of NDA-loaded nanoparticles to detect cellular GSH variations (Figure 16).

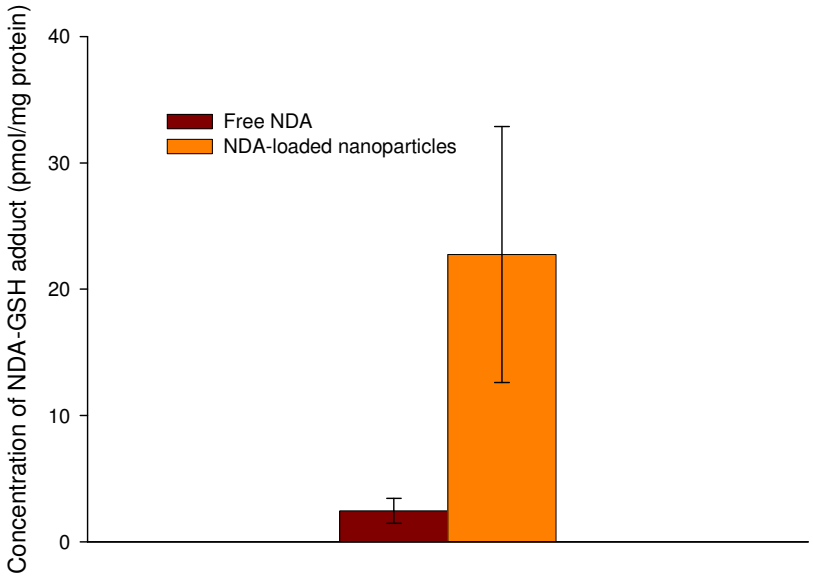

Figure 15. Comparison of NDA-GSH adduct concentration in yeast cell extracts after 20-min incubation with 100 µM of the free probe or with the equivalent amount of NDA-loaded nanoparticles. Values are the means of 5 independent experiments ± S.D.

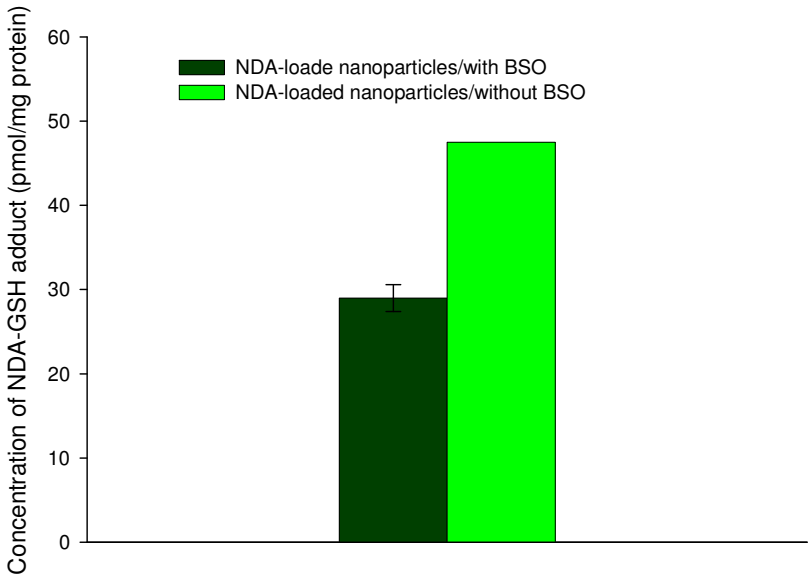

Figure 16. Comparison of NDA-GSH adduct concentration in yeast cell extracts after 20-min incubation with NDA-loaded nanoparticles at a concentration of 100 µM without (n = 1) or after treatment with BSO (n = 3). Values are shown as mean ± S.D.

5.1.4. Cytotoxicity of nanoparticles and NDA

At last, the impact of NDA and corresponding nanoparticles on the viability of yeast cells was tested. The difficulty was that NDA caused the change of the color of yeast pellets especially visible with the naked eye at a concentration of NDA ≥ 100 µM (from beige to brown with increasing the concentration from 100 to 1 000 µM, data not shown). This phenomenon interfered with the measurement of the blue color appearance resulting from the formazon formation from MTT by viable cells. The problem was solved that the absorbance of the cells untreated with NDA (control cells and cells treated with the blank nanoparticles) was read against the sterile medium (as for the calibration curve in order to calculate the number of cells). However, the absorbance of the cells treated with free NDA or NDA-loaded nanoparticles was read against the absorbance of the cells treated with NDA or NDA-loaded nanoparticles (the same NDA concentration), but not treated with MTT. A typical calibration curve showing the relationship between absorbance of formazon produced by vital cells and cell number is presented in Figure 17.

Detailed results concerning the cytotoxicity of either blank nanoparticles, free or encapsulated NDA are summarized in Table 16. For each tested product, at least 3 sets of

experiment were carried out (3 independent cultures). In each experiment for a given product, the determination of cell viability was performed in triplicate (incubation of yeast cells with the product following MTT assay). Based on the mean absorbance, the cell number was calculated from the calibration curve. In turn, number of vital cells after the incubation with the tested product was compared to the number of untreated cells and expressed in percentage to calculate cell viability.

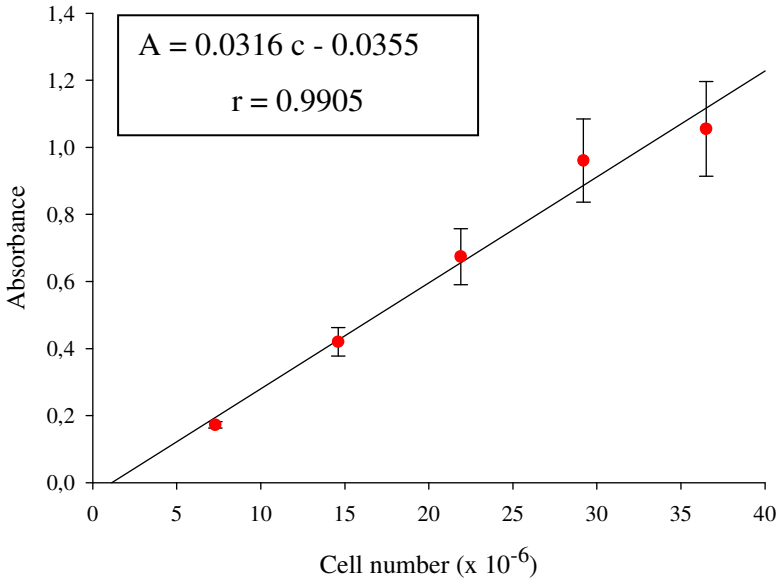

Figure 17. Calibration curve for the determination of cell number according to MTT assay (mean values ± S.D., n = 3).

As seen in Figure 18, based on the MTT test results, calculated viability of a *Candida albicans* strain after 20-min treatment with blank nanoparticles, 100 µM of free NDA, or an equivalent concentration of NDA encapsulated in nanoparticles, was 94.4 ± 12.1 (n = 6), 51.5 ± 18.3 (n = 6) and 96.1 ± 20.2% (n = 3), respectively. It appears that blank nanoparticles do not affect viability of yeast cells. In the considered experiment, the concentration of blank nanoparticles was 0.8 mg/ml (the same as that for NDA-loaded nanoparticles). Additionally, the higher concentration of blank nanoparticles were also tested (1.6 and 2.4 mg/ml) and the obtained cell viability was practically unchanged after incubation with the higher concentration of blank nanoparticles (90.5 ± 6.6 and 102.6 ± 8.1%, respectively, n = 3, data not shown).

Table 16.The processing way of selected data concerning the cytotoxicity study.

Culture treatment	A 1	A 2	A3	Mean	Cell number (x 10^{-6})	**Viability (%)**
Culture 1						
untreated (control)	0.575	0.681	0.702	0.653	21.78	100.00
blank nanoparticles	0.668	0.681	0.704	0.684	22.78	**104.60**
NDA solution	0.461	0.324	0.459	0.415	14.25	**65.42**
NDA – nanoparticles	0.424	0.438	0.541	0.468	15.92	**73.12**
Culture 2						
untreated (control)	0.807	0.818	0.992	0.872	28.73	100.00
blank nanoparticles	0.699	0.624	0.765	0.696	23.15	**80.58**
NDA solution	0.570	0.623	0.637	0.610	20.43	**71.10**
NDA – nanoparticles	0.926	0.895	1.099	0.973	31.93	**111.13**
Culture 3						
untreated (control)	0.805	0.750	0.707	0.754	24.98	100.00
blank nanoparticles	0.681	0.627	0.740	0.683	22.73	**90.96**
NDA solution	0.483	0.415	0.595	0.498	16.87	**67.53**
NDA - nanoparticles	0.712	0.663	0.986	0.787	26.03	**104.18**

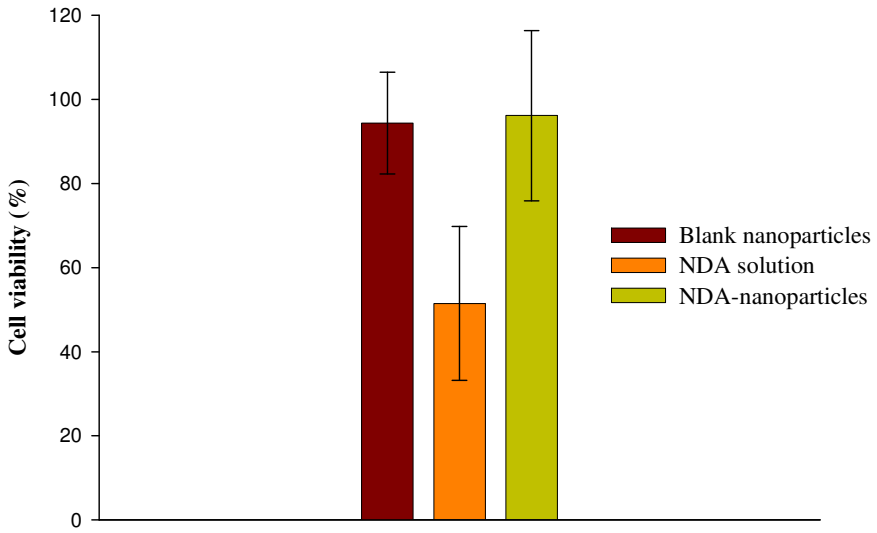

Figure 18. Comparison of cell viability after 20-min incubation with blank nanoparticles, NDA solution (n = 6) or NDA-loaded nanoparticles (n = 3) (final NDA concentration: 100 µM). Values are shown as mean ± S.D.

Simultaneously, NDA-loaded nanoparticles had a very high mean cell viability, however, a large distribution of results was seen (n = 3). As shown in Figure 18, the lowest viability of cells, suggesting a cytotoxic effect of the tested product, was observed after treatment with non-encapsulated NDA, with the minimum and maximum result of 31.6 and 71.1%, respectively (n = 6). Moreover, two additional NDA concentrations were tested (50 and 200 μM) as free NDA (data not shown). Observed viability of yeast cells were 36.6 ± 8.0% and 27.0 ± 7.0%, respectively. Surprisingly, even a lower cell viability was detected with the lower NDA concentration. Nevertheless, the evidence was that NDA solutions at the tested concentrations were cytotoxic against *Candida albicans* after 20-min treatment.

5.2. Encapsulation of salmon calcitonin

5.2.1. Method validation of salmon calcitonin determination by HPLC

The optimized analytical procedure for sCT determination by HPLC was evaluated for selectivity, linearity, detection and quantification limits (LOD,LOQ), and accuracy/precision.

- Selectivity

Before qualitative and quantitative analysis of sCT in the drug release medium (5% acetic acid solution) and two media for the indirect or direct determination of sCT encapsulation efficiency (0.1% PVA solution and acetate buffer pH 5.2/0.02% Tween 80, respectively), the selectivity of HPLC method was confirmed by the lack of peaks corresponding to the retention time of sCT (17.0 min) in the HPLC chromatograms of analyzed blanc solutions or samples of blank nanoparticles.

- Linearity

Identification and quantification of sCT in various media were performed by the HPLC method. sCT was identified by a comparison of the retention time of the peak in the chromatograms of standard sCT solution and the analyzed samples. Quantitative measurement of sCT was carried out on the basis of peak areas. The linear dependence between peak areas and sCT concentrations in standard solutions was examined. The parameters of the calibration curve equations and the correlation coefficients in three media were calculated (Table 17). As seen in Table 17, the linear regression was characterized by good correlation coefficients ($r \geq 0.999$).

- Detection and quantification limits

The LOD (signal-to-noise ratio = 3) was equal to 0.05 µg of sCT/ml, while the LOQ (signal-to-noise ratio = 10) was 0.1 µg of sCT /ml.

- Accuracy and precision

The inter-day accuracy and precision of the sCT determination by HPLC were determined by mean recovery and relative standard deviation (R.S.D.), respectively (Table 18). The accuracy of the method was estimated for three sCT concentrations in standard solutions (the lowest, medium and the highest within the calibration curve range) for each medium type, and expressed as mean recovery. The precision was estimated for the same sCT concentrations in standard solutions (the lowest, medium and the highest) for each medium

type (Table 18). The precision was expressed as R.S.D [R.S.D.% = (S.D. × 100)/mean sCT concentration].

Table 17. The parameters of inter-day calibration curves of sCT determination by HPLC prepared in various media (5% acetic acid solution; 0.1% PVA solution; acetate buffer pH 5.2/0.02% Tween 80) (mean ± S.D., n=3).

Parameter	Medium		
	5% CH_3COOH	**0.1% PVA**	**Acetate buffer/Tween**
Linearity range (µg/ml)	0.1 – 5.0	1.0 – 20.0	0.1 – 10.0
Coefficient of correlation (r)	0.9990 ± 0.0008	0.9994 ± 0.0005	1.000 ± 0.0000
Slope (a)	130 450 ± 3 796	131 686 ± 21 476	139 515 ± 71
Intercept (b)	-22 640 ± 10 395	-81 557 ± 22 626	-3 474 ± 4 247

Table 18. The inter-day precision (R.S.D.%) and accuracy (mean recovery) of the HPLC method for sCT determination in various media (A - 5% acetic acid solution; B - 0.1% PVA solution; C - acetate buffer pH 5.2/0.02% Tween 80) (n = 3).

A)

sCT concentration in standard solution (µg/ml)	Recovery ± S.D. (%) (Accuracy)	R.S.D. (%) (Precision)
0.1	219.0 ± 76.2	23.2
1.0	94.5 ± 4.8	12.8
5.0	100.5 ± 1.1	1.7

B)

sCT concentration in standard solution (µg/ml)	Recovery ± S.D. (%) (Accuracy)	R.S.D. (%) (Precision)
1.0	122.1 ± 21.4	22.4
5.0	93.5 ± 4.4	24.9
20.0	100.2 ± 0.6	16.6

C)

sCT concentration in standard solution (µg/ml)	Recovery ± S.D. (%) (Accuracy)	R.S.D. (%) (Precision)
0.1	118.0 ± 26.3	4.4
1.0	96.5 ± 6.0	6.3
10.0	100.1 ± 0.2	0.1

5.2.2. Method validation of salmon calcitonin determination by ELISA

Although, the commercial kit was validated, preliminary trials were taken to check whether the change of the human serum into rat serum could influence the parameters of the calibration curves. First, the sCT standards in human serum of the kit (concentrations: 0; 7; 22; 120; 330; 450 pg/ml) were 2-fold diluted in pooled rat serum, and no influence was observed for the calibration curve parameters (very similar equations) and level of recovery for sCT controls of the kit. Then, the calibration curve was constructed only in rat serum by appropriate dilutions of sCT stock solution (1 mg/ml) in pooled rat serum (concentrations: 0; 10; 25; 100; 250; 500 pg/ml) (Figure 19). Moreover, an attempt was made that sCT standards in rat serum were spiked with additional amounts of rat calcitonin. However, no significant change was observed for the parameters of the calibrations curve equation, indicating that no cross reaction occurred over the calibration curve range, i.e. the assay is highly specific for sCT, and rat calcitonin was not detectable.

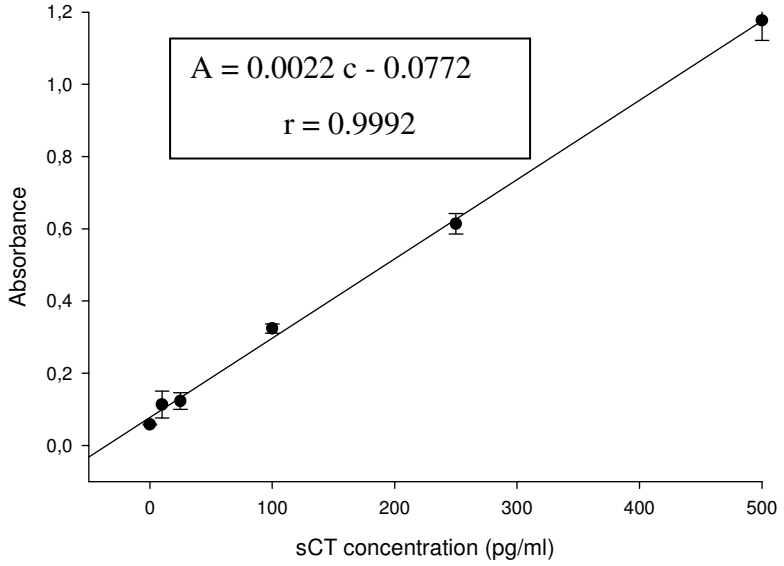

Figure 19. Typical calibration curve for sCT determination in rat serum by ELISA (subcutaneous administration) (mean ± S.D., n = 3).

The LOQ of sCT in rat serum was equal to 20 pg/ml and was calculated by interpolation of the mean absorbance plus 3 standard deviations (S.D.) of 3 replicates of the pooled blank rat serum. For the concentration range of sCT between 10 and 500 pg/ml (Figure 19) the calibration curves exhibited a good linearity with $r \geq 0.99$. The precision (expressed as R.S.D.%) and the accuracy (expressed as mean recovery of sCT) of sCT determination in rat serum (subcutaneous administration) are presented in Table 19.

Table 19. The intraday and interday precision (R.S.D. %) and accuracy (mean recovery in %) of sCT determination in rat serum by ELISA (subcutaneous administration).

sCT concentration in control solution (pg/ml)	R.S.D. (%) (Precision)		Recovery ± S.D. (%) (Accuracy)	
	Intraday (n=2)	Interday (n=3)	Intraday (n=2)	Interday (n=4)
20	4.6	26.4	69.5 ± 8.2	106.4 ± 28.1
200	6.6	9.7	102.2 ± 6.7	115.0 ± 11.2

The same kit and analytical procedure (preparation of the calibration curve in pooled rat serum) was used to determine sCT concentration in rat serum after oral administration. However, some analytical problems have arisen. As a matter of fact, the *in vivo* study of the oral administration was conducted almost one year later from the time of the first *in vivo* study with sc administration, thus, the kits were repurchased, and had a different serial number, which was most probably the reason for analytical problems with the sensitivity of the assay. The LOQ of sCT in rat serum was equal to 100 pg/ml and was calculated by interpolation of the mean absorbance plus 3 S.D. of 4 replicates of the pooled blank rat serum. For the concentration range of sCT between 100 and 500 pg/ml, the calibration curves exhibited a linearity with $r > 0.98$ (Figure 20). The precision (expressed as R.S.D. %) and the accuracy (expressed as mean recovery of sCT) of sCT determination in rat serum (oral administration) are presented in Table 20.

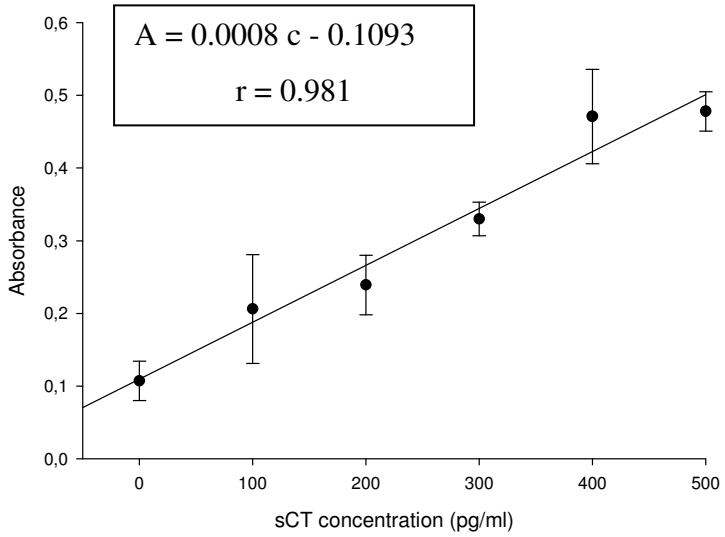

Figure 20. Typical calibration curve for sCT determination in rat serum by ELISA (oral administration) (mean ± S.D., n = 3).

As seen in Tables 19 and 20, some of the interday variations in the precision exceeded 20%. However, according to the manufacturer's instructions, the color of the final product may develop more quickly or more slowly than the recommended incubation time (15 min) depending on the localized room temperature and it is recommended to monitor visually the color development to optimize the incubation time and stop the reaction on appropriate time. Thus, the most important for this kind of methods is to proceed simultaneously with standards and unknown samples using the same microplate.

Table 20. The intraday and interday precision (R.S.D. %) and accuracy (mean recovery in %) of sCT determination in rat serum by ELISA (oral administration) (n = 3).

sCT concentration in control solution (pg/ml)	R.S.D. (%) (Precision)		Recovery ± S.D. (%) (Accuracy)	
	Intraday	Interday	Intraday	Interday
150	51.0	8.2	126.6 ± 64.6	139.6 ± 11.5
350	20.6	33.2	122.8 ± 25.4	95.0 ± 31.6

5.2.3. *In vitro* characterization of calcitonin-loaded nanoparticles

Table 21 demonstrates the general characteristics (mean diameter, zeta potential, encapsulation efficiency) of blank or sCT-loaded nanoparticles prepared with PLGA H, PLGA S, Eudragit RS or blends of two polymers. Moreover, polydispersity index was checked and yield of production was calculated for each formulation. Results in Table 21 indicate that the mean diameter and zeta potential were affected by the polymer type and in certain cases by the encapsulation of sCT. Mean diameter of nanoparticles was rather large (379-625 nm) and did not exhibit any practical significance for the loaded and unloaded nanoparticles made of one single polymer. Only polymer blended nanoparticles (PLGA H/RS and PLGA S/RS) loaded with sCT had a quite larger mean diameter than unloaded ones, but no statistical difference was observed. On the other hand, the smallest nanoparticles were obtained with Eudragit® RS (approximately 450 nm), and the influence of Eudragit® RS on reducing particle size was observed in nanoparticles composed of Eudragit® RS and PLGA. In spite of relatively high S.D. values for the particle size measurements, polydispersity index, which indicates the width of the size distribution and has a value between 0 and 1 (0 being for mono-disperse particles), were below 0.5 for each batch. The yield of the preparation process

(defined by the weight of nanoparticles recovered after lyophilization with respect to the initial weight of all the compounds) reached 70-80 %.

Table 21. General characteristics of blank or sCT-loaded nanoparticles prepared with PLGA H, PLGA S, Eudragit® RS or blends of two polymers (1:1). Data represent the mean ± S.D., n = 3 for blank nanoparticles, n = 4-9 for sCT-loaded nanoparticles. * Statistically significant differences from blank nanoparticles ($p \leq 0.05$).

Formulation	Mean diameter (nm)		Zeta potential (mV)		Encapsulation efficiency (%) (indirect method)
	Blank	sCT	Blank	sCT	sCT
PLGA H	610 ± 167	598 ± 137	- 16 ± 2	- 11 ± 3 *	83 ± 7
PLGA S	625 ± 139	609 ± 86	- 16 ± 1	- 12 ± 3 *	75 ± 3
PLGA H/RS	421 ± 45	555 ± 101	+ 30 ± 4	+ 52 ± 1*	69 ± 3
PLGA S/RS	379 ± 5	468 ± 110	+ 50 ± 4	+ 51 ± 2	75 ± 4
RS	456 ± 4	441 ± 24	+ 41 ± 8	+ 42 ± 5	72 ± 7

Unfortunately, due to the limited accessibility to the SEM analysis, presented SEM micrographs (Figure 21) are those performed only for one formulation type - PLGA H nanoparticles containing sCT. In the SEM images, nanoparticles displayed in spherical shapes with smooth surface and showed in certain regions small aggregation. However, the sample was lyophilized and the appearance of aggregates could occur. As expected, particles seen in SEM images had the size of < 1 µm. The images supported the PSC analysis, nonetheless, the PCS analysis was carried out in suspension before lyophilization of particles.

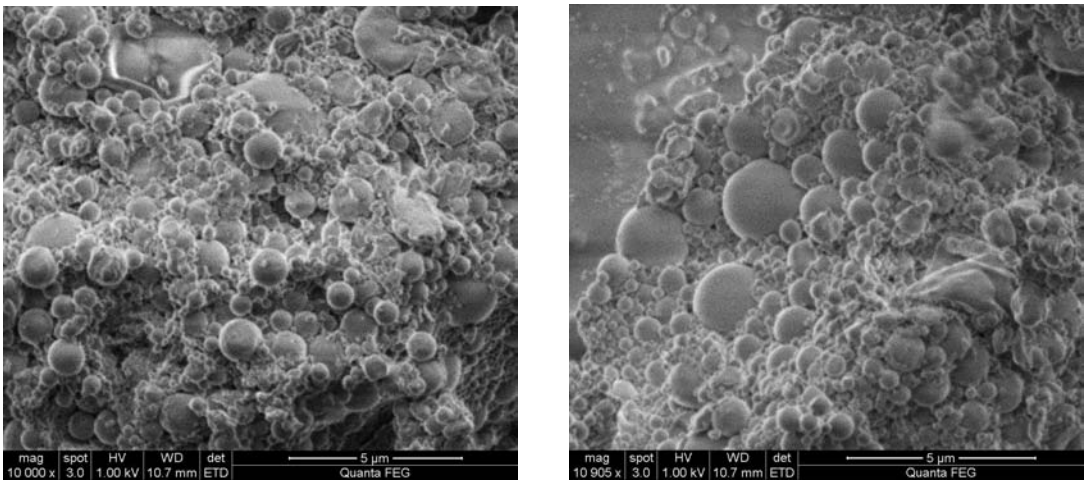

Figure 21. SEM images of sCT-loaded nanoparticles composed of PLGA H.

As supposed, the charge of nanoparticles (Table 21) was dependent primarily on the polymer type. Since Eudragit® RS is a polycationic polymer, nanoparticles composed of this polymer type displayed high positive zeta potential. Instead, as reported in Table 21, unloaded and loaded nanoparticles composed of PLGA H or PLGA S demonstrated similar negative zeta potential. However, there was a statistically significant change in zeta potential value before and after loading with sCT for PLGA H, PLGA S and PLGA H/RS nanoparticles. When PLGA was blended with Eudragit® RS, the resultant nanoparticles had high positive zeta potential. Once again, the change in the parameter after blending was observed towards the values characteristic of Eudragit® RS nanoparticles.

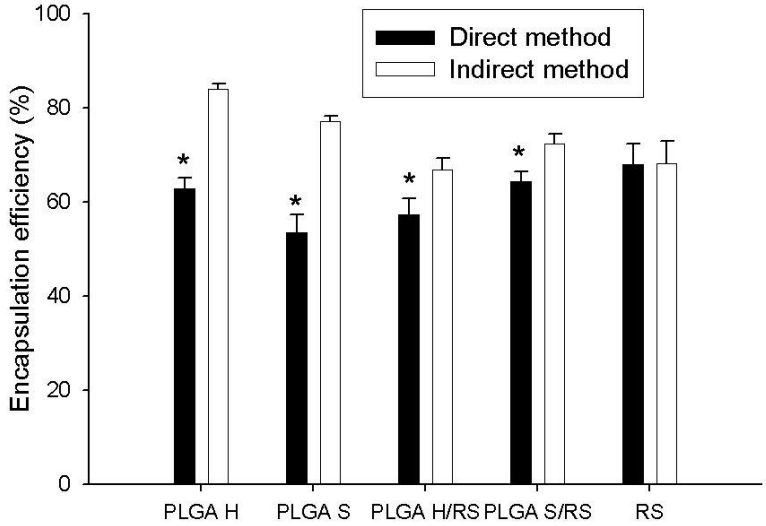

Figure 22. Comparison of encapsulation efficiencies of sCT-loaded nanoparticles as determined by direct (extraction) or indirect method (mean ± S.D., n = 3). * Statistically significant differences from indirect method ($p \leq 0.05$).

In order to determine the encapsulation efficiency of the peptide within the nanoparticles and to avoid under- or overestimation, two different techniques (referred to as direct and indirect method) were applied. It should be mentioned that nominal core loading was relatively low (2 μg sCT/mg polymer which equals 0.2%). However, the encapsulation efficiencies were rather high and satisfactory with a view to further *in vivo* studies (Table 21, Figure 22). According to the indirect method (Table 21), encapsulation efficiencies had higher values (69-83% depending on the formulation) compared to those determined by the direct (extraction) method. A comparison between the mean encapsulation efficiency values obtained by the extraction or indirect method is presented in Figure 22. The same results were obtained only in the case of Eudragit® RS nanoparticles. However, a statistical difference (but without practical significance) was observed for the rest of formulations. The lower values

obtained in the extraction method could be probably due to strong calcitonin - polymer interaction and/or retention of sCT at the water/organic interface after the dissolution of particles in an organic solvent (ethyl acetate) which do not allow an efficient extraction of calcitonin towards the aqueous phase. Further calculations for *in vitro* and *in vivo* study took into account only the results provided by the indirect method, since the determination of the peptide content in the nanoparticles by this method appeared reliable, less laborious and time-consuming.

In the adsorption study carried out under similar conditions as for the *in vitro* release study, sCT was tested regarding its tendency to adsorb to blank nanoparticles or to the glass vials in two different media: 5% acetic acid solution and 0.1% PVA solution. For this experiment, 3 blank formulations, selected for further *in vivo* study (PLGA H, PLGA H/RS, RS), were used. Bound peptide fraction was calculated from the difference between the initial (total) and remaining (free) sCT concentration. The obtained results indicate that there was almost no adsorption of sCT onto blank nanoparticles. The amount of peptide remaining in the supernatant throughout 24 h was in the range of 98-100% of the initial amount for positively charged PLGA H/RS and RS nanoparticles in both media. In the case of negatively charged PLGA H blank nanoparticles, the amount of peptide remaining after 24 h was 94.5 ± 2.9% and 89.7 ± 3.6% of the initial amount in 5% acetic solution acid and 0.1% PVA solution, respectively. Since no significant decrease of concentration was observed during 24 h of the experiment, it was assumed that no adsorption onto blank nanoparticles had occurred and suggested that the observed slight reduction of the sCT concentration (blank PLGA H nanoparticles) had been rather due to its instability in the tested medium and/or due to weak adsorption onto the glass.

5.2.4. Calcitonin *in vitro* stability and release from nanoparticles

Figure 23 presents the effect of pH on the sCT stability in aqueous solution at 37°C for 72 h. The peptide was considerably more stable in 5% acetic acid solution (pH 2.4) and in 2.3 M acetate buffer pH 4.3 than in PBS pH 7.4. In PBS at 37°C, 43% of the initial peptide amount was degraded within 24 h and 80% after 3 days. On the contrary, 94, 75 and 59% of the initial amount still remained in 5% acetic acid solution after 3, 14 and 42 days, respectively (data not shown). It should be mentioned that additional stability test for sCT in 5% acetic acid solution was conducted as a control for the entire duration of the *in vitro* release study (42 days). The results make it clear that sCT in PBS solution quickly undergoes

degradation rendering this medium not suitable for the *in vitro* release study. The degradation products generated mainly in PBS pH 7.4 were detected by HPLC (additional peaks in the chromatograms), but not identified. However, during the preliminary trials, the reduction of sCT disulfide bridge was performed with the help of dithiothreitol and the retention time of the reduced peptide was compared with the retention time of sCT in the chromatograms corresponding to the stability samples in different media. As a result, in these media, the reduction of the disulfide bridge did not occur.

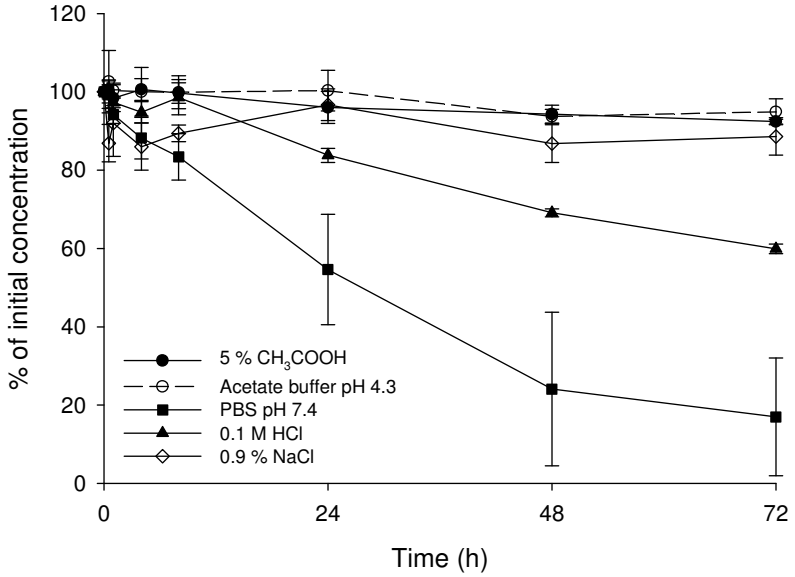

Figure 23. Stability of salmon calcitonin at 37°C in different media (mean ± S.D., n = 3).

Figure 24 shows the *in vitro* release profiles of calcitonin-loaded nanoparticles by representing the percentage of sCT released with respect to the amount of sCT encapsulated as a function of time. An initial calcitonin release of around 10% was observed within the first few hours of the release study with PLGA H and PLGA S particles. Then, extended and low release can be seen from both formulations during the 3-4 weeks incubation period corresponding to the release *via* diffusion of the entrapped peptide. This phase was followed by a slight increase in the peptide release after 3 or 4 weeks for PLGA H and PLGA S, respectively. The cumulative percentage of calcitonin released from both type of PLGA particles was found to be incomplete and around 21% at best. Some morphological changes of PLGA nanoparticles suspension were observed during the *in vitro* release test. Morphological changes proceeded with time and the nanoparticles started to agglomerate. Finally after 2 or 3 weeks, a large block of polymer formed and the suspension became more transparent and viscous.

On the contrary, Eudragit® RS nanoparticles displayed a completely different release profile with an immediate and total release of sCT within only 1 h. However, when Eudragit® RS was blended with PLGA H or PLGA S, nanoparticles showed a similar release profile characterized by an initial burst release of 80-100% of the encapsulated sCT within few hours. Thereafter, the release profiles reached quickly a plateau. It could be concluded that Eudragit® RS had a modifying accelerating effect on the sCT release.

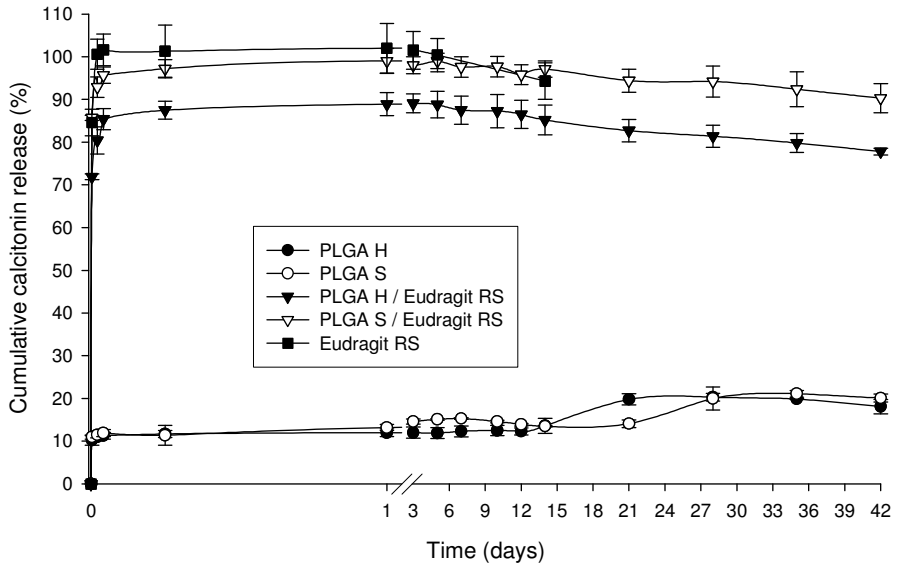

Figure 24. Percentage of cumulative calcitonin release in 5% acetic acid solution from nanoparticles composed of PLGA H, PLGA S, blend of PLGA H/Eudragit® RS, blend of PLGA S/Eudragit® RS or Eudragit® RS (mean ± S.D., n = 3).

The pH of the release medium was measured at the end of each release test. There was no significant change of pH after 6 weeks of incubation compared to pH of a fresh 5% acetic acid solution (pH = 2.4).

5.2.5. *In vivo* studies

Subcutaneous administration

Calcitonin solution and three formulations containing sCT (PLGA H nanoparticles, PLGA H/RS nanoparticles, RS nanoparticles) were administered subcutaneously in anaesthetized, fasted, male Wistar rats and the serum concentration of sCT was measured (ELISA) as a function of time (Figure 25). Pharmacokinetic parameters are summarized in Table 22. When sCT was administered as a solution at 50 µg/kg, the serum concentration of

sCT increased to 2 142 pg/ml at 45 min after administration, and then quickly decreased to negligible concentration detected by ELISA after 10 h ($AUC_{0\text{-}10\,h}$ = 4 561 pg/ml x h).

Table 22. Pharmacokinetic parameters after sc administration of sCT-loaded nanoparticles and sCT solution as reference.

Formulation (sCT dose)	Relative bioavailability (%)	T_{max} (h)	C_{max} (pg/ml)
sCT solution (50 µg/kg)	-	0.75	2 142 ± 688
PLGA H nanoparticles (100 µg/kg)	131.7	1	3 617 ± 1 686
PLGA H/RS nanoparticles (100 µg/kg)	83.4	1	3 420 ± 1 146
RS nanoparticles (100 µg/kg)	138.7	1	2 392 ± 1 187

All the nanoparticle formulations administered at a sCT dose of 100 µg/kg led to a delayed t_{max} (1 h), an increased C_{max}, and AUC values compared to those of the control solution. The initial calcitonin peak must be related with *in vivo* burst release of calcitonin from nanoparticles and its absorption from the sc tissue. For all the nanoparticle formulations, the mean serum concentration time profiles were comparable to that of calcitonin solution. However, in the case of the calcitonin solution, the last concentration of calcitonin over LOQ of the ELISA was observed after 8 h, but for the PLGA H nanoparticles mean sCT concentration was still 35 pg/ml at 72 h after administration. In this study, relative bioavailability after sc administration of sCT encapsulated in nanoparticles compared to the sCT solution was 132% and 139% for PLGA H and RS nanoparticles, respectively. This suggests that sCT was more bioavailable after sc injection from sCT-loaded nanoparticles than from sCT solution. Only in the case of blended nanoparticles (PLGA H/RS nanoparticles), bioavailability of sCT was not improved compared to the solution (relative bioavailability equal to 83%).

A)

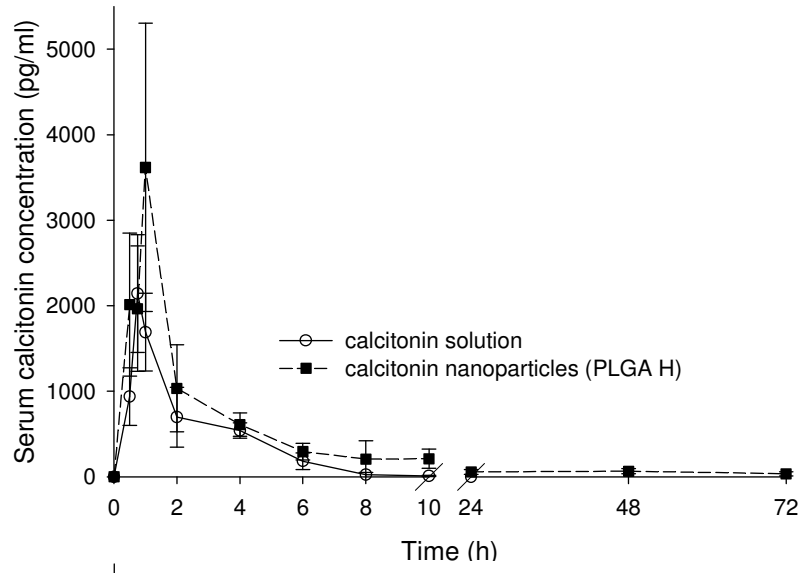

B)

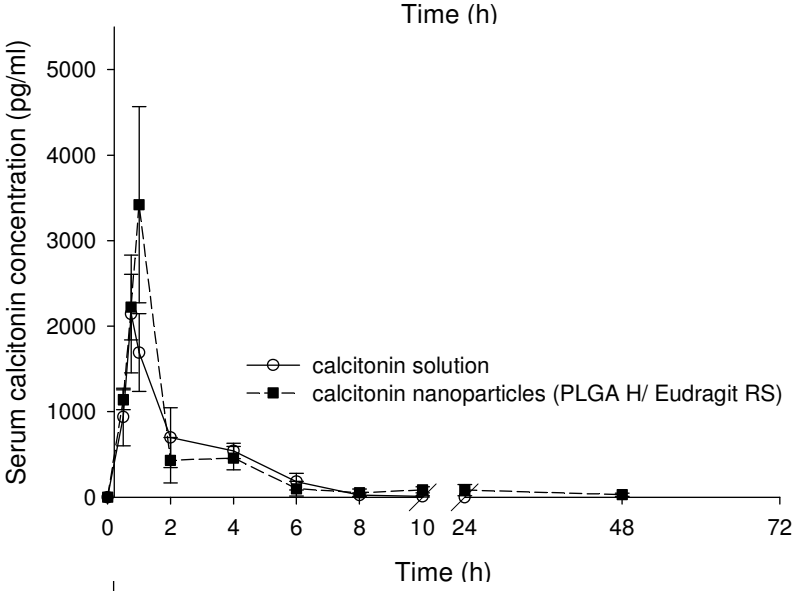

C)

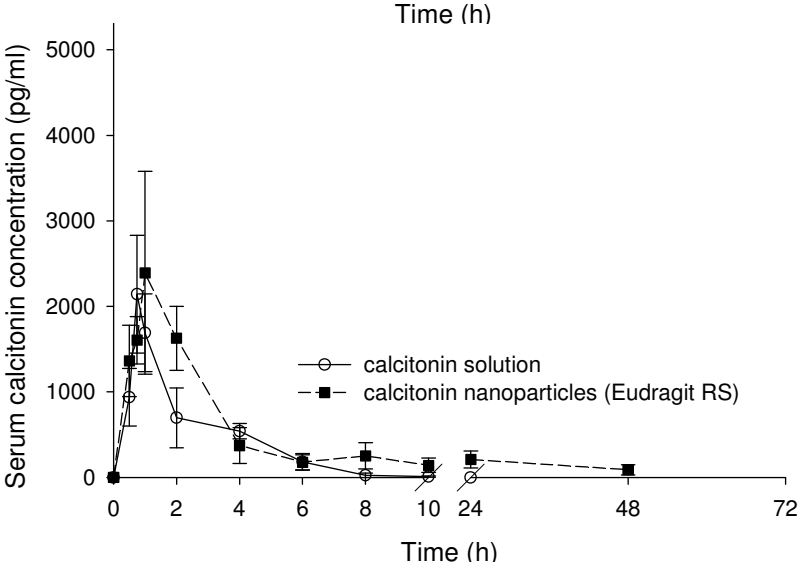

Figure 25. Calcitonin concentrations in rat serum after sc administration of sCT solution at a dose of 50 µg/kg or sCT-loaded nanoparticles at a dose of 100 µg/kg prepared from A) PLGA H; B) PLGA H/Eudragit® RS; and C) Eudragit® RS (mean values ± S.D., n = 5).

Oral administration

Calcitonin solution and three types of nanoparticle formulations containing sCT (PLGA H nanoparticles, PLGA H/RS nanoparticles, RS nanoparticles – the same as for sc administration) were administered intragastrically to Wistar rats and the obtained sera were assayed by ELISA. However, the measured absorbance coming from all the samples was either on the level of blank rat serum or the calculated concentrations were below the LOQ, i.e. ≤ 100 pg/ml. Thus, calcitonin was detected in some samples, but the results were not quantifiable.

A)

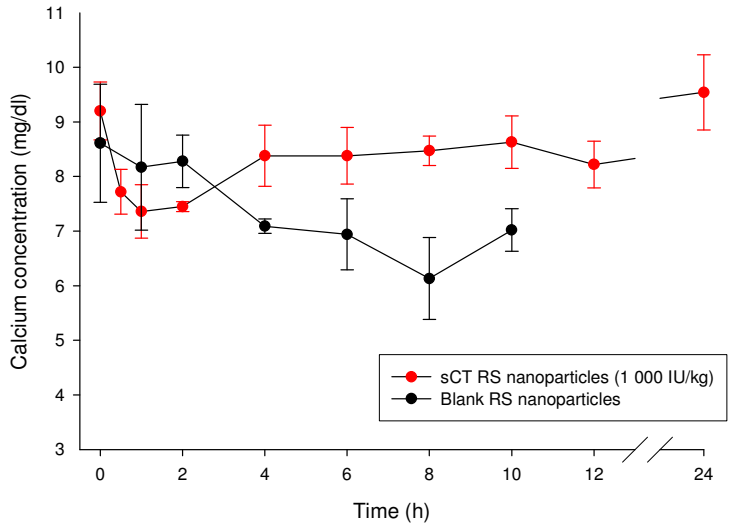

B)

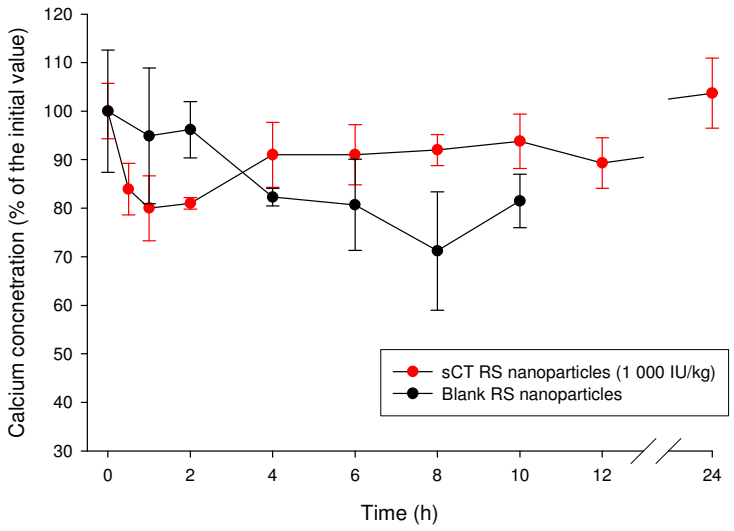

Figure 26. Changes of the calcium concentration in rat serum expressed A) in mg/dl or B) as % of the initial value after oral administration of Eudragit® RS-composed blank nanoparticles or nanoparticles containing calcitonin (mean ± S.D., n = 7).

Additionally, calcium concentration was measured in rat sera obtained after oral administration of nanoparticles. The initial value (considered as 100%) of the average calcium concentration in rats before the treatment was 8.72 ± 0.88 mg/dl (R.S.D.% = 10.1%, n = 34). Figure 26 A shows the changes of calcium concentrations and the same changes are expressed as % of basal in Figure 26 B. As seen, after administration of RS nanoparticles, the calcium concentration decreased to approximately 80% within the first 4 h and then the weak hypocalcemic effect was maintained within 12 h. However, in the case of blank RS nanoparticles the decrease was also observed after 4 h after administration.

A)

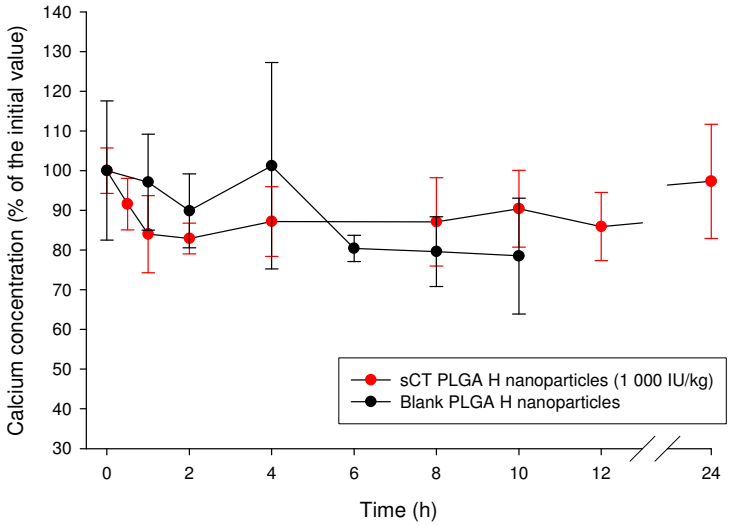

B)

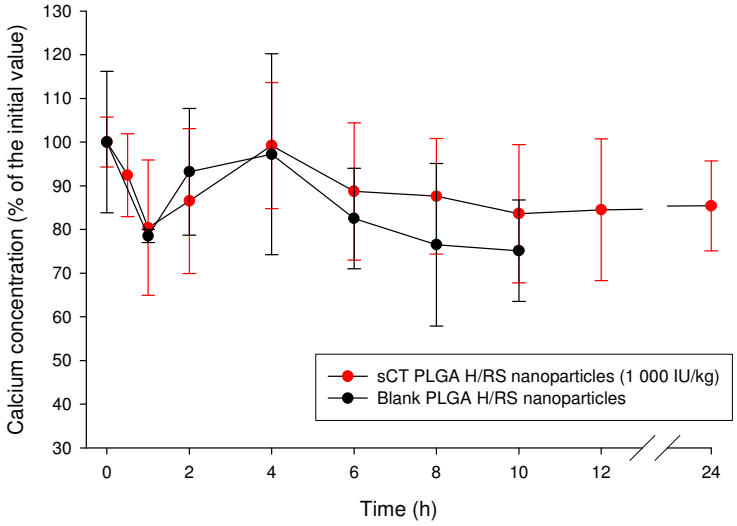

Figure 27. Changes of the calcium concentration in rat serum (as % of the initial value) after oral administration of blank or sCT-loaded nanoparticles composed of A) PLGA H or B) PLGA H/RS (mean ± S.D., n = 7).

Furthermore, sCT-loaded PLGA H nanoparticles seemed to decrease the serum calcium concentration for 12 h as well when compared to the blank nanoparticles. Instead,

sCT encapsulated in blended nanoparticles (PLGA H/RS) triggered the same effect as blank nanoparticles did, and no improvement in hypocalcemic activity was observed (if any) with comparison to the nanoparticles made from the single polymer. It should be noted that the administration of blank nanoparticles in each case provoked a delayed and a more or less significant decrease in calcium concentration indicating that the procedure of *per os* administration and blood sampling (cardiac puncture) could likely have an influence on the blood calcium level in rats.

5.2.6. DSC study

The purpose of this study was to evaluate potential influence of either formulation of polymer(s) into nanoparticles or sCT encapsulation into nanoparticles on the thermal properties of the polymer(s). Therefore, pure polymers, blank nanoparticles and loaded nanoparticles were analyzed by DSC and some examples of the obtained thermograms are presented in Figure 28. In the DSC curves, for all the samples, only glass transition occurred since the breakdown of the baseline was observed, and the transition appeared as a step transition and not as a peak, indicating that in the used temperature range, the polymer(s) reached its T_g when heated and underwent in its rubbery state. Average T_g of pure polymers, blank and loaded nanoparticles is presented in Table 23.

Table 23. Glass transition temperature (°C) (considered as a mid-point of transition from the second heating) of pure polymers, blank and loaded nanoparticles (mean ± S.D., n = 3).

	Pure polymer(s)	Blank nanoparticles	sCT-loaded nanoparticles
PLGA H	44.5 ± 0.74	43.3 ± 0.3	41.1 ± 0.6
PLGA S	42.3 ± 0.4	42.4 ± 0.2	42.0 ± 0.3
PLGA H/RS	-	48.6 ± 0.2	47.8 ± 0.2
PLGA S/RS	-	42.9 ± 0.4	45.7 ± 0.3
Eudragit RS	51.6 ± 0.6	52.1 ± 0.7	52.3 ± 1.1

For two types of PLGA polymers, blank and loaded nanoparticles deriving from them, similar T_g values were observed in the temperature range 41 – 45°C. Similarly, in the case of blank and loaded nanoparticles composed of Eudragit® RS, the T_g values did not change, but were higher (approximately 52°C) and the appeared transition was larger and less distinct compared to PLGA polymers and nanoparticles (Figure 28 C). Instead, blank and loaded PLGA H/RS nanoparticles and loaded PLGA S/RS nanoparticles demonstrated intermediate

T_g values between the values for each individual polymer, most likely indicating that the two polymeric fractions were miscible after formulation.

For pure sCT, the DSC analysis was not performed since in order to detect any changes it would require for one run a few milligrams of the peptide, which is relatively expensive. Besides, pure PVA, as an ingredient present in lyophilized nanoparticles (residual PVA) despite of washing, was also analyzed and the glass transition or other phenomena were not observed in the second heating in the temperature range -20°C to 80°C.

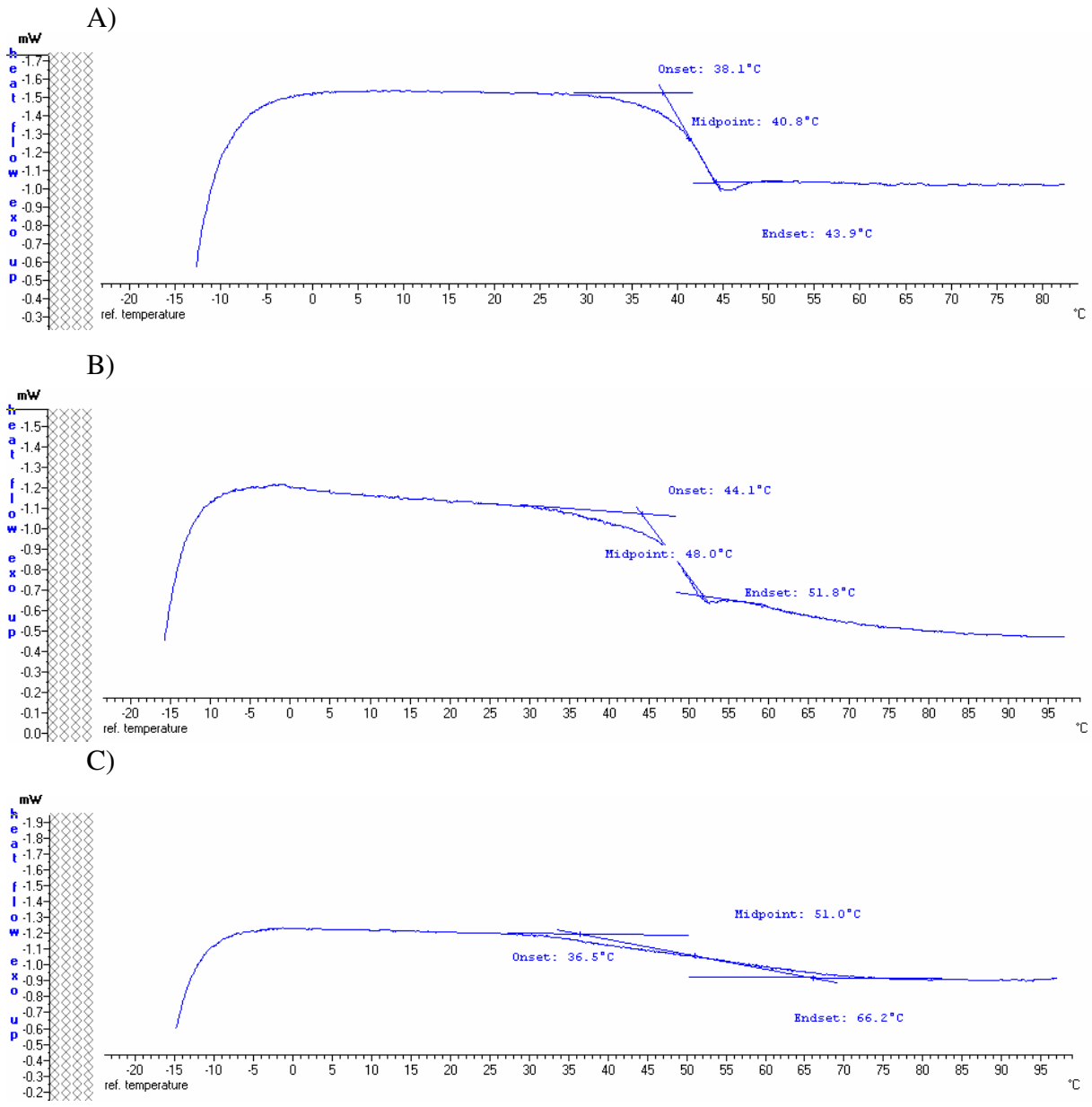

Figure 28. DSC thermograms of A) sCT-loaded PLGA H nanoparticles, B) sCT-loaded PLGA H/RS nanoparticles and C) sCT-loaded RS nanoparticles.

6. DISCUSSION

6.1. Encapsulation of glutathione-selective fluorogenic probes

The preparation of the considered probe-loaded nanoparticles was based on the well known oil/water simple emulsion solvent evaporation method which is intended particularly for encapsulation of hydrophobic active agents (Hombreiro-Perez*, et al.*, 2000). Physicochemical properties of polymeric nanoparticles (including polymer nature, particle size and size distribution, surface charge, encapsulation efficiency, release kinetics, *etc.*) may have significant influence on the *in vivo* behavior of an active agent incorporated in the nanoparticles and released from. In this work, the choice of Eudragit® E as a polymeric matrix relied mainly upon its high solubility in acidic conditions and rendering nanoparticles positively charged. Eudragit® E is a polycationic non biodegradable polymer with dimethylaminoethyl functional groups (Figure 29 A). Because of these groups, the material is soluble under acidic conditions up to pH 5, but it becomes swellable and permeable above this critical pH (according to the manufacturer specification).

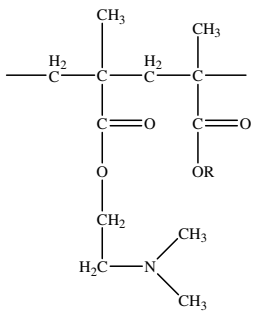

R = CH_3, C_4H_9

A

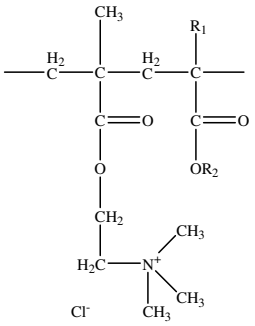

R_1 = H, CH_3
R_2 = CH_3, C_2H_5

B

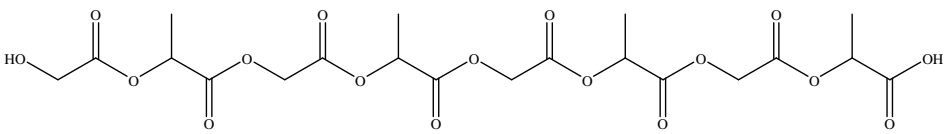

C

Figure 29. Schematic structure of the polymers used for the preparation of nanoparticles: A) Eudragit® E; B) Eudragit® RS; C) uncapped PLGA.

The idea was based on the assumption that positively-charged nanoparticles should interact favorably with yeast wall/membrane of opposite charge, and the release of the probe inside lysosomal vesicles (acidic environment) after endocytosis should occur. This approach can be exemplified by the work of Haining *et al.* (2004), who studied the use of pH-sensitive microparticles composed of a phospholipid and Eudragit® E as vaccine delivery vehicles for peptide antigens. These particles, after phagocytosis by antigen presenting cells, released the encapsulated antigen in the low pH environment of the phagosome, thereby improving antigen presentation to lymphocytes and enhancing the response to peptide vaccines (Haining, *et al.*, 2004).

A)

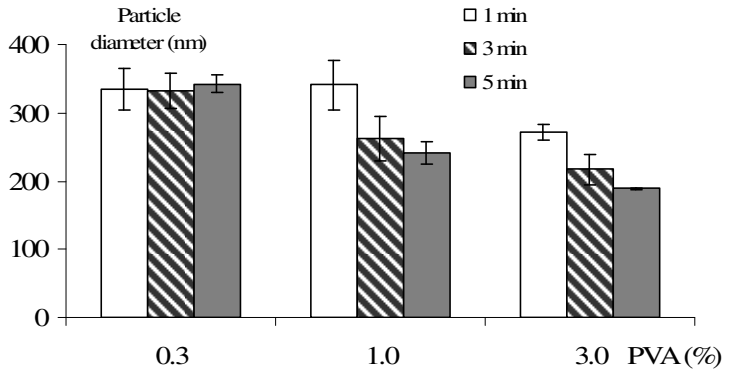

B)

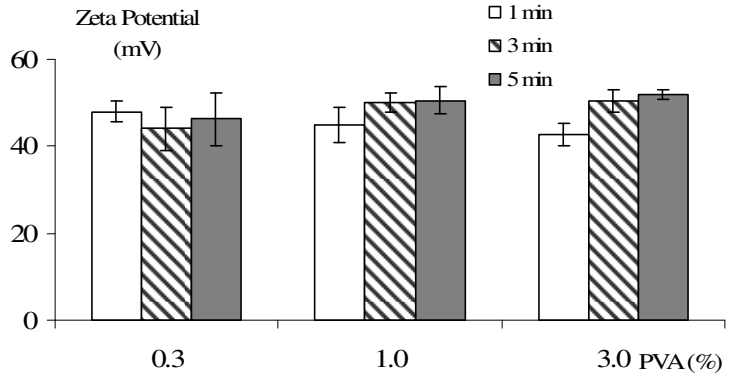

Figure 30. Influence of PVA concentration and ultrasonication time (1, 3 or 5 min) on A) the particle size and B) zeta potential of OPA-loaded nanoparticles (means ± S.D., n = 3) (Martenka, 2004, Główka, *et al.*, 2006).

The preparation method of the probe-loaded nanoparticles was previously optimized in terms of PVA content and ultrasonication time (Figure 30) on the basis of the size and zeta potential monitoring of the obtained nanoparticles (Martenka, 2004, Główka, *et al.*, 2006). The probe used for this optimization protocol was OPA. As a result, high and positive zeta potential of particles remained rather constant and independent on the tested preparation parameters. The lowest size of nanoparticles loaded with OPA (188.8 ± 1.3 nm; n = 3) was

observed for 3% PVA and a 5 min-period of sonication**.** Thus, these conditions were retained for further preparation of NDA-loaded nanoparticles. The NDA-loaded particle diameter, polydispersity index and zeta potential were very close to those measured with OPA-loaded nanoparticles (Table 15). In other words, the change of the encapsulated active agent did not considerably affect these fundamental properties of the formulation.

In contrast, encapsulation efficiency of OPA and NDA in lyophilized nanoparticles prepared under the same optimized conditions was completely different. In both cases, encapsulation efficiency was determined directly by total dissolution of nanoparticles in acidic medium and the released probe was then determined by HPLC after the derivatization reaction. A 23-fold higher encapsulation efficiency was observed for NDA than for OPA (Table 15). This might be the result of the higher hydrophobicity of NDA. It is now well known that the more hydrophobic active substance is, the higher encapsulation efficiency can be achieved with the simple emulsion solvent evaporation method. Due to the higher nanoencapsulation efficiency of NDA, this probe was consequently chosen for cellular application.

With regard to the *in vitro* release of NDA from nanoparticles in 0.1 M HCl, as expected, a complete release of the probe was immediately observed, due to the dissolution of the polymer in acidic medium. Indeed, as mentioned above, Eudragit® E is a pH-sensitive polymer that dissolves at pH up to 5 by salt formation, thus allowing the complete release of the encapsulated probe. However, at pH 7.0, the release profile was characterized by a large initial amount of the probe released (about 70%), followed by a progressive and incomplete release up to 1 h. The initial burst release could be explained by the imperfect encapsulation of the probe inside nanoparticles resulting from the unstable nature of the emulsion droplets during the solvent removal step. This potential instability may lead to a part of the loaded probe to locate at the nanoparticle surface, thereby rapidly released (Lu & Park, 1995). In addition, Eudragit® E becomes permeable above pH 5, involving swelling and release of the encapsulated probe into the dissolution medium by diffusion through pores from the polymeric network. The incomplete release of the probe from nanoparticles resulted probably from the short time of the release study (1 h), but a complete release could be expected within 2 h. It should be bore in mind that loading of yeast cells with NDA encapsulated in nanoparticles was conducted within only 20 min.

With respect to the study in yeast cells, previously optimized parameters by Diez *et al* (2005) concerning cell extraction and loading were used for the purpose of this experiment. At first, two extraction media (PBS solution pH 7.0 and borate buffer pH 9.2) and two

physical processes for cell lysis (freezing cycle or ultrasonic homogenization) were compared in terms of the highest extraction rate of NDA-GSH from cells. The evidence was that combining a cell freezing cycle and borate buffer has given rise to the highest efficiency of extraction of NDA-GSH adduct. NDA-GSH adduct was clearly identified in yeast extracts and quantified. Thus, full selectivity was obtained *versus* endogenous compounds, as demonstrated by the chromatograms of cell extracts loaded or not with NDA (Figure 12 B and C). Moreover, it has been confirmed that no NDA- γ-GluCys adduct was detected in the cell extracts and neither release of NDA-GSH adduct from cells nor extracellular GSH reaction with NDA occur during the cell loading with NDA. Additionally, labeling of cellular GSH with NDA, in the yeast strain used as a cellular model was optimized as a function of NDA concentration (20, 100 and 500 µM), and the incubation time (10, 20 and 30 min). According to Diez *et al.* (2005), 100 µM and 20 min seemed to be optimal NDA concentration and loading period, respectively. Most likely, these parameters should be optimized if any other prokaryotic or eukaryotic cell types are studied (Diez*, et al.*, 2005).

Furthermore, cells were also loaded with free OPA in the same conditions than those previously optimized for NDA, i.e. concentration of 100 µM and 20-min incubation and for extraction step (cell freezing cycle and borate buffer pH 9.2). As a result, 1.8-fold less concentration of the OPA-GSH adduct was found in cell extracts compared to the NDA-GSH adduct concentration. Since NDA is more lipophilic than OPA, it was concluded that NDA could penetrate the cell with a better yield than OPA. However, other mechanisms can act with a different intensity, such as the reactivity of OPA and NDA with the amino or sulfhydryl groups of cell wall components. Besides, OPA seemed to be less selective than NDA (many other peaks in the chromatograms corresponding to unidentified cytosolic components which react with OPA) (Diez*, et al.*, 2005).

In the present work, the improvement of the fluorogenic probe uptake by cells using nanoparticles was evaluated. This is confirmed by the results of the HPLC measurements of the NDA-GSH adduct concentration in cell extracts. The 9.2-fold higher NDA-GSH adduct concentration was found in cell extracts after incubation of cells with NDA-loaded nanoparticles in comparison with incubation with the free NDA (Figure 15). Moreover, a better probe penetration into cells is also supported by the microscopic images of the fluorescence resulting from the NDA-GSH adduct formation (Martenka, 2004, Główka*, et al.*, 2006). The fluorescence in yeast cells loaded with blank nanoparticles, NDA (free or encapsulated) and Nile Red-loaded nanoparticles was examined using confocal laser scanning microscopy (CLSM) in a qualitative way (Figure 31). For these experiments, a red marker of

cellular membranes (*Urtica dioica* agglutinin, specific for saccharides containing *N*-acetylglucosamine, and conjugated to tetramethylrhodamine isothiocyanate) was used to visualize the plasmic membrane of yeast cells. This red labeling was particularly visible in images of cells after incubation with blank nanoparticles (Figure 31 b). This also confirmed that no green fluorescence was observed from other potential sources (polymers or cells).

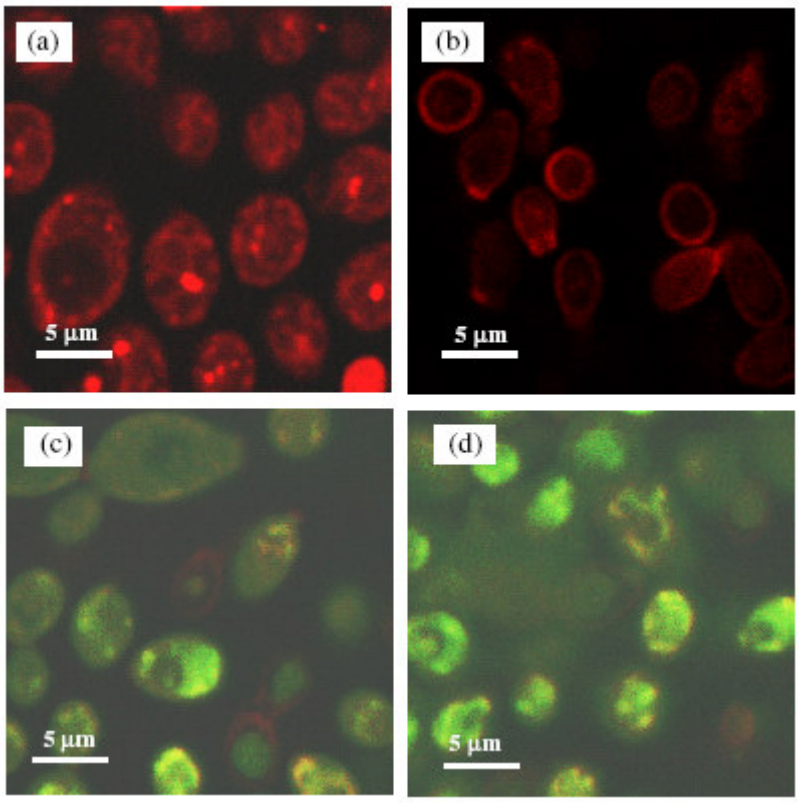

Figure 31. CLSM images of *Candida albicans* cells incubated with: (a) Nile Red-loaded nanoparticles, (b) blank nanoparticles, (c) free NDA, (d) NDA-loaded nanoparticles. Cells presented in (b)–(d) were marked by a red marker of cellular membranes (Główka, *et al.*, 2006).

Red labeling of cell membranes definitely demonstrates that green fluorescence was located inside the cells. It was evident that the observed green fluorescence corresponded to the intracellular formation of the NDA-GSH adduct. A more intense green fluorescence was observed with the use of encapsulated NDA (Figure 31 d) when compared to the free probe (Figure 31 c). An enhanced cellular uptake of the probe could be explained by an adhesion of positively charged nanoparticles on cells surface. This could create a higher concentration gradient that would enhance the probe transport across cell wall and membranes. Most probably, nanoparticles may also be endocytosed by cells followed by the release of the probe inside cells. Overall, a positive effect of nanoparticles on NDA-GSH adduct formation was

observed and HPLC measurements and CLSM imaging lead to a similar conclusion. Moreover, green fluorescence of NDA-GSH adduct was maintained relatively for a longer period of time using NDA-loaded nanoparticles. However, Figure 31 a demonstrates also that nanoparticles were internalized. In this case, the phenoxazine dye Nile Red was encapsulated in nanoparticles and applied to cultured cells in order to assess the intracellular penetration of nanoparticles. Nile Red is a fluorescent and lipophilic dye, which can be efficiently incorporated into nanoparticles. The internalization was confirmed when *Candida albicans* were incubated with Nile Red-loaded nanoparticles since red fluorescence was observed inside cells. Some labeling of the cell membranes occurred as well, probably due to the adhesion of the polycationic Nile Red-loaded nanoparticles to the membrane. This is an expected step of internalization. As a conclusion, obtained CLSM images prove the adsorption to the surface of cells and the intracellular penetration of the probe-loaded nanoparticles (Martenka, 2004, Główka*, et al.*, 2006).

Finally, the impact of NDA and corresponding nanoparticles on the viability of the yeast cells was tested. No data concerning the cytotoxicity of NDA are available in the literature. Blank nanoparticles, 100 μM of free NDA, and an equivalent concentration of NDA-loaded nanoparticles were added to a *Candida albicans* culture for 20 min and the MTT test was applied: the calculated viability was 105 ± 9, 66 ± 15 and 73 ± 6% (n = 3), respectively. It appears that blank nanoparticles do not affect the viability of yeast cells and both free NDA and NDA-loaded nanoparticles have a similar cytotoxic effect. However, the structurally closed compound OPA is claimed to have a high disinfective effect on bacteria by reacting with wall components, and it exhibits a minimum bactericidal concentration of 745 μM for 30 min application on *Pseudomonas fluorescens* (Simoes, *et al.,* 2005).

6.2. Encapsulation of salmon calcitonin

Treatment of osteoporosis today has focused on the long-term use of antiresorptive drugs. In this context, sCT, a powerful inhibitor of osteoclast activity, is of particular interest, not only because of its ability to prevent bone loss and to decrease fracture risk, but also because of analgesic activity and lack of serious side effects (Reginster, 1995, Body, 2002). sCT, unlike the bisphosphonates, has only a transitory action and is quickly eliminated from the skeleton (Body, 2002). A unique advantage of sCT, unshared by any other antiresorptive agent, is its analgesic effect on bone pain previously demonstrated in clinical studies (Gennari, 2002, Munoz-Torres*, et al.*, 2004). Calcitonin is especially recommended for patients who fail to respond to or cannot tolerate bisphosphonate medications or are unable to take bisphosphonates because of impaired renal function (Silverman, 2003). Nasal administration constitutes a therapeutic option that is particularly attractive for women who do not wish to take or do not tolerate estrogens, or for whom estrogens are contraindicated (Silverman, 1997). sCT has been used for many years in the management of osteoporosis because of a higher potency than calcitonin from several other species, and a lesser tendency to aggregate than the human form (Gaudiano*, et al.*, 2005).

In order to improve patient compliance and comfort of administration during a long-term therapy, there is an ongoing effort to develop either a sustained-release delivery system for calcitonin or a delivery system administered *via* other route, especially an oral one. Both of them should effectively deliver an active peptide to the systemic circulation and maintain its therapeutic levels. Both are promising and offer new opportunities in the treatment and prevention of osteoporosis. On the other hand, calcitonin is often considered as a model peptide for developing an oral peptide/protein delivery system or studying associated instability issues, due to the high calcitonin activity (low doses needed) and a large therapeutic window.

As mentioned, various injectable prolonged or controlled delivery systems have been proposed for calcitonin, mainly involving biodegradable microparticles (see section 2.2.4.1). Furthermore, oral systems (nanoparticles in most cases), protecting calcitonin against digestion in the gastrointestinal tract, and favoring its interaction with the intestinal epithelium, have also been studied (see section 2.2.4.2.). But so far, only a few satisfactory results have been obtained *in vivo* and development of such formulations still remains a challenge.

The aim of this work was to develop polymeric nanoparticles loaded with sCT composed of a single biodegradable (PLGA) or non biodegradable (Eudragit® RS) polymer and assess the influence of polymer blending (mixed nanoparticles composed of one biodegradable and one non biodegradable polymer) on the *in vitro* and *in vivo* characteristics. Biodegradable PLGA-based nanoparticles were preliminary intended as a parenteral sustained release system, and non biodegradable Eudragit RS-composed nanoparticles as an oral formulation. However, in order to identify the impact of the polymer type on the bioavailability of calcitonin, biodegradable as well as non biodegradable nanoparticles were administered *via* both routes (subcutaneously and orally).

Preparation and in vitro characterization of nanoparticles

The preparation of sCT-loaded nanoparticles was based on the double emulsion solvent evaporation method which is intended particularly for encapsulation of hydrophilic drugs such as proteins and peptides. In the course of calcitonin encapsulation, sonication was used in order to reduce the size of droplets, but the amount of organic solvent was minimized compared to the preparation of insulin-loaded nanoparticles previously developed in Department of Pharmaceutical Technology in Nancy (Damge*, et al.*, 2007).

PVA was used as a surfactant not only for stabilizing emulsions during nanoencapsulation, but it is also important in preventing aggregation and contributing to stabilization of encapsulated peptides or proteins (Youan, *et al.*, 2003). PVA is frequently used since it forms particles of relatively small size and uniform size distribution. In this study, PVA of low molecular weight was used at a very low concentration (0.1%), especially as nanoparticles were planned to be administered subcutaneously. In order to minimize the possible toxicity of the residual amount of PVA, the nanoparticles were washed when administered parenterally. However, a small fraction of PVA may still remain associated with nanoparticles despite repeated washing steps. According to the results of Sahoo et al. (2002), the residual PVA amount was 2% (w/w) of nanoparticles when used 0.5% PVA solution (of the same low molecular weight as used in this work) for formulating PLGA nanoparticles by multiple emulsion solvent evaporation technique. Moreover, a decrease in PVA concentration in the external aqueous phase resulted in the decrease in the residual PVA amount associated with nanoparticles (Sahoo, et al., 2002). Instead, orally administered PVA is safe and approved (DeMerlis & Schoneker, 2003). It should be mentioned that PVA is unacceptable for parenteral application because of its potential toxicity and there is no concentration limit for residual PVA in the final parenteral product. On the other hand, only little is known on the

toxicity of residual PVA used as an excipient and there are only few studies concerning acute or subacute toxicity. However in the very early study of Hall C.E. and Hall O. (1963), daily sc injection to rats of 1 ml of a 5% solution of medium molecular weight PVA after 4 weeks induced many toxic symptoms (e.g. severe hypertension, abdominal swelling, cardiac hypertrophy). Nevertheless, in the same study, low molecular weight PVA (as used in this study) was not found in any tissues and elicited no systemic effects (Hall & Hall, 1963).

The choice of PLGA copolymers as polymeric matrix of nanoparticles for sc delivery was obvious, since PLGA is biodegradable, biocompatible and approved by most drug agencies worldwide. In addition, the diversity of chemical composition makes feasible to develop controlled release system of desirable properties. Besides, much is already known about these polymer types since they have been widely studied for many years. Two types of PLGA copolymers of the same high inherent viscosity (indicating high molecular weight) were used in this work: PLGA H (uncapped, free carboxyl end groups) and PLGA S (esterified end groups). Furthermore, Eudragit® RS was chosen since it is a well known polymer for oral solid dosage forms (Figure 29 B and C). Due to its dissolution properties (pH-independent swelling, insoluble and permeable in the gastrointestinal fluids), Eudragit® RS is a suitable matrix or coating material allowing a controlled drug release. A polymeric matrix made from this type of polymer swells and becomes permeable allowing diffusion of the embedded drug. Additionally, positively charged groups (quaternary amino groups) in Eudragit® RS are responsible for its mucoadhesive properties. In this work, degradable (PLGA) and non-degradable polymers (Eudragit® RS) were mixed in order to evaluate the possibilities of modulating the release properties of such nanoparticles. Polymer blending has been already evaluated in drug delivery systems because of their ability to combine properties of different polymers in one particle. Blends of Eudragit® and PLGA have been recently described in the preparation of heparin-loaded nanoparticles as potential oral carriers (Jiao, *et al.*, 2001, Hoffart, *et al*., 2002) and ciprofloxacin-loaded nanoparticles (Dillen, *et al*., 2006).

It this work, 5 different formulations were obtained (PLHA H, PLGA S, PLGA H/RS, PLGA S/RS, RS). The SEM micrographs (Figure 21) revealed spherical shape of particles and smooth surface. The particle size was rather large (379 – 625 nm), nevertheless, it was suitable for sc injection. Evidently smaller particle size was obtained with Eudragit® RS. Most likely, quaternary ammonium groups of Eudragit® RS stabilized the first emulsion and prevented fast coalescence of the droplets resulting in smaller particles as previously reported (Chernysheva, *et al.*, 2003).

As expected, Eudragit® RS gave high positive charge to blank as well as sCT-loaded nanoparticles. Interestingly, when Eudragit® RS was blended with negatively charged PLGA polymers, the resultant nanoparticles had positive zeta potential. It could be suggested that hydrophobic PLGA backbone chains were anchored into the bulk phase of Eudragit® RS, and that, consequently, the amine groups in the Eudragit® backbone were oriented outside towards the aqueous phase, resulting in a highly positively charged surface (Chernysheva, *et al*., 2003). Bearing in mind that sCT is positively charged at pH < 10.4 (pI) (Tsai, *et al*., 1996), calcitonin interactions with PLGA H, having negatively ionized free carboxylic end groups in the polymer chain, should be favored. For this reason, an increase of electrostatic binding would be expected between negatively charged PLGA H and sCT involving a positive zeta potential in drug-loaded nanoparticles or a smaller negative one at least. As a matter of fact, zeta potential of sCT-loaded PLGA H nanoparticles was slightly less negative compared to unloaded nanoparticles, most likely indicating that the peptide was rather incorporated into the matrix than adsorbed onto the surface. At the opposite, it was expected that nanoparticles prepared with PLGA S (capped by an alkyl chain group at its terminal end) would have no charge on their surface. In this sense, PLGA S should not electrostatically interact with the drug. However, as reported in Table 21, blank and loaded nanoparticles composed of PLGA H or PLGA S demonstrated similar negative zeta potential.

With regard to encapsulation efficiency of sCT in nanoparticles, the highest efficiency (83%, according to the indirect method) was achieved by PLGA H nanoparticles which could be explained in a similar way, i.e. a favorable interaction of positively charged calcitonin with the free carboxyl groups in the polymer. This speculation was in accordance with Blanco and Alonso (1997) who successfully encapsulated BSA in nanospheres using solvent evaporation technique (Blanco & Alonso, 1997). Moreover, the lower values of encapsulation efficiency obtained in the extraction method for PLGA polymers could be partially due to the strong electrostatic calcitonin - polymer interaction. It is already well known that the state of the terminal groups in PLGA polymers and the inherent viscosity related to their molecular weights are two important factors in the drug encapsulation and release properties (Gao, *et al*., 2006). However, in this study, since both polymers displayed similar viscosity, only the state of PLGA end groups was considered to be an important factor, but in fact the state of the end group did not affect the encapsulation efficiency of sCT.

With regard to thermal analysis (DSC) of pure polymers and polymeric particles, the conclusion could be that there was no significant influence of either formulation of polymer(s) into nanoparticles (including potential plasticizing effect of PVA or the use of

solvent evaporation and lyophilization) or sCT encapsulation into nanoparticles on the thermal properties of the polymer(s). All the formulations displayed T_g values higher than 40°C when stored at 2-8°C and protected from moisture (desiccator) after lyophilization. This suggests that during storage the polymers are in their glassy state (lesser tendency to undergo the changes due to the lower mobility of the polymer chains). However, to broaden the knowledge about the potential T_g changes during long term storage of nanoparticles, the DSC study should be continued, provided that nanoparticles are stored under temperature and relative humidity controlled conditions. On the other hand, there is no confidence that the polymers are still in the glassy state at 37°C when exposed to aqueous environment (*in vitro* drug release and *in vivo* conditions), since water can strongly act on PLGA as a plasticizer (Friess & Schlapp, 2002).

In the next step, the adsorption of sCT to blank nanoparticles was studied in two media: 5% acetic acid solution and 0.1% PVA solution under experimental conditions similar to those of the *in vitro* drug release. However, in this experiment no adsorption was observed in both media for 3 formulations (PLGA H, PLGA H/RS, RS). In earlier reports, it has been demonstrated that adsorption of sCT onto polymers was strongly dependent on pH. According to Dani and DeLuca (2001), very little adsorption onto blank PLGA microspheres was observed at pH 4.0. However, in their study, the adsorption increased dramatically at pH 7.4 (Dani & DeLuca, 2001). This was consistent with the earlier work (Tsai*, et al.*, 1996) on sCT adsorption onto PLGA polymers. Indeed, maximum adsorption occurred near the pI of sCT (pI = 10.4) and almost no adsorption was observed at pH less than 6. Results obtained by Johansen *et al.* (1998) prove the importance of such adsorption study to be conducted. In their study, incomplete *in vitro* release of tetanus toxoid from PLGA microspheres was shown to be partly due to adsorption on the glass vials used for the release test and also on the surface of the PLGA microspheres, wherefrom it was released (Johansen*, et al.*, 1998). Additionally, less adsorption of sCT on soda lime silica glass was found in acetate buffer pH 4.3 (Law & Shih, 1999). As a conclusion, the choice of the 5% acetic acid solution was confirmed as the release medium since acidic pH could prevent calcitonin readsorption onto nanoparticles. Nevertheless, surface adsorption of a peptide drug to a container may always occur but equilibrium is reached in the first few hours (Law & Shih, 1999). Additionally, in this work, 0.1% PVA solution, used as an external phase during the preparation method, was also tested as an adsorption medium. Since no affinity of sCT onto the blank nanoparticles was observed in this medium, it could be suggested that a real encapsulation of sCT within the particles had

occurred during the nanoparticle preparation excluding sCT-polymer interaction based on adsorption mechanism.

In vitro calcitonin release from nanoparticles

Before selecting the release medium, the study on calcitonin stability was performed under conditions similar to the *in vitro* release study. Among different tested media (5% acetic acid solution, 2.3 M acetate buffer pH 4.3, PBS pH 7.4, 0.1 M HCl, 0.9% NaCl) (Figure 23), the peptide was considerably more stable in acidic solutions (5% acetic acid solution pH 2.4, acetate buffer pH 4.3), especially when compared to the PBS pH 7.4 (80% of the initial peptide amount was degraded after 3 days), which was consistent with previous reports (Lee*, et al.*, 1992, Dani & DeLuca, 2001). Dani and DeLuca (2001) reported similar results in acetate buffer pH 4.0 at 37°C with a last stability measurement conducted at 22 days which showed that 63% of the initial calcitonin amount was still present. In order to avoid possible sCT aggregation induced by metal ions (Cholewinski*, et al.*, 1996) present in the acetate buffer, 5% acetic acid solution was finally selected as the release medium. Besides, this solution was recommended by the manufacturer in terms of the best storage stability. Additionally, at the end of the *in vitro* release study, pH of the release medium was measured and no significant change in pH was observed compared to the fresh medium.

The stability of peptide and protein drugs is a relevant problem in formulation. It is evident that a slow and progressive degradation of sCT results in loss of its pharmacological activity. It has been already well confirmed that degradation of sCT in an aqueous solution depends on time, temperature and pH (Lee*, et al.*, 1992, Dani & DeLuca, 2001, Dijkhuizen-Radersma*, et al.*, 2002). Thus, care should be taken in the formulation study of calcitonin to prevent its degradation during preparation, storage and release from the delivery system.

Furthermore, the positive effect of acetic acid on calcitonin stability during *in vitro* release experiments has already been reported. For instance, van Dijkhuizen-Radersma *et al.* (2002) carried out the release of calcitonin from poly(ether-ester) films either in a 0.1 M phosphate or in a 0.2 mM acetic acid buffer, both at pH 4.3 to exclude pH effects. In their study, the total calcitonin release was only 20-25% in phosphate buffer medium, whereas acetic acid buffer resulted in a release of 80-100%. On the other hand, this also suggests that the calcitonin release profile is highly dependent on the release medium composition. There are many examples of how the drug release from PLGA matrices can be influenced by pH of the release medium. Zolnik and Burgess (2007) studied the effect of acidic pH on PLGA microspheres degradation and dexamethasone release. PLGA microspheres of two different

molecular weights were investigated and both exhibited a triphasic release profile at pH 7.4 as well as at pH 2.4. The initial burst and lag phases were similar for both pH values, while the secondary burst release phase was substantially accelerated at pH 2.4. Accelerated drug release from PLGA at low pH may occur as a result of the catalysis of the ester linkage breakage of the polymer backbone enhancing polymer erosion. Nevertheless, at pH 2.4, the mechanism of drug release did not change from that under usual conditions (pH 7.4) (Zolnik & Burgess, 2007). Since drug release profiles from PLGA delivery systems can range from days to months, Zolnik and Burgess (2007) proposed acidic pH conditions for accelerated release testing of such systems for quality control purposes as well as to aid in formulation design.

According to Jiang *et al*. (2002), most authors have investigated the effect of PLGA characteristics (e.g. molecular weight and copolymer ratio) on the release kinetics, but the importance of the *in vitro* release conditions was neglected. They suggested that a number of studies focused on protein release kinetics without sufficient attention to protein stability resulting in unpredictable and incomplete protein release kinetics. As an example, in the study of Jiang *et al*. (2002), lysozyme showed conformational stability and complete release from PLGA microparticles in acetate buffer pH 4.0 and in glycine buffer pH 2.5, whereas in PBS pH 7.4 the protein showed a trend toward aggregation and adsorption resulting in slow and incomplete release terminated by 27% cumulative release (Jiang*, et al.*, 2002).

In this study, the chosen PLGA polymers had high molecular weight and differed in the type of the end groups. The presence of free carboxyl groups in the polymer chain of PLGA H should increase the degradation rate of the polymer, and thereby accelerate the drug release kinetics (Blanco & Alonso, 1997). Unexpectedly, both uncapped and capped PLGA appeared to release sCT at a similar very low and slow rate without significant difference. To explain the incomplete release of sCT from PLGA nanoparticles, various factors could be taken under consideration. However, incomplete release of the drug was observed only in the case of PLGA nanoparticles. It should be emphasized that complete release from Eudragit® RS alone, PLGA H/RS and PLGA S/RS nanoparticles most likely indicates that no aggregation of the calcitonin had occurred either due to the formulation process or the release medium. The incomplete release from PLGA nanoparticles is not due to the instability or adsorption of calcitonin since acetic acid solution prevents calcitonin degradation and adsorption phenomenon to PLGA or glass vials as mentioned before. That is why, the most probable reason for the incomplete release is a production of some calcitonin-polymer conjugates.

This can be explained by the results of Lucke *et al*. (2002). In their study, PLA and PLGA microspheres were investigated concerning the possible acylation of encapsulated sCT. Peptide integrity was monitored by HPLC-MS analysis during the release study in PBS pH 7.4 for four weeks. Interestingly, sCT was acylated by lactic and glycolic acid units inside degrading microspheres in a time-dependent manner. Moreover, oligomers that stem from polymer degradation and accumulate inside degrading microspheres were also the source of peptide acylation. The authors also found that pH appears to play a major role in the mechanism of the acylation reaction, since at pH 2 the amount of acylated sCT was significantly increased compared to the solutions at pH 5. According to Lucke *et al*. (2002), raising the pH inside eroding PLA or PLGA matrices by adding bases or an enhancement of degradation products release from the system seems to be highly desirable and useful approach to slow down and suppress the acylation process (Lucke*, et al.*, 2002). Moreover, Na *et al.* (2003) have also confirmed the acylation of sCT in the PLGA microspheres during the release study in PBS pH 7.4 monitored by CE and matrix-assisted laser desorption-ionization time-of-flight mass spectrometry (MALDI-TOF MS). The authors determined the acylation products to be adducts with glycolic acid units and suggested the primary amino group to be the major target for peptide acylation (Na*, et al.*, 2003).

It is known that a proper choice of release medium is important for the estimation and prediction of *in vivo* results but quite difficult (if possible) to make with peptides and proteins. Calcitonin stability upon incubation in the release medium is a major condition to achieve complete *in vitro* drug release especially over a long period of time. Nevertheless, the release and activity of encapsulated calcitonin should be mainly estimated under *in vivo* conditions.

In vivo studies

Since PLGA H and S nanoparticles as well as PLGA H/RS and PLGA S/RS nanoparticles displayed very similar *in vitro* characteristics in terms of size, zeta potential, encapsulation efficiency and release of calcitonin only 3 of 5 formulations were selected for further *in vivo* study in rats: PLHA H, PLGA H/RS and RS nanoparticles. All of them were administered either subcutaneously or orally. Although non biodegradable, PLGA H/RS and RS nanoparticles were also administered *via* sc injection, with a view to serving as reference for determination of the relative bioavailability (if applicable) after oral administration and to making a comparison with PLGA H. Besides, such an administration may also allow determining the influence of positive charge on *in vivo* behavior of nanoparticles after sc administration.

With RS and PLGA H/RS nanoparticles, no delayed release characteristics were observed *in vitro* (Figure 24) and it was considered that no sustained calcitonin concentration in blood would be provided. Interestingly, Eudragit® RS nanoparticles sustained the release of calcitonin at least over 48 h, similarly to the PLGA H nanoparticles (Figure 25). Thus, it is obvious that sCT blood levels in rats did not correlate qualitatively with *in vitro* release results in 5% acetic acid solution. In contrast to *in vitro* results, PLGA H nanoparticles seemed to release sCT very quickly after injection. However, due to the stability issues, the *in vitro* release was carried out in an acetic acid solution which is far from the local sc physiological environment both in terms of pH and viscosity. Thus, it was not surprising that correlation between *in vitro* release and *in vivo* behavior of the peptide drug was not achieved.

According to Lee and Sinko (2000), after sc administration of sCT solution to dogs, the absolute sCT bioavailability showed large variability and was 21, 53 and 23% at a dose of 10, 20 and 1 000 µg, respectively (Lee & Sinko, 2000). Sinko *et al.* (1995) have reported even lower absolute sCT bioavailability in rats after sc administration: 16.2 ± 5.1% (administered doses: 1, 10, 25 and 100 µg) (Sinko*, et al.*, 1995). However, the absolute bioavailability following sc injection of 100 IU (~ 15 µg/dose) in humans is higher and comes to 71% according to the package leaflet for Novartis Pharma Miacalcin® Injection. In this study, the sCT dose was 50 µg/kg (~ 300 IU/kg) or 100 µg/kg (~ 600 IU/kg) in the case of sCT solution or sCT-loaded nanoparticles, respectively. Obviously, the bioavailability was adjusted for the dose in calculations, and then, a comparison was performed. Since the formulation was considered as sustained drug delivery system, it was expected that the initial calcitonin concentrations in plasma could be lower than those after sCT solution administration. That is why, the sCT dose in nanoparticles was 2-fold higher compared to sCT solution in order to ensure sufficient calcitonin concentration in plasma. It should be known that Sinko *et al.* (1995) have already demonstrated that pharmacokinetic parameters for iv and sc administration of sCT are independent of dose, thus sCT gives liner pharmacokinetics.

As a result of this study, sCT was more bioavailable after sc injection from sCT-loaded nanoparticles than from sCT solution (at best relative bioavailability of 139% for PLGA H nanoparticles) and sCT was still detected until 3 days after injection of nanoparticles. Most likely, the amount of sCT to be released from the polymeric matrix was quickly depleted after injection and too low to maintain longer than 3 days the drug concentration in blood over the limit of sCT quantification by ELISA. However, Dani and DeLuca (2001) reported that sc administration to rats of 500 µg/kg sCT dose (~ 3 000 IU/kg) in PLGA microspheres resulted in elevated serum sCT levels for at least 6 days, and

detectable levels were observed for 9 days following administration. However, administration of 1 mg/kg dose (~ 6 000 IU/kg) of sCT-loaded microspheres produced elevated serum sCT levels beyond 9 days, with levels returning to baseline after 12 days and this was thought to be promising as a 2-week formulation. Nevertheless, the doses used by Dani and DeLuca (2001) were 5 or 10-fold higher than those used in this study for sc administration (~ 600 IU/kg).

In the report of Sinko *et al*. (1995), the authors concluded that the calcium lowering effects increase with increasing sCT plasma concentrations, but reaching a maximum effect after which additive lowering does not occur. This maximum effect occurs at extremely low concentrations of the peptide in plasma, which were in their study below the LOQ of the assay (radioimmunoassay, LOQ = 80 pg/ml). However, due to the linearity of the sc and iv pharmacokinetic data, the authors estimated that the maximal calcium lowering effect occurs at a sCT plasma concentration of approximately 10 pg/ml. Additionally, it has been demonstrated a dose-response relationship following sc sCT administration in rats, indicating that the maximal calcium lowering effect which occurs at a sCT plasma concentration of approximately 10 pg/ml corresponds to sc minimum dose equal to 10.2 ng/rats. This is because the pharmacodynamic effect (calcium lowering) *versus* dose relationship is nonlinear and saturable (Sinko*, et al.*, 1995). Additionally, Hastewell *et al.* (1992), reported that to achieve a maximal decrease in the plasma calcium level in rats, plasma hCT levels of 600 pg/ml must be reached (Hastewell*, et al.*, 1992), which seems to be logical taking into account that sCT is at least 30 times more potent than hCT. In this *in vivo* study, the last plasma sCT measurements (after 48 or 72 h) exceeding 10 pg/ml for each formulation suggest that most likely calcium lowering effect was prolonged at least for 2-3 days, although almost the entire amount of sCT seemed to be released from nanoparticles within 1 day following sc administration.

Since, in most reports, results from animal studies are based on serum calcium levels, it is difficult to directly compare the bioavailability results of this study with those of other studies. In addition, different calcitonins (e.g. salmon, human, bovine) and methods for calculations of bioavailability (absolute or relative) were used in different animal models. The current formulation of sCT-loaded PLGA H nanoparticles could be further improved to sustain the calcitonin concentration in blood for a longer period of time. For instance, an increased calcitonin core loading in the nanoparticles seems to be necessary or some additives could be included in the formulation to decrease the burst release right after the injection. By

optimizing the formulation parameters, PLGA H nanoparticles encapsulating calcitonin might be potentially utilized for the injectable sustained delivery system of this hormone.

Nevertheless, bioavailability is not the only parameter useful to assess *in vivo* efficacy of a formulation after administration to subjects. In most reports, a pharmacodynamic response to sCT, i.e. the plasma calcium lowering effect, is studied to characterize novel formulations containing sCT and calculate oral bioavailability. However, relying on pharmacodynamic results can easily lead to overestimation of the bioavailability (Sinko*, et al.*, 1995). However, it should be mentioned that analytical methods for determination of sCT in blood samples have been reported difficult due to very low sCT concentrations in plasma, rapid elimination and problems associated with calcitonin stability and assay sensitivity.

Taking into account all the obtained results, completely different *in vitro* and *in vivo* release of sCT from PLGA H nanoparticles is quite surprising. Thus, the following hypothesis could be constructed. At acidic pH during *in vitro* drug release study, the PLGA H particles could exist in the glassy state with hampered mobility of the polymer chains resulting in lower diffusivity of water and slower drug release. Additionally, the prolonged contact of calcitonin with the polymeric matrix could give rise to the peptide acylation with time as the matrix was gradually degraded. In contrast, at physiological pH after sc injection, the polymer could be in the rubbery state (due to the decrease of T_g) resulting in higher molecular mobility and diffusivity of water, and consequently faster drug release. This explanation is supported by the results of Faisant *et al*. (2006). In their study, 5-fluorouracil was rapidly and completely released within 3 days from PLGA microparticles at high pH (carbonate buffer pH 10.8). In phosphate buffer pH 7.4, an intermediate release rate was observed (22 days), whereas at low pH (phosphate buffer pH 4.5 and citrate buffer pH 1.3) drug release was very slow (37 days). Next, they determined T_g of microparticles in wet state after exposure to the different release media. The reason for these differences in drug release was the change of T_g: the T_g was above 37°C at acidic pH (buffers pH 1.3 and 4.5), whereas it was below 37°C in the case of buffers pH 7.4 and 10.8. Thereby, at pH 7.4 the PLGA polymer was in the rubbery state and released the drug faster (Faisant*, et al.*, 2006).

With regard to oral administration, calcitonin solution and three nanoparticulate formulations (the same as for sc injection) administered intragastrically did not display any sCT concentrations in rat sera above LOQ of ELISA (100 pg/ml). However, following administration of sCT-loaded RS nanoparticles, the calcium concentration decreased to approximately 80% within the first 4 h and then the weak hypocalcemic effect was maintained within 12 h. Similarly, sCT-loaded PLGA H nanoparticles seemed to decrease the

serum calcium concentration for 12 h, indicating that negative charge must not be a limitation on interactions with anionic mucus in the gastrointestinal tract. Instead, sCT encapsulated in blended positively charged nanoparticles (PLGA H/RS) triggered the same effect as blank nanoparticles did, and no improvement in hypocalcemic activity was observed (if any) when compared to the nanoparticles made from the single polymer. It should be noted that the administration of blank nanoparticles in each case provoked a delayed and a more or less significant decrease (starting approximately after 4 h after administration) of calcium concentration, indicating that the procedure of drug administration and blood sampling could likely have the influence on the blood calcium level in rats. Nevertheless, it is reasonable to suppose that sCT was released from nanoparticles and maintained its biological activity resulting in the decrease of calcium level particularly within first 4 h. In this sense, nanoparticles prepared from Eudragit® RS seems to be the most promising formulations.

By comparison to other studies, the obtained results indicate rather medium or weak hypocalcemic effect of the studied formulations, especially as compared to the study of Prego *et al.* (2006). In their study, nanocapsules, consisted of an oily core and coated with chitosan, triggered a high hypocalcemic effect remaining on the level of 70-80% of basal and prolonged for 24 h, following oral administration to rats (sCT dose of 500 IU/kg) (Prego*, et al.*, 2006). Interesting results were also obtained by Yoo and Park (2004). They prepared PLGA nanoparticles loaded with sCT-fatty acid complex and administered into the stomach of rats. For a sCT dose of 60 μg/kg (~ 360 IU/kg), the plasma concentration of sCT soared to ~ 600 pg/ml after 2 h and then slowly decreased (after 12 h the sCT plasma concentration was still ~ 100 pg/ml), and the calculated bioavailability was approximately 0.4%. However, when sCT was orally administered as free sCT at 160 μg/kg (~ 960 IU/kg), negligible amounts of sCT were detected by ELISA (Yoo & Park, 2004). It is worthy to quote Hastewell *et al.* (1992) who reported that the absolute bioavailability following intracolonic administration of hCT to rats was in the range 0.2-0.9%. However, when sCT was administered intraduodenally in rats, the absolute bioavailability was 0.022% (Sinko*, et al.*, 1995). These differences may be attributed to less enzymatic degradation of calcitonin in the colon that in the duodenum. Additionally, colonoscopicaly administered hCT in humans was absorbed across the distal colonic mucosa in low amount with an absolute bioavailability of 0.00-0.22% (Antonin*, et al.*, 1992).

7. CONCLUSIONS

7.1. Encapsulation of glutathione-selective fluorogenic probes

1. The method used for preparation of nanoparticles allowed to obtain positively charged pH-sensitive 220-nm particles with a low polidispersity index.
2. Two selective fluorogenic probes useful for the labeling of intracellular GSH, OPA and NDA, were incorporated into nanoparticles. However, only NDA was successfully encapsulated into polymeric nanoparticles (higher encapsulation efficiency), most probably due to a higher hydrophobicity compared to OPA. For this reason, this probe was consequently chosen for cellular application.
3. The HPLC method permitted to identify and quantify the NDA-GSH adduct formed in yeast cells after their incubation with the free or encapsulated probe and extraction of the adduct. HPLC results (9.2-fold higher NDA-GSH adduct concentration found in cell extracts after incubation of cells with NDA-loaded nanoparticles in comparison with incubation with the free NDA) demonstrated a better penetration of the probe and its uptake by yeast cells when encapsulated in nanoparticles compared to the free probe.
4. The mechanism of the enhanced cellular uptake of the probe by means of nanoparticles could be associated with the nature of the polymer. Since Eudragit® E is a pH-sensitive polycationic polymer, the adhesion of nanoparticles onto microbial cells, allowing an easier internalization of nanoparticles followed by an immediate dissolution of nanoparticles and release of the probe inside cells, should be favored.
5. The use of NDA-loaded nanoparticles is a promising approach for intracellular GSH labeling coupled with *in situ* methods, such as FC and confocal microscopy, as most of this equipment includes an argon laser with an emission line at 488 nm, well fitted to the excitation of the NDA-GSH adduct.

7.2. Encapsulation of salmon calcitonin

1. The method used for preparation of nanoparticles allowed to successfully incorporate sCT, a polypeptide drug, into polymeric nanoparticles with high encapsulation efficiencies (69-83% depending on the formulation) which were sufficient to administer in animals an appropriate dose of sCT encapsulated in nanoparticles even *via* an oral route. The particle size of the obtained nanoparticles was relatively large (380-625 nm), but suitable for parenteral administration.
2. Calcitonin stability upon incubation in the release medium at 37°C is a major condition to achieve complete *in vitro* drug release especially over a long period of time.
3. PLGA nanoparticles were characterized by a slow and incomplete *in vitro* calcitonin release, unconventionally conducted in 5% acetic acid solution, which could be explained by the acylation of the encapsulated sCT in the polymeric matrix due to the appearance of the polymer degradation products.
4. Eudragit® RS had a modifying accelerating effect on the *in vitro* calcitonin release from the blended nanoparticles composed of both biodegradable (PLGA) and non biodegradable (Eudragit® RS) polymer.
5. It was demonstrated that after a single sc injection of sCT-loaded nanoparticles (PLGA H and Eudragit® RS nanoparticles) to rats, elevated serum sCT levels could be sustained for 3 days and the achieved sCT bioavailability from nanoparticles was increased compared to sCT solution. Nevertheless, only PLGA nanoparticles could be considered as a sustained delivery system for calcitonin due to biodegradability and biocompatibility of this polymer.
6. A slight hypocalcemic effect in rats after single oral administration of sCT-loaded nanoparticles composed of Eudragit® RS could suggest the protection of sCT against the enzymatic degradation in the gastrointestinal tract.
7. The use of sCT-loaded polymeric nanoparticles is a promising approach as a sustained injectable or oral calcitonin delivery system, however, the present formulations need to be further improved.

8. REFERENCES

[1] Akamatsu T, Minemoto M & Uyeda M (2005) Evaluation of the antimicrobial activity and materials compatibility of orthophthalaldehyde as a high-level disinfectant. *J Int Med Res* **33**: 178-187.

[2] Allemann E, Leroux J-C & Gurny R (1998) Polymeric nano- and microparticles for the oral delivery of peptides and peptidomimetics. *Adv Drug Deliv Rev* **34**: 171–189.

[3] Amodeo P, Motta A, Strazzullo G & Castiglione Morelli MA (1999) Conformational flexibility in calcitonin: the dynamic properties of human and salmon calcitonin in solution. *J Biomol NMR* **13**: 161–174.

[4] Antonin KH, Saano V, Bieck P, Hastewell J, Fox R, Lowe P & Mackay M (1992) Colonic absorption of human calcitonin in man. *Clin Sci* **83**: 627-631.

[5] Arum SM (2008) New developments surrounding the safety of bisphosphonates. *Curr Opin Endocrinol Diabetes Obes* **15**: 508-513.

[6] Arvinte T & Drake AF (1993) Comparative study of human and salmon calcitonin secondary structure in solutions with low dielectric constants. *J Biol Chem* **268**: 6408-6414.

[7] Arvinte T, Cudd A & Drake AF (1993) The structure and mechanism of formation of human calcitonin fibrils. *J Biol Chem* **268**: 6415-6422.

[8] Azria M, Copp DH & Zanelli JM (1995) 25 years of salmon calcitonin: from synthesis to therapeutic use. *Calcif Tissue Int* **57**: 405-408.

[9] Bagger YZ, Tanko LB, Alexandersen P*, et al.* (2005) Oral salmon calcitonin induced suppression of urinary collagen type II degradation in postmenopausal women: A new potential treatment of osteoarthritis. *Bone* **37**: 425 – 430.

[10] Barhoumi R, Bailey RH & Burghardt RC (1995) Kinetic analysis of glutathione in anchored cells with monochlorobimane. *Cytometry* **19**: 226-234.

[11] Barratt G (2003) Colloidal drug carriers: achievements and perspectives. *Cell Mol Life Sci* **60**: 21-37.

[12] Basan H, Gumusderelioglu M & Orbey MT (2007) Release characteristics of salmon calcitonin from dextran hydrogels for colon-specific delivery. *Eur J Pharm Biopharm* **65**: 39–46.

[13] Baudys M, Mix D & Kim SW (1996) Stabilization and intestinal absorption of human calcitonin. *J Control Release* **39**: 145-151.

[14] Bellomo G, Palladini G & Vairetti M (1997) Intranuclear distribution, function and fate of glutathione and glutathione-S-conjugate in living rat hepatocytes studied by fluorescence microscopy. *Microsc Res Techniq* **36**: 243-252.

[15] Bernkop-Schnurch A (2000) Chitosan and its derivatives: potential excipients for peroral peptide delivery systems. *Int J Pharm* **194**: 1–13.

[16] Bernkop-Schnurch A, Kast CE & Guggi D (2003) Permeation enhancing polymers in oral delivery of hydrophilic macromolecules: thiomer/GSH systems. *J Control Release* **93**: 95– 103.

[17] Beveridge T, Niederer W, Nuesch E & Petrin A (1976) Pharmacokinetic study with synthetic salmon calcitonin (Sandoz). *Z Gastroenterol Verh* **10**: 12-15.

[18] Bilati U, Allemann E & Doelker E (2005) Strategic approaches for overcoming peptide and protein instability within biodegradable nano- and microparticles. *Eur J Pharm Biopharm* **59**: 375–388.

[19] Blanco MD & Alonso MJ (1997) Development and characterization of protein loaded poly(lactide-co-glycolide) nanospheres *Eur J Pharm Biopharm* **43**: 287-294.

[20] Bodmeier R & Maincent P (1998) Polymeric Dispersions as Drug Carriers *Pharmaceutical Dosage Forms: Disperse Systems*, Vol. 3 (Lieberman HA, Rieger MM & Banker GS), 87-127. Informa Health Care, New York.
[21] Body JJ (2002) Calcitonin for the long-term prevention and treatment of postmenopausal osteoporosis. *Bone* **30**: 75S–79S.
[22] Buclin T, Rochat MC, Burckhardt P, Azria M & Attinger M (2002) Bioavailability and biological efficacy of a new oral formulation of salmon calcitonin in healthy volunteers. *J Bone Miner Res* **17**: 1478-1485.
[23] Cai J, Chen Y, Seth S, Furukawa S, Compans RW & Jones DP (2003) Inhibition of Influenza infection by glutathione. *Free Radical Bio Med* **34**: 928-936.
[24] Camera E & Picardo M (2002) Analytical methods to investigate glutathione and related compounds in biological and pathological processes. *J Chromatogr B* **781**: 181-206.
[25] Capelle MAH, Gurny R & Arvinte T (2007) High throughput screening of protein formulation stability: practical considerations. *Eur J Pharm Biopharm* **65**: 131–148.
[26] Capelle MAH, Gurny R & Arvinte T (2009) A high throughput protein formulation platform: case study of salmon calcitonin. *Pharm Res* **26**: 118-128.
[27] Caruthers SD, Wickline SA & Lanza GM (2007) Nanotechnological applications in medicine. *Curr Opin Biotech* **18**: 26-30.
[28] Cereser C, Guichard J, Drai J*, et al.* (2001) Quantitation of reduced and total glutathione at the femtomole level by high-performance liquid chromatography with fluorescence detection: application to red blood cells and cultured fibroblasts. *J Chromatogr B* **752**: 123-132.
[29] Chaturvedula A, Joshi DP, Anderson C, Morris RL, Sembrowich WL & Bangaa AK (2005) *In vivo* iontophoretic delivery and pharmacokinetics of salmon calcitonin. *Int J Pharm* **297**: 190-196.
[30] Chernysheva Y, Babak VG, Kildeeva N, Boury F, Benoit JP, Ubrich N & Maincent P (2003) Effect of the type of hydrophobic polymers on the size of nanoparticles obtained by emulsification-solvent evaporation. *Mendeleev Commun* **13**: 65-68.
[31] Chesnut III CH, Azria M, Silverman S, Engelhardt M, Olson M & Mindeholm L (2008) Salmon calcitonin: a review of current and future therapeutic indications. *Osteoporos Int* **19**: 479–491.
[32] Chesnut III CH, Silverman S, Andriano K*, et al.* (2000) A randomized trial of nasal spray salmon calcitonin in postmenopausal women with established osteoporosis: the prevent recurrence of osteoporotic fractures study. *Am J Med* **109**: 267-276.
[33] Cholewinski M, Luckel B & Horn H (1996) Degradation pathways, analytical characterization and formulation strategies of a peptide and a protein. Calcitonin and human growth hormone in comparison. *Pharm Acta Helv* **71**: 405-419.
[34] Clarke SJ, Hollmann CA, Zhang Z, et al. (2006) Photophysics of dopamine-modified quantum dots and effects on biological systems. *Nat Mater* **5**: 409-417.
[35] Clausen AE, Kast CE & Bernkop-Schnurch A (2002) The role of glutathione in the permeation enhancing effect of thiolated polymers. *Pharm Res* **19**: 602-608.
[36] Combe B, Cohen C & Aubin F (1997) Equivalence of nasal spray and subcutaneous formulations of salmon calcitonin. *Calcif Tissue Int* **61**: 10–15.
[37] Copp DH, Davidson AGF & Cheney BA (1961) Evidence for a new parathyroid hormone which lowers blood calcium. *Proc Can Fed Biol Soc* **4**: 17.
[38] Couvreur P, Barratt G, Fattal E, Legrand P & Vauthier C (2002) Nanocapsule technology: a review. *Crit Rev Ther Drug Car Sys* **19**: 99-134.
[39] Damge C, Maincent P & Ubrich N (2007) Oral delivery of insulin associated to polymeric nanoparticles in diabetic rats. *J Control Release* **117**: 163-170.

[40] Dani BA & DeLuca PP (2001) Preparation, characterization, and *in vivo* evaluation of salmon calcitonin microspheres. *AAPS PharmsciTech* **2**: E22.
[41] Deas O, Dumont C, Mollereau B*, et al.* (1997) Thiol-mediated inhibition of FAS and CD2 apoptotic signaling in activated human peripheral T cells. *Int Immunol* **9**: 117-125.
[42] Delie F & Blanco-Prieto MJ (2005) Polymeric particulates to improve oral bioavailability of peptide drugs. *Molecules* **10**: 65-80.
[43] DeMerlis CC & Schoneker DR (2003) Review of the oral toxicity of polyvinyl alcohol (PVA). *Food Chem Toxicol* **41**: 319–326.
[44] Devalapally H, Chakilam A & Amiji MM (2007) Role of nanotechnology in pharmaceutical product development. *J Pharm Sci* **96**: 2547-2565.
[45] Diaz RV, Llabres M & Evora C (1999) One-month sustained release microspheres of ^{125}I-bovine calcitonin. *In vitro-in vivo* studies. *J Control Release* **59**: 55–62.
[46] Dickinson DA & Forman HJ (2002) Cellular glutathione and thiols metabolism. *Biochem Pharmacol* **64**: 1019-1026.
[47] Diez L, Martenka E, Dabrowska A, Coulon J & Leroy P (2005) Assessment of in situ cellular glutathione labeling with naphthalene-2,3-dicarboxaldehyde using high-performance liquid chromatography. *J Chromatogr B* **827**: 44-50.
[48] Dijkhuizen-Radersma R, Nicolas HM, Weert M, Blom M, Groot K & Bezemer JM (2002) Stability aspects of salmon calcitonin entrapped in poly(etherester) sustained release systems. *Int J Pharm* **248**: 229-237.
[49] Dillen K, Vandervoort J, van den Mooter G & Ludwiga A (2006) Evaluation of ciprofloxacin-loaded Eudragit RS100 or RL100/PLGA nanoparticles. *Int J Pharm* **314**: 72-82
[50] Dogru ST, Calis S & Oner F (2000) Oral multiple w/o/w emulsion formulation of a peptide salmon calcitonin: *in vitro-in vivo* evaluation. *J Clin Pharm Ther* **25**: 435-443.
[51] Dorkoosh FA, Verhoef JC, Rafiee-Tehrani M, Borchard G & Junginger HE (2002) Peroral drug delivery systems for peptides and proteins. *S.T.P. Pharma Sci* **12**: 213-221.
[52] Dziurla MA, Leroy P, Strunkmann GW*, et al.* (2004) Measurement of glutathione in activated sludges. *Water Res* **38**: 236–244.
[53] Ettinger B, Black DM, Mitlak BH*, et al.* (1999) Reduction of vertebral fracture risk in postmenopausal women with osteoporosis treated with raloxifene: results from a 3-year randomized clinical trial *JAMA* **282**: 637-645.
[54] Faisant N, Akiki J, Siepmann F, Benoit JP & Siepmann J (2006) Effects of the type of release medium on drug release from PLGA-based microparticles: experiment and theory. *Int J Pharm* **314**: 189-197.
[55] Franco R, Schoneveld OJ, Pappa A & Panayiotidis MI (2007) The central role of glutathione in the pathophysiology of human diseases. *Arch Phys Biochem* **113**: 234-258.
[56] Friess W & Schlapp M (2002) Release mechanisms from gentamicin loaded poly(lactic-co-glycolic acid) (PLGA) microparticles. *J Pham Sci* **91**: 845-856.
[57] Fu K, Klibanov AM & Langer R (2000) Protein stability in controlled-release systems. *Nat Biotechnol* **18**: 24-25.
[58] Gao P, Ding P, Xu H, Yuan Z, Chen D, Wei J & Chen D (2006) *In vitro* and *in vivo* characterization of huperzine A loaded microspheres made from end-group uncapped poly(D,L-lactide acid) and poly(D,L-lactide-co-glycolide acid). *Chem Pharm Bull* **54**: 89-93.
[59] Gao X, Yang L, Petros JA, Marshall F, Simons JW & Nie S (2005) *In vivo* molecular and cellular imaging with quantum dots. *Curr Opin Biotech* **16**: 63–72.
[60] Garcia-Fuentes M, Prego C, Torres D & Alonso MJ (2005) A comparative study of the potential of solid triglyceride nanostructures coated with chitosan or poly(ethylene glycol) as carriers for oral calcitonin delivery. *Eur J Pharm Sci* **25**: 133–143.

[61] Gate L, Vauthier C, Couvreur P, Tew KD & Tapiero H (2001) Glutathione-loaded poly(isobutylcyanoacrylate) nanoparticles and liposomes: comparative effects in murine erythroleukemia and macrophage-like cells *S.T.P. Pharma Sci* **11**: 355-361.
[62] Gaudiano MC, Colone M, Bombelli C, Chistolini P, Valvo L & Diociaiuti M (2005) Early stages of salmon calcitonin aggregation: Effect induced by ageing and oxidation processes in water and in the presence of model membranes. *Biochim Biophys Acta* **1750**: 134-145.
[63] Gennari C (2002) Analgesic effect of calcitonin in osteoporosis. *Bone* **30**: 67S-70S.
[64] Główka E, Lamprecht A, Ubrich N, Maincent P, Lulek J, Coulon J & Leroy P (2006) Enhanced cellular uptake of a glutathione selective fluorogenic probe encapsulated in nanoparticles. *Nanotechnology* **17**: 2546-2552.
[65] Goldberg M & Gomez-Orellana I (2003) Challenges for the oral delivery of macromolecules. *Nat Rev Drug Discov* **2**: 289-295.
[66] Gombotz WR & Pettit DK (1995) Biodegradable polymers for protein and peptide drug delivery. *Bioconjugate Chem* **6**: 332-351.
[67] Guggi D, Krauland AH & Bernkop-Schnurch A (2003) Systemic peptide delivery *via* the stomach: *in vivo* evaluation of an oral dosage form for salmon calcitonin. *J Control Release* **92**: 125-135.
[68] Gutscher M, Pauleau A-L, Marty L*, et al.* (2008) Real-time imaging of the intracellular glutathione redox potential. *Nat Methods* **5**: 553-559.
[69] Haining WN, Anderson DG, Little SR*, et al.* (2004) pH-triggered microparticles for peptide vaccination. *J Immnunol* **173**: 2578–2585.
[70] Hall CE & Hall O (1963) Polyvinyl alcohol nephrosis: relationship of degree of polymerization to pathophysiological effects. *P Soc Exp Biol Med* **112**: 86–91.
[71] Hanczko R, Jambor A, Perl A & Molnar-Perl I (2007) Advances in the o-phthalaldehyde derivatizations. Comeback to the o-phthalaldehyde–ethanethiol reagent. *J Chromatogr A* **1163**: 25–42.
[72] Harris ST, Watts NB, Genant HK*, et al.* (1999) Effects of risedronate treatment on vertebral and nonvertebral fractures in women with postmenopausal osteoporosis: a randomized controlled trial. *JAMA* **282**: 1344-1352.
[73] Hastewell J, Lynch S, Williamson I, Fox R & Mackay M (1992) Absorption of human calcitonin across the rat colon *in vivo*. *Clin Sci* **82**: 589-594.
[74] Haugland RP (2005) The Handbook - A Guide to Fluorescent Probes and Labeling Technologies (10th edn). Invitrogen Corp., Eugene, OR, USA.
[75] Hayter C (2003) An EPSRC view of the nanotechnology horizon. *Mat Sci Eng C* 23: 703-705.
[76] He X, Zhong Z, Guo Y, et al. (2007) Gold nanoparticle-based monitoring of the reduction of oxidized to reduced glutathione. *Langmuir* **23**: 8815-8819.
[77] Hedley DW & Chow S (1994) Evaluation of methods for measuring cellular glutathione content using flow cytometry. *Cytometry* **15**: 349-358.
[78] Hoffart V, Ubrich N, Simonin C*, et al.* (2002) Low molecular weight heparin-loaded polymeric nanoparticles: formulation, characterization, and release characteristics. *Drug Dev Ind Pharm* **28**: 1091-1099.
[79] Hombreiro-Perez M, Zinutti C, Lamprecht A*, et al.* (2000) The preparation and evaluation of poly(ε-caprolactone) microparticles containing both a lipophilic and a hydrophilic drug. *J Control Release* **65**: 429–438.
[80] Ikegame M, Ejiri S & Ozawa H (2004) Calcitonin-induced change in serum calcium levels and its relationship to osteoclast morphology and number of calcitonin receptors. *Bone* **35**: 27– 33.

[81] Jain KK (2008) Nanomedicine: application of nanobiotechnology in medical practice. *Med Princ Pract* **17**: 89-101.
[82] Jiang G, Woo BH, Kang F, Singh J & DeLuca PP (2002) Assessment of protein release kinetics, stability and protein polymer interaction of lysozyme encapsulated poly(D,L-lactide-co-glycolide) microspheres. *J Control Release* **79**: 137-145.
[83] Jiao YY, Ubrich N, Marchand-Arvier M, Vigneron C, Hoffman M & Maincent P (2001) Preparation and *in vitro* evaluation of heparin-loaded polymeric nanoparticles. *Drug Deliv* **8**: 135-141.
[84] Johansen P, Corradin G, Merkle HP & Gander B (1998) Release of tetanus toxoid from adjuvants and PLGA microspheres: how experimental set-up and surface adsorption fool the pattern. *J Control Release* **56**: 209-217.
[85] Karsdal Ma, Sondergaard BC, Arnold M & Christiansen C (2007) Calcitonin affects both bone and cartilage. A dual action treatment for osteoarthritis? *Ann NY Acad Sci* **1117**: 181–195.
[86] Karsdal MA, Henriksen K, Arnold M & Christiansen C (2008) Calcitonin – a drug of the past or for the future? Physiologic inhibition of bone resorption while sustaining osteoclast numbers improves bone quality. *Biodrugs* **22**: 137-144.
[87] Kawamura K, Matsumoto T, Nakahara T, Hirano M, Uchimura H & Maeda H (2000) Improved method for determination of beta-phenylethylamine in human plasma by solid-phase extraction and high-performance liquid chromatography with fluorescence detection. *J Liq Chrom & Rel Technol* **23**: 1981–1993.
[88] Kawashima Y, Yamamoto H, Takeuchi H & Kuno Y (2000) Mucoadhesive DL-lactide/glycolide copolymer nanospheres coated with chitosan to improve oral delivery of elcatonin. *Pharm Dev Technol* **5**: 77–85.
[89] Kawashima Y, Yamamoto H, Takeuchi H, Hino T & Niwa T (1998) Properties of a peptide containing DL-lactide:glycolide copolymer nanospheres prepared by novel emulsion solvent diffusion methods. *Eur J Pharm Biopharm* **45**: 41-48.
[90] Keck CM & Muller RH (2006) Drug nanocrystals of poorly soluble drugs produced by high pressure homogenisation. *Eur J Pharm Biopharm* **62**: 3-16.
[91] Kerppola TK (2006) Visualization of molecular interactions by fluorescence complementation. *Nat Rev Mol Cell Biol* **7**: 449–456.
[92] Kidd PM (1997) Glutathione: systemic protectant against oxidative and free radical damage. *Altern Med Rev* **2**: 155-176.
[93] Kidron M, Dinh S, Menachem Y*, et al.* (2004) A novel per-oral insulin formulation: proof of concept study in non-diabetic subjects. *Diabetic Med* **21**: 354-357.
[94] Kretlow JD, Klouda L & Mikos AG (2007) Injectable matrices and scaffolds for drug delivery in tissue engineering. *Adv Drug Deliv Rev* **59**: 263-273.
[95] Kulinsky VI & Kolesnichenko LS (2007) Mitochondrial glutathione. *Biochemistry (Moscow)* **72**: 698-701.
[96] Kutlan D, Presits P & Molnar-Perl I (2002) Behavior and characteristics of amine derivatives obtained with o-phthaldialdehyde/3-mercaptopropionic acid and with o-phthaldialdehyde/N-acetyl-L-cysteine reagents. *J Chromatogr A* **949**: 235–248.
[97] Lai MC & Topp EM (1999) Solid-state chemical stability of proteins and peptides. *J Pharm Sci* **88**: 489-500.
[98] Lamba S, Pandit A, Sanghi SK*, et al.* (2008) Determination of aliphatic amines by high-performance liquid chromatography-amperometric detection after derivatization with naphthalene-2,3-dicarboxaldehyde. *Anal Chim Acta* **614**: 190–195.
[99] Lamprecht A, Yamamoto H, Takeuchi H & Kawashima Y (2004) pH-Sensitive microsphere delivery increases oral bioavailability of calcitonin. *J Control Release* **98**: 1-9.

[100] Law SL & Shih CL (1999) Adsorption of calcitonin to glass. *Drug Dev Ind Pharm* **25**: 253-256.
[101] Lee KC, Lee YJ, Song HM, Chun CJ & DeLuca PP (1992) Degradation of synthetic salmon calcitonin in aqueous solution. *Pharm Res* **9**: 1521-1523.
[102] Lee KC, Soltis EE, Newman PS, Buron KW, Mehta RC & DeLuca PP (1991) *In vivo* assessment of salmon calcitonin sustained release from biodegradable microspheres. *J Control Release* **17**: 199-206.
[103] Lee KC, Tak KK, Park MO*, et al.* (1999) Preparation and characterization of polyethylene-glycol-modified salmon calcitonins. *Pharm Dev Technol* **4**: 269-275.
[104] Lee KC, Park M-O, Na DH*, et al.* (2003) Intranasal delivery of PEGylated salmon calcitonins: hypocalcemic effects in rats. *Calcif Tissue Int* **73**: 545-549.
[105] Lee YH & Sinko PJ (2000) Oral delivery of salmon calcitonin. *Adv Drug Deliv Rev* **42**: 225–238.
[106] Lenton KJ, Therriault H & Wagner JR (1999) Analysis of glutathione and glutathione disulfide in whole cells and mitochondria by postcolumn derivatization high-performance liquid chromatography with ortho-phthalaldehyde. *Anal Biochem* **274**: 125–130.
[107] Leroy P, Nicolas A, Wellmann M, Michelet F, Oster T & Siest G (1993) Evaluation of o-phthalaldehyde as bifunctional fluorogenic post-column reagent for glutathione in LC. *Chromatographia* **36**: 130-134.
[108] Letchford K & Burt H (2007) A review of the formation and classification of amphiphilic block copolymer nanoparticulate structures: micelles, nanospheres, nanocapsules and polymersomes. *Eur J Pharm Biopharm* **65**: 259–269.
[109] Lewicki K, Marchand S, Matoub L, Lulek J, Coulon J & Leroy P (2006) Development of a fluorescence-based microtiter plate method for the measurement of glutathione in yeast. *Talanta* **70**: 876–882.
[110] Lowe PJ & Temple CS (1994) Calcitonin and insulin in isobutylcyanoacrylate nanocapsules: protection against proteases and effect on intestinal absorption in rats. *J Pharm Pharmacol* **46**: 547-552.
[111] Lu C, Zu Y & Yam VW-W (2007) Nonionic surfactant-capped gold nanoparticles as postcolumn reagents for high-performance liquid chromatography assay of low-molecular-mass biothiols. *J Chromatogr A* **1163**: 328–332.
[112] Lu RH, Kopeckova P & Kopecek J (1999) Degradation and aggregation of human calcitonin *in vitro*. *Pharm Res* **16**: 359-367.
[113] Lu W & Park TG (1995) Protein release from poly(lactic-co-glycolic acid) microspheres: protein stability problems. *J Pharm Sci Technol* **49**: 13–19.
[114] Lucke A, Kiermaier J & Gopferich A (2002) Peptide acylation by poly(α-hydroxy esters). *Pharm Res* **19**: 175-181.
[115] Lyritis GP & Trovas G (2002) Analgesic effects of calcitonin. *Bone* **30**: 71S–74S.
[116] Malkov D, Angelo R, Wang H-Z, Flanders E, Tang H & Gomez-Orellana I (2005) Oral delivery of insulin with the Eligen® Technology: Mechanistic studies. *Curr Drug Deliv* **2**: 191-197.
[117] Manica DP, Lapos JA, Jones AD & Ewing AG (2003) Analysis of the stability of amino acids derivatized with naphthalene-2,3-dicarboxaldehyde using high-performance liquid chromatography and mass spectrometry. *Anal Biochem* **322**: 68-78.
[118] Manicourt DH, Devogelaer JP, Azria M & Silverman S (2005) Rationale for the potential use of calcitonin in osteoarthritis. *J Musculoskelet Neuronal Interact* **5**: 285-293.
[119] Martenka E (2004) Praca magisterska: Nanocząstki i ich zastosowanie do wprowadzania sond fluorogennych do komórek drożdży (Mémoire de Master: Rôle des nanoparticules dans la pénétration des sondes fluorescentes sélectives du glutathion chez la levure *Candida albicans*)

[120] Matsuyama T, Morita T, Horikiri Y, Yamahara H & Yoshino H (2006) Improved nasal absorption of salmon calcitonin by powdery formulation with N-acetyl-L-cysteine as a mucolytic agent. *J Control Release* **115**: 183-188.
[121] Medintz IL, Mattoussi H & Clapp AR (2008) Potential clinical applications of quantum dots. *Int J Nanomed* **3**: 151-167.
[122] Mehta R, Jeyanthi R, Calis S, Thanoo B, Burton K & DeLuca P (1994) Biodegradable microspheres as depot system for parenteral delivery of peptide drugs. *J Control Release* **29**: 375-384.
[123] Michelet L, Zaffagnini M, Massot V*, et al.* (2006) Thioredoxins, glutaredoxins, and glutathionylation: new crosstalks to explore. *Photosynth Res* **89**: 225-245.
[124] Mieyal JJ, Gallogly MM, Qanungo S, Sabens EA & Shelton MD (2008) Molecular mechanisms and clinical implications of reversible protein S-glutathionylation. *Antioxid Redox Sign* **10**: 1941-1988.
[125] Moriarty DF, Vagts S & Raleigh DP (1998) A role for the C-terminus of calcitonin in aggregation and gel formation: a comparative study of C-terminal fragments of human and salmon calcitonin. *Biochem Biophys Res Commun* **245**: 344–348.
[126] Morimoto K, Katsumata H, Yabuta T, Iwanaga K, Kakemi M, Tabata Y & Ikada Y (2001) Evaluation of gelatin microspheres for nasal and intramuscular administrations of salmon calcitonin. *Eur J Pharm Sci* 179–185.
[127] Muller M, Zechmann B & Zellnig G (2004) Ultrastructural localization of glutathione in *Cucurbita pepo* plants. *Protoplasma* **223**: 213-219.
[128] Mundargi RC, Babu VR, Rangaswamy V, Patel P & Aminabhavi TM (2008) Nano/micro technologies for delivering macromolecular therapeutics using poly(D,L-lactide-co-glycolide) and its derivatives. *J Control Release* **125**: 193–209.
[129] Munoz-Torres M, Alonso G & Raya MP (2004) Calcitonin therapy in osteoporosis. *Treat Endocrinol* **3**: 117-132.
[130] Na DH, Youn YS, Lee SD, Son MW, Kim WB, DeLuca PP & Lee KC (2003) Monitoring of peptide acylation inside degrading PLGA microspheres by capillary electrophoresis and MALDI-TOF mass spectrometry. *J Control Release* **92**: 291-299.
[131] Na DH, Youn YS, Park EJ*, et al.* (2004) Stability of PEGylated salmon calcitonin in nasal mucosa. *J Pharm Sci* **93**: 256-261.
[132] Orwar O, Fishman HA, Ziv NE, Scheller RH & Zare RN (1995) Use of 2,3-naphthalenedicarboxaldehyde derivatization for singlel-cell analysis of glutathione by capillary electrophoresis and histochemical localization by fluorescence microscopy. *Anal Chem* **67**: 4261 -4268.
[133] Ostergaard H, Tachibana C & Winther JR (2004) Monitoring disulfide bond formation in the eukaryotic cytosol. *J Cell Biol* **166**: 337-345.
[134] Panyam J & Labhasetwar V (2003) Biodegradable nanoparticles for drug and gene delivery to cells and tissue. *Adv Drug Deliver Rev* **55**: 329–347.
[135] Parak WJ, Pellegrino T & Plank C (2005) Labelling of cells with quantum dots. *Nanotechnology* **16**: R9–R25.
[136] Parmentier C, Wellman M, Nicolas A, Siest G & Leroy P (1999) Simultaneous measurement of reactive oxygen species and reduced glutathione using capillary electrophoresis and laser-induced fluorescence detection in cultured cell lines. *Electrophoresis* **20**: 2938-2944.
[137] Paroni R, Vecchi ED, Cighetti G, Arcelloni C, Fermo I, Grossi A & Bonini P (1995) HPLC with o-phthalaldehyde precolumn derivatization to measure total, oxidized, and protein-bound glutathione in blood, plasma, and tissue. *Clin Chem* **41**: 448-454.

[138] Pinto Reis C, Neufeld RJ, Ribeiro AJ & Veiga F (2006) Nanoencapsulation I. Methods for preparation of drug-loaded polymeric nanoparticles. *Nanomedicine: Nanotechnology, Biology, and Medicine* **2**: 8-21.
[139] Plosker GL & McTavish D (1996) Intranasal salcatonin (salmon calcitonin). A review of its pharmacological properties and role in the management of postmenopausal osteoporosis. *Drug Aging* **8**: 378-400.
[140] Prabhu S, Tran LP & Betageri GV (2005) Effect of co-solvents on the controlled release of calcitonin polypeptide from *In situ* biodegradable polymer implants. *Drug Deliv* **12**: 393-398.
[141] Prego C, Fabre M, Torres D & Alonso MJ (2006) Efficacy and mechanism of action of chitosan nanocapsules for oral peptide delivery. *Pharm Res* **23**: 549-556.
[142] Prousky J (2008) The treatment of pulmonary diseases and respiratory-related conditions with inhaled (nebulized or aerosolized) glutathione. *Evid Based Complement Alternat Med* **5**: 27-35.
[143] Purdue BW, Tilakaratne N & Sexton PM (2002) Molecular pharmacology of the calcitonin receptor. Receptor Channel 8: 243–255.
[144] Qin J, Ye N, Yu L*, et al.* (2005) Simultaneous and ultrarapid determination of reactive oxygen species and reduced glutathione in apoptotic leukemia cells by microchip electrophoresis. *Electrophoresis* **26**: 1155-1162.
[145] Rahman I, Kode A & Biswas SK (2006) Assay for quantitative determination of glutathione and glutathione disulfide levels using enzymatic recycling method. *Nat Protoc* **1**: 3159-3165.
[146] Rammouz G, Lacroix M, Garrigues JC, Poinsot V & Couderc F (2007) The use of naphthalene-2,3-dicarboxaldehyde for the analysis of primary amines using high-performance liquid chromatography and capillary electrophoresis. *Biomed Chromatogr* **21**: 1223-1239.
[147] Reginster JY (1995) Treatment of bone in elderly subjects: calcium, vitamin D, fluor, bisphosphonates. *Horm Res* **43**: 83-88.
[148] Resch-Genger U, Grabolle M, Cavaliere-Jaricot S, Nitschke R & Nann T (2008) Quantum dots versus organic dyes as fluorescent labels. *Nat Methods* **5**: 763-775.
[149] Riegler J & Nann T (2004) Application of luminescent nanocrystals as labels for biological molecules. *Anal Bioanal Chem* **379**: 913–919.
[150] Rouhier N, Lemaire SD & Jacquot J-P (2008) The role of glutathione in photosynthetic organisms: emerging functions for glutaredoxins and glutathionylation. *Annu Rev Plant Biol* **59**: 143–166.
[151] Saby S, Leroy P & Block J-C (1999) *Escherichia coli* resistance to chlorine and glutathione synthesis in response to oxygenation and starvation. *Appl Environ Microbiol* **65**: 5600-5603.
[152] Sahoo SK, Panyam J, Prabha S & Labhasetwar V (2002) Residual polyvinyl alcohol associated with poly (D,L-lactide-coglycolide) nanoparticles affects their physical properties and cellular uptake. *J Control Release* **82**: 105–114.
[153] Santra S, Xu J, Wang K & Tan W (2004) Luminescent nanoparticles probes for bioimaging. *J Nanosci Nanotech* **4**: 590-598.
[154] Schultz C (2009) Fluorescent revelations. *Chem Biol* **16**: 107-111.
[155] Schwarzlander M, Fricker MD, Muller C*, et al.* (2008) Confocal imaging of glutathione redox potential in living plant cells. *J Microsc* **231**: 299-316.
[156] Shah RB & Khan MA (2004 A) Protection of salmon calcitonin breakdown with serine proteases by various ovomucoid species for oral drug delivery. *J Pharm Sci* **93**: 392-406.
[157] Shah RB & Khan MA (2004 B) Regional permeability of salmon calcitonin in isolated rat gastrointestinal tracts: transport mechanism using Caco-2 cell monolayer. *AAPS J* **6**: 1-5.

[158] Shah RB, Siddiqui A, Shah G & Khan MA (2003) A validated HPLC assay for simultaneous analysis of salmon calcitonin and duck ovomucoid. *Pharmazie* **58**: 620-622.
[159] Sharma P, Brown S, Walter G, Santra S & Moudgil B (2006) Nanoparticles for bioimaging. *Adv Colloid Interface Sci* **123-126**: 471-485.
[160] Sheehan D, Meade G, Foley VM & Dowd CA (2001) Structure, function and evolution of glutathione transferases: implications for classification of non-mammalian members of an ancient enzyme superfamily. *Biochem J* **360**: 1-16.
[161] Shen W-C (2003) Oral peptide and protein delivery: unfulfilled promises? *Drug Discov Today* **8**: 607-608.
[162] Shimada K & Mitamura K (1994) Derivatization of thiol-containing compounds. *J Chromatogr B* **659**: 227-241.
[163] Sies H (1999) Glutathione and its role in cellular functions. *Free Radical Bio Med* **27**: 916-921.
[164] Sigurjonsdottir JF, Loftsson T & Masson M (1999) Influence of cyclodextrins on the stability of the peptide salmon calcitonin in aqueous solution. *Int J Pharm* **186**: 205-213.
[165] Silverman SL (1997) Nasal calcitonin. *Endocrine* **6**: 199-202.
[166] Silverman SL (2003) Calcitonin. *Endocrinol Metab Clin North Am* **32**: 273-284.
[167] Silverman SL & Azria M (2002) The analgesic role of calcitonin following osteoporotic fracture. *Osteoporos Int* **13**: 858–867.
[168] Simoes M, Pereira MO & Vieira MJ (2005) Validation of respirometry as a short-term method to assess the efficacy of biocides. *Biofouling* **21**: 9–17.
[169] Simons C, Walsh SE, Maillard J-Y & Russell AD (2000) A note: ortho-phthalaldehyde proposed mechanism of action of a new antimicrobial agent. *Lett Appl Microbiol* **31**: 299-302.
[170] Sinko PJ, Smith CL, McWhorter LT, Stern W, Wagner E & Gilligan JP (1995) Utility of pharmacodynamic measures for assessing the oral bioavailability of peptides. 1. Administration of recombinant salmon calcitonin in rats. *J Pharm Sci* **84**: 1374-1378.
[171] Smirnova GV & Oktyabrsky ON (2005) Glutathione in bacteria. *Biochemistry (Moscow)* **70**: 1199-1211.
[172] Soppimath KS, Aminabhavi TM, Kulkarni AR & Rudzinski WE (2001) Biodegradable polymeric nanoparticles as drug delivery devices. *J Control Release* **70**: 1-20.
[173] Stevenson CL & Tan MM (2000) Solution stability of salmon calcitonin at high concentration for delivery an implantable system. *J Peptide Res* **55**: 129-139.
[174] Stratton LP, Dong A, Manning MC & Carpenter JF (1997) Drug delivery matrix containing native protein precipitates suspended in a poloxamer gel. *J Pharm Sci* **86**: 1006-1010.
[175] Takeuchi H, Matsui Y, Yamamoto H & Kawashima Y (2003) Mucoadhesive properties of carbopol or chitosan-coated liposomes and their effectiveness in the oral administration of calcitonin to rats. *J Control Release* **86**: 235–242.
[176] Takizawa T & Robinson JM (2000) FluoroNanogold is a bifunctional immunoprobe for correlative fluorescence and electron microscopy. *J Histochem Cytochem* **48**: 481-485.
[177] Tanko LB, Bagger YZ, Alexandersen P*, et al.* (2004) Safety and efficacy of a novel salmon calcitonin (sCT) technology-based oral formulation in healthy postmenopausal women: acute and 3-month effects on biomarkers of bone turnover. *J Bone Miner Res* **19**: 1531-1538.
[178] Tasset C, Barette N, Thysman S, Ketelslegers JM, Lemoine D & Preat V (1995) Polyisobutylcyanoacrylate nanoparticles as sustained release system for calcitonin. *J Control Release* **33**: 23-30.
[179] Tauskela JS, Hewitt K, Kang LP*, et al.* (2000) Evaluation of glutathione-sensitive fluorescent dyes in cortical culture. *Glia* **30**: 329-341.

[180] Thirawong N, Thongborisute J, Takeuchi H & Sriamornsak P (2008) Improved intestinal absorption of calcitonin by mucoadhesive delivery of novel pectin–liposome nanocomplexes. *J Control Release* **125**: 236–245.
[181] Thomas D, Klein K, Manavathu E, Dimmock JR & Mutus B (1991) Glutathione levels during thermal induction of the yeast-to-mycelial transition in *Candida albicans*. *FEMS Microbiol Lett* **77**: 331-334.
[182] Tortiglione C, Quarta A, Tino A, Manna L, Cingolani R & Pellegrino T (2007) Synthesis and biological assay of GSH functionalized fluorescent quantum dots for staining *Hydra wulgaris*. *Bioconjugate Chem* **18**: 829-835.
[183] Townsend DM, Tew KD & Tapiero H (2003) The importance of glutathione in human disease. *Biomed Pharmacother* **57**: 145-155.
[184] Trapani A, Laquintana V, Denora N*, et al.* (2007) Eudragit RS 100 microparticles containing 2-hydroxypropyl-B-cyclodextrin and glutathione: physicochemical characterization, drug release and transport studies. *Eur J Pharm Sci* **30**: 64-74.
[185] Treumer J & Valet G (1986) Flow-cytometric determination of glutathione alterations in vital cells by o-phthaldialdehyde (OPT) staining. *Exp Cell Res* **163**: 518-524.
[186] Tsai T, Mehta RC & DeLuca PP (1996) Adsorption of peptides to poly(D,L-lactide-co-glycolide): 2. Effect of solution properties on the adsorption. *Int J Pharm* **127**: 43-52.
[187] Tseng W-L, Lee K-H & Chang H-T (2005) Using Nile Red-adsorbed gold nanoparticles to locate glutathione within erythrocytes. *Langmuir* **21**: 10676-10683.
[188] Ublacker GA, Johnson JA, Siegel FL & Mulcahy RT (1991) Influence of glutathione S-transferases on cellular glutathione determination by flow cytometry using monochlorobimane. *Cancer Res* **51**: 1783-1788.
[189] Vasir JK, Reddy MK & Labhasetwar VD (2005) Nanosystems in drug targeting: opportunities and challenges. *Curr Nanosci* **1**: 47-64.
[190] Vila A, Sanchez A, Tobıo M, Calvo P & Alonso MJ (2002) Design of biodegradable particles for protein delivery. *J Control Release* **78**: 15–24.
[191] Wallach S, Farley JR, Baylink DJ & Brenner-Gati L (1993) Effects of calcitonin on bone quality and osteoblastic function. *Calcif Tissue Int* **52**: 335-339.
[192] Wang F, Tan WB, Zhang Y, Fan X & Wang M (2006) Luminescent nanomaterials for biological labelling. *Nanotechnology* **17**: R1-R13.
[193] Wang J, Chow D, Heiati H & Shen W-C (2003) Reversible lipidization for the oral delivery of salmon calcitonin. *J Control Release* **88**: 369–380.
[194] Wang L, Wang L, Xia T, Bian G, Dong L, Tang Z & Wang F (2005) A highly sensitive assay for spectrofluorimetric determination of reduced glutathione using organic nano-probes. *Spectrochim Acta A* **61**: 2533–2538.
[195] Wang W (1999) Instability, stabilization, and formulation of liquid protein pharmaceuticals. *Int J Pharm* **185**: 129-188.
[196] Weert M, Hennink WE & Jiskoot W (2000) Protein instability in poly(lactic-co-glycolic acid) microparticles. *Pharm Res* **17**: 1159-1167.
[197] Windisch V, DeLuccia F, Duhau L, Herman F, Mencel JJ, Tang S-Y & Vuilhorgne M (1997) Degradation pathways of salmon calcitonin in aqueous solution. *J Pharm Sci* **86**: 359-364.
[198] Winterbourn C (1993) Superoxide as an intracellular radical sink. *Free Radical Bio Med* **14**: 85-90.
[199] Witschi A, Reddy S, Stofer B & Lauterburg BH (1992) The systemic availability of oral glutathione. *Eur J Clin Pharmacol* **43**: 667-669.
[200] Wu G, Fang Y-Z, Yang S, Lupton JR & Turner ND (2004) Glutathione metabolism and its implications for health. *J Nutr* **134**: 489-492.

[201] Yamamoto H, Kuno Y, Sugimoto S, Takeuchi H & Kawashima Y (2005) Surface-modified PLGA nanosphere with chitosan improved pulmonary delivery of calcitonin by mucoadhesion and opening of the intercellular tight junctions. *J Control Release* **102**: 373-381.
[202] Yoo HS & Park TG (2004) Biodegradable nanoparticles containing protein-fatty acid complexes for oral delivery of salmon calcitonin. *J Pharm Sci* **93**: 488-495.
[203] Youan BC, Hussain A & Nguyen NT (2003) Evaluation of sucrose esters as alternative surfactants in microencapsulation of proteins by the solvent evaporation method. *AAPS PharmSci* **5**: 22.
[204] Youn YS, Jung JY, Oh SH, Yoo SD & Lee KC (2006) Improved intestinal delivery of salmon calcitonin by Lys^{18}-amine specific PEGylation: Stability, permeability, pharmacokinetic behavior and *in vivo* hypocalcemic efficacy. *J Control Release* **114**: 334-342.
[205] Youn YS, Kwon MJ, Na DH, Chae SY, Lee S & Lee KC (2008) Improved intrapulmonary delivery of site-specific PEGylated salmon calcitonin: Optimization by PEG size selection. *J Control Release* **125**: 68-75.
[206] Yu WW, Chang E, Drezek R & Colvin VL (2006) Water-soluble quantum dots for biomedical applications. *Biochem Biophys Res Commun* **348**: 781–786.
[207] Zaidi M, Inzerillo AM, Moonga BS, Bevis PJR & Huang CL-H (2002) Forty years of calcitonin - where are we now? A tribute to the work of Iain Macintyre, FRS. *Bone* **30**: 655-663.
[208] Zechmann B, Zellnig G & Muller M (2005) Changes in the subcellular distribution of glutathione during virus infection in *Cucurbita pepo* (L.). *Plant Biol* **7**: 49-57.
[209] Zechmann B, Muller M & Zellnig G (2006) Intracellular adaptations of glutathione content in *Cucurbita pepo* L. induced by treatment with reduced glutathione and buthionine sulfoximine. *Protoplasma* **227**: 197–209.
[210] Zechmann B, Mauch F, Sticher L & Muller M (2008) Subcellular immunocytochemical analysis detects the highest concentrations of glutathione in mitochondria and not in plastids. *J Exp Bot* **59**: 4017–4027.
[211] Zolnik BS & Burgess DJ (2007) Effect of acidic pH on PLGA microsphere degradation and release. *J Control Release* **122**: 338-344.

If there are more than 8 authors, only the names of the first three authors are indicated in the References.

Abstract

Polymeric nanoparticles are defined as submicronic solid colloidal carriers composed of polymers. Nanoparticles have been studied for many years and considered to have the potential to improve drug delivery to the desired site of action, including intracellular targeting, and to enable delivery of poorly soluble, poorly absorbed or unstable drugs such as proteins and peptides.

In this work, two considerably different types of active substances have been chosen for encapsulation in polymeric nanoparticles: fluorogenic probes for intracellular targeting of the reduced glutathione (GSH), namely *ortho*-phthaldialdehyde (OPA) and naphthalene-2,3-dicarboxaldehyde (NDA), as well as salmon calcitonin (sCT). Nanoparticles have been loaded with the selective fluorogenic probe for the labeling of intracellular GSH, an important biomarker of oxidative stress, and the potential ability of nanoparticles to enhance the probe uptake by cells has been evaluated. On the other hand, sCT is a polypeptide hormone used mainly for the treatment of osteoporosis. The development of a sustained injectable or oral delivery system for sCT would enhance the clinical usefulness of this polypeptide drug.

The probe or sCT-loaded nanoparticles were obtained using a simple or double emulsion solvent evaporation method, respectively. Nanoparticles were prepared with the well known Eudragit® polymers, however the biodegradable polymers based on the copolymers of lactic and glycolic acids (PLGA) were also used with the aim of the development of injectable sCT-loaded nanoparticles. Then, the obtained nanoparticles were thoroughly characterized, e.g. in terms of the size, zeta potential, encapsulation efficiency, drug (probe) release, cytotoxicity (probe-loaded nanoparticles) or microscopic morphology and thermal properties (sCT-loaded nanoparticles). The NDA-loaded particle diameter was approximately 220 nm, while the particle size of various sCT formulations was in the range 380-625 nm. Due to a higher encapsulation efficiency of NDA (~48%) than OPA (~2%), only the former was selected for further study in yeast cells. However, sCT was more efficiently incorporated into nanoparticles (encapsulation efficiency: 69-83% for all the formulations). NDA-loaded nanoparticles were incubated with yeast cells (*Candida albicans*) and intracellular NDA-GSH adduct levels determined by HPLC after cell lysis increased by about 9-times in comparison with the free probe. In the case of sCT, the *in vivo* study was conducted in Wistar rats, and it was demonstrated that after subcutaneous injection of sCT-loaded PLGA nanoparticles, elevated serum sCT levels could be sustained for 3 days and the achieved sCT bioavailability from nanoparticles was increased compared to sCT solution. Furthermore, after oral administration of sCT-loaded nanoparticles in rats, encouraging results were obtained in the case of one of the formulations.

In conclusion, the active molecules incorporated in polymeric nanoparticles achieved the better cellular uptake (NDA) and bioavailability (sCT) that the non encapsulated ones.

Streszczenie

Nanocząstki polimerowe to submikronowe cząstki koloidalne, zaliczane do tzw. *advanced drug delivery systems*. Stanowią one kulistą matrycę polimerową, w której inkorporowana substancja aktywna jest rozpuszczona bądź zawieszona. Badania nad wykorzystaniem nanocząstek jako nośników leków trwają od wielu lat ze względu na potencjalne zastosowanie w terapii celowanej, w tym osiąganie przez substancję aktywną celów wewnątrzkomórkowych (*intracellular targeting*) oraz możliwość dostarczania *per os* substancji leczniczych słabo rozpuszczalnych, źle wchłanianych z przewodu pokarmowego lub nietrwałych (peptydy i białka). Do potencjalnych korzyści biofarmaceutycznych wynikających ze stosowania nośników polimerowych zaliczyć należy m.in. możliwość interakcji nanonośników z powierzchnią komórek (np. nabłonka jelit), efekt przedłużonego/kontrolowanego uwalniania leku czy ochronne działanie nośnika w odniesieniu do substancji aktywnej. Ponadto wymiary nanocząstek (< 1000 nm), decydują o możliwości podania dożylnego, a także o całkowitym wchłanianiu nanocząstek z inkorporowanym lekiem z przewodu pokarmowego.

Celem niniejszej pracy była ocena wpływu inkorporowania wybranych substancji aktywnych do nanocząstek na ich przenikanie w warunkach *in vivo*. W nanocząstki inkorporowano dwa rodzaje substancji aktywnych: sondy fluorogenne - aldehyd *o*-ftalowy (OPA) lub aldehyd-2,3-diformylowy (NDA) oraz kalcytoninę łososiową (sCT).

OPA i NDA stosowane są m.in. do derywatyzacji i oznaczania stężenia zredukowanego glutationu (GSH), ważnego biomarkera stresu oksydacyjnego, metodami chromatograficznymi lub elektroforetycznymi.

Z kolei sCT to hormon polipeptydowy zbudowany z 32 aminokwasów działający nawet do 40 razy silniej w porównaniu do endogennej kalcytoniny ludzkiej. Dzięki zdolności obniżania aktywności osteolitycznej osteoklastów, stymulacji mineralizacji kości i działania przeciwbólowego, kalcytonina znajduje zastosowanie w leczeniu takich schorzeń jak osteoporoza, choroba Paget'a, przerzuty nowotworowe do kości czy hiperkalcemia. Obecnie kalcytonina podawana jest w formie iniekcji lub częściej donosowo, co nie zapewnia odpowiedniego komfortu wielu pacjentom zmuszonym do stosowania tych postaci leku. Stąd też od kilku lat prowadzone są intensywne badania nad opracowaniem bądź postaci do wstrzyknięć o przedłużonym uwalnianiu bądź formy doustnej tego polipeptydowego hormonu. Jednak, podobnie jak wiele innych leków o budowie peptydowej lub białkowej, kalcytonina ulega rozkładowi w przewodzie pokarmowym pod wpływem enzymów trawiennych, a po podaniu parenteralnym wykazuje krótki okres półtrwania. Opracowanie którejś z w/w postaci farmaceutycznych kalcytoniny z pewnością przyczyniłoby się do zwiększenia zastosowania klinicznego tego hormonu.

Wybrane sondy fluorogenne (NDA lub OPA) do znakowania wewnątrzkomórkowego GSH inkorporowano do polimerowych nanocząstek, a następnie ocenie poddano zdolność otrzymanych

nanocząstek do polepszenia wychwytu sondy przez komórki drożdży (*Candida albicans*). Nanocząstki otrzymano z Eudragitu® E, polimeru dobrze znanego w technologii farmaceutycznej, stosując metodę emulgowania z wytworzeniem emulsji typu o/w z następującym odparowaniem rozpuszczalnika organicznego. Następnie przeprowadzono szczegółową charakterystykę nanocząstek, obejmującą m.in. pomiar wielkości cząstek, potencjału zeta, stopnia inkorporacji sondy do nanocząstek i cytotoksyczności. Uzyskane nanocząstki z NDA wykazały wysoki dodatni potencjał zeta, a wielkość cząstek wyniosła około 220 nm. Ze względu na znacznie wyższy poziom inkorporacji do nanocząstek NDA (~48%) niż OPA (~2%), dalsze badania na komórkach drożdży przeprowadzono jedynie z nanocząstkami zawierającymi NDA. Po inkubacji komórek z wolnym NDA lub inkorporowanym do nanocząstek (stężenie NDA w obu przypadkach: 100 μM), komórki były poddane lizie. Stężenie adduktu NDA-GSH w ekstraktach z komórek drożdży było oznaczone metodą HPLC z detekcją spektrofluorymetryczną. Inkorporacja NDA do nanocząstek, spowodowała około 9-krotny wzrost stężenia adduktu NDA-GSH w ekstraktach z drożdży w porównaniu z poziomami tego adduktu oznaczonymi przy użyciu sondy nie inkorporowanej. Zatem inkorporacja w polimerowe nanocząstki skutkowała lepszą penetracją NDA do komórek.

Z kolei, nanocząstki zawierające sCT otrzymano metodą emulgowania wielokrotnego (w/o/w) z następującym odparowaniem rozpuszczalnika organicznego. Do otrzymywania nanocząstek użyto: Eudragit® RS oraz biodegradowalny kopolimer kwasu mlekowego i glikolowego (PLGA) 50:50 w dwóch odmianach różniących się budową grup końcowych w łańcuchu polimerowym (PLGA H i PLGA S). Wykorzystując 3 różne polimery (osobno lub łącznie) w stosunku 1:1 otrzymano 5 różnych formulacji: Eudragit® RS, PLGA H, PLGA S, PLGA H/Eudragit® RS, PLGA S/Eudragit® RS. Otrzymane nanocząstki scharakteryzowano pod kątem ich wielkości i potencjału zeta oraz przeprowadzono obserwacje powierzchni nanocząstek za pomocą skaningowego mikroskopu elektronowego (SEM). Właściwości termiczne czystych polimerów, pustych nanocząstek i nanocząstek z kalcytoniną oceniono różnicową kalorymetrią skaningową (DSC). Średnia wielkość nanocząstek z sCT wyniosła pomiędzy 380-625 nm zależnie od typu polimeru. Nanocząstki z polimerów biodegradowalnych (PLGA) posiadały ujemny potencjał zeta, natomiast w przypadku nanocząstek z polikationowego Eudragitu® RS oraz z mieszanin obu polimerów potencjał zeta był dodatni. Obserwacje liofilizowanych nanocząstek za pomocą SEM wykazały budowę sferyczną i stosunkowo gładką powierzchnię oraz potwierdziły wielkość cząstek wynoszącą poniżej 1 μm. Stopień inkorporacji kalcytoniny oznaczony metodą pośrednią (oznaczanie kalcytoniny nie zainkorporowanej do nanocząstek w zewnętrznej fazie rozpraszającej emulsji) wahał się od 69 do 83% zależnie od rodzaju formulacji. Był on porównywalny z wynikami uzyskanymi metodą bezpośrednią (rozpuszczenie nanocząstek w rozpuszczalniku organicznym i ekstrakcja sCT do fazy wodnej). Do oznaczeń sCT wykorzystano gradientową metodę HPLC. Badania uwalniania sCT z nanocząstek przeprowadzono niekonwencjonalnie w 5% roztworze kwasu octowego ze względu na niewystarczającą trwałość substancji leczniczej w klasycznych płynach akceptorowych. W warunkach

in vitro, stwierdzono bardzo powolne uwalnianie sCT z nanocząstek otrzymanych z obu polimerów biodegradowalnych (po 6 tygodniach – około 21%). Natomiast uwalnianie sCT z nanocząstek z Eudragitu® RS oraz z mieszanin Eudragitu® RS i PLGA było całkowite w ciągu zaledwie kilku godzin. Niekompletne uwalnianie sCT z nanocząstek z obu polimerów biodegradowalnych można wytłumaczyć tworzeniem się koniugatów pomiędzy peptydem a produktami degradacji polimerów.

Do badań *in vivo* wybrano 3 rodzaje formulacji (Eudragit® RS, PLGA H, Eudragit® RS/PLGA H). Szczurom rasy Wistar podano jednorazowo podskórnie lub bezpośrednio do żołądka bądź roztwór wodny kalcytoniny (dawka podskórna: 300 IU/kg, dawka *per os*: 1000 IU/kg) bądź wodną zawiesinę nanocząstek zawierających sCT (dawka podskórna: 600 IU/kg, dawka *per os*: 1000 IU/kg). Następnie szczurom pobierano krew, a w uzyskanej surowicy szczurzej oznaczano zawartość sCT metodą ELISA oraz, w przypadku podania do żołądka, oznaczano także stężenie wapnia (II) metodą spektrofotometryczną. Po podskórnym wstrzyknięciu szczurom nanocząstek z PLGA H zawierających sCT, zaobserwowano maksymalne stężenie sCT w surowicy po 1 h (C_{max} = 3,6 ng/ml), utrzymujące się stężenia sCT przez co najmniej 3 doby oraz lepszą biodostępność sCT z nanocząstek w porównaniu z jej biodostępnością z roztworu (biodostępność względna na poziomie 132%). Pozytywne wyniki stwierdzono również po podaniu doustnym szczurom nanocząstek z Eudragitu® RS, dla których uzyskano około 20% obniżenie poziomu wapnia (II) w surowicy szczurzej przez pierwsze 4 h od momentu podania. Może to wskazywać na ochronne działanie nanocząstek przed rozkładem sCT w przewodzie pokarmowym.

Podsumowując, na podstawie uzyskanych wyników badań można stwierdzić, że nanocząstki wydają się być obiecującymi nośnikami zarówno do wprowadzania sond fluorogennych do komórek, jak i do inkorporowania polipeptydów w celu polepszenia ich dostępności biologicznej.

Résumé

Les nanoparticules polymériques sont définies comme des transporteurs solides colloïdaux présentant une taille inférieure au micromètre. Etudiées depuis de nombreuses années, les nanoparticules présentent la capacité d'améliorer le transport et le ciblage des médicaments vers un site d'action défini mais également la capacité de transporter des substances actives peu solubles, faiblement absorbées ou fragiles telles que des protéines ou des peptides.

Dans ce travail, deux types de substances actives ont été encapsulées au sein de nanoparticules: d'une part des sondes fluorogéniques pour le ciblage du glutathion réduit (GSH) intracellulaire, à savoir l'*ortho*-phthaldialdehyde (OPA) et le naphtalène-2,3-dicarboxaldehyde (NDA), et d'autre part la calcitonine de saumon (sCT). L'OPA et le NDA sont deux sondes fluorogéniques sélectives pour le marquage du GSH intracellulaire, biomarqueur du stress oxydant. L'objectif de cette étude a été ainsi d'évaluer la capacité des nanoparticules à améliorer l'absorption de ces sondes par les cellules. Lors de la seconde étude, la sCT qui est une hormone polypeptidique utilisée principalement dans le traitement de l'ostéoporose a été encapsulée dans des nanoparticules. Le développement d'une forme orale ou injectable à libération prolongée de la sCT permettrait d'en améliorer significativement son utilité clinique.

Lors de ce travail, les nanoparticules d'OPA ou de NDA ainsi que des nanoparticules de sCT (à base d'Eudragit®, polymère polycationique non biodégradable couramment utilisé) ont été préparées respectivement à l'aide de techniques de simple ou de double émulsion avec évaporation du solvant. Cependant, des polymères biodégradables ont également été utilisés tels que les copolymères de l'acide lactique et de l'acide glycolique lors de la fabrication de nanoparticules injectables de sCT. Les nanoparticules obtenues ont été caractérisées en terme de taille, potentiel zêta, taux d'encapsulation, libération *in vitro* du principe actif, cytotoxicité (cas des nanoparticules de NDA) ou encore au niveau de leurs propriétés thermiques (cas des nanoparticules de sCT). Les particules chargées de NDA ont présenté des diamètres de l'ordre de 220 nm alors que les particules chargées de sCT présentaient des tailles fluctuant entre 380 et 625 nm. Au regard d'une meilleure encapsulation du NDA (~ 48%) comparativement à l'OPA (~ 2%), seules les nanoparticules de NDA ont été testées sur les levures (*Candida albicans*). L'encapsulation de la sCT au sein des nanoparticules s'est révélée plus efficace au vue des valeurs de taux d'encapsulation comprises entre 69% et 83 %. Les nanoparticules chargées de NDA ont été incubées en présence de levures et la concentration en adduit NDA-GSH intracellulaire était augmentée environ 9 fois par rapport à la concentration en adduits formés à partir de la sonde libre. Dans le cas de la sCT, l'étude *in vivo* menée chez des rats Wistar a démontré que, après une injection sous-cutanée de nanoparticules, les taux sériques élevés obtenus pouvaient être maintenus pendant 3 jours et que la biodisponibilité de la sCT augmentait par rapport à la solution de sCT administrée seule. Enfin, après une administration orale de nanoparticules de sCT chez le rat, des résultats encourageants ont été obtenus pour l'une des formulations.

En conclusion, les substances actives incorporées au sein des nanoparticules polymériques ont permis une meilleure pénétration cellulaire du NDA et une meilleure biodisponibilité de la sCT par rapport à ces mêmes molécules non encapsulées.

List of figures

List of tables

OŚWIADCZENIE

Niniejszym oświadczam, iż jestem autorem pracy doktorskiej p.t.:

Wprowadzanie sond fluorogennych i cząsteczek farmakologicznie aktywnych w nanocząstki celem zwiększenia ich penetracji w komórkach

Encapsulation of fluorogenic probes and pharmacologically active molecules into nanoparticles for enhancing cellular uptake

Praca ta została przeze mnie napisana samodzielnie (bez jakiegokolwiek udziału osób trzecich), przy wykorzystaniu wykazanej w pracy literatury przedmiotu i materiałów źródłowych, stanowi ona pracę oryginalną, nie narusza praw autorskich oraz dóbr osobistych osób trzecich i jest wolna od jakichkolwiek zapożyczeń.

Oświadczam również, że wymieniona praca nie zawiera danych i informacji, które zostały uzyskane w sposób niedozwolony prawem oraz nie była dotychczas przedmiotem żadnej urzędowej procedury związanej z uzyskaniem stopnia naukowego: doktor nauk farmaceutycznych, a złożona przeze mnie dyskietka/płyta CD zawiera elektroniczny zapis przedstawionej przeze mnie pracy.

Jednocześnie oświadczam, że nieodpłatnie udzielam Uniwersytetowi Medycznemu im. Karola Marcinkowskiego w Poznaniu licencji do korzystania z wyżej wymienionej pracy bez ograniczeń czasowych i terytorialnych w zakresie obrotu nośnikami, na których pracę utrwalono przez: wprowadzanie do obrotu, użyczenie lub najem egzemplarzy w postaci elektronicznej a nadto upoważniam Uniwersytet Medyczny im. Karola Marcinkowskiego w Poznaniu do przechowywania i archiwizowania pracy w zakresie wprowadzania jej do pamięci komputera oraz do jej zwielokrotniania i udostępniania w formie elektronicznej oraz drukowanej.

Imię i nazwisko .....Eliza Główka.....

Data, podpis .....07.04.2009 r.....